RETROGRADE TRANSPORT MEDIATED ER RECYCLING OF WNTLESS

by

Puttachai Ratchasanmuang

A thesis submitted to the Faculty of the University of Delaware in partial fulfillment of the requirements for the degree of Master of Science in Biological Sciences

Fall 2011

RETROGRADE TRANSPORT MEDIATED ER RECYCLING OF WNTLESS

by

Puttachai Ratchasanmuang

Approved: _____
Erica M. Selva, Ph.D.
Professor in charge of thesis on behalf of the Advisory Committee

Approved: _____
Randall L. Duncan, Ph.D.
Chair of the Department of Biological Sciences

Approved: _____
George H. Watson, Ph.D.
Dean of the College of Arts and Sciences

Approved: _____
Charles G. Riordan, Ph.D.
Vice Provost for Graduate and Professional Education

ACKNOWLEDGMENTS

I would like to first acknowledge my advisor Dr. Erica M. Selva for being exceptionally supportive and showing unending dedication to me and my project. I can't thank her enough for being an amazing advisor who goes out of her way to help me. Throughout this research, she forced me to think critically for myself but at the same time has always been there if I ever needed her. In time of exhaustion and despair, she has always been the pillar of light that encourages me to keep going. To say that this project would not have become as successful as it has without her would be an understatement.

I would like to acknowledge all the past and present members of the Selva lab. In one way or another, they have contributed to my research. I especially like to thank Dr. David Raden and Rich Wittmeyer who were extremely helpful when I was first starting out in the lab. I would like to thank both the graduate students currently in the lab, Babak Basiri and Senel Sencer Tektas, for their great ideas and being wonderful colleagues. Also I would to thank the undergraduate students for their enthusiastic nature that brightens my day. I especially want to thank Erica Boetefuer who is always been more than willing to help. I would also like to thank Scott Tibbetts, Alicia Liu, and Allison McCague for always keeping the lab entertaining. I wish them all best of luck in their future endeavors.

I would like to thank my committee members Dr. Melinda Duncan and Dr. Jia Song for their source of ideas and encouragement. They have been more than understanding and flexible with their time. I am also thankful to the University of Delaware's Biological Sciences Department and my funding, for without them this project would not have happened.

I would like to thank my parents David and Suttida Brown, who have given me nothing less than their utmost love and support. Through their constant encouragement and guidance I have learned to strive to be the best that I can be. Lastly, I want to thank my brother Jeffery and all my family in Thailand, for without them I would not be here today.

Sincerely,

Puttachai Ratchasanmuang

TABLE OF CONTENTS

LIST OF FIGURES

ABSTRACT

Wnts are secreted signaling molecules that have numerous functions during organismal development and are important in adult stem cell maintenance. While extensive study has elucidated many of the Wnt signaling mechanisms within signal-receiving cells, the process of Wnt maturation within signal producing cells remains poorly understood. Within the developing *Drosophila* wing imaginal disc, Wntless (Wls) and the retromer complex are required to sustain secretion of Wingless (Wg), the prototypical *Drosophila* Wnt. Wls directly binds Wg and escorts it through the secretory system for plasma membrane deployment. The retromer complex recycles Wls back to the secretory system to maintain Wls levels needed for continuous Wg secretion. The retromer complex is known to recycle cell surface proteins back to the Golgi, which has led to the broad view that Wls initially binds Wg within the Golgi. Here we present data showing Wls initially engages Wg within the endoplasmic reticulum (ER). This result leads to the hypothesis that Wls must be transported from the Golgi to the ER following retromer mediated Golgi targeting. To test this hypothesis, we performed β-COP and Yip1A RNAi knockdowns to specifically block Golgi to ER retrograde transport in Wg expressing cells. β-COP is a component of COPI coatomer vesicles shown to be important for retrograde transport. Whereas Yip1A is a protein that regulates the membrane association of Rab protein shown to regulate the retrograde transport of Shiga toxin from the Plasma membrane to the ER. Remarkably, the β-COP and YipA1 knockdowns phenocopy Wls and retromer mutant phenotypes, Wg accumulation within producing

cells and adult wing nicks. RNAi induced Wg retention and wing nicks are rescued by over-expression of *wls* in knockdown cells. This suggests Wg accumulation results from insufficient ER levels of Wls since it is required for Wg transport and deployment. These data suggest a model where Wls cycles from the ER to the plasma membrane with its Wg cargo and then returns to the ER for additional rounds of Wg export via Golgi mediated retromer targeting followed by Golgi to ER retrograde transport.

Chapter 1

INTRODUCTION

The Wnt family of signaling molecules regulates numerous processes in animal development and has been shown to be important for maintaining adult homeostasis[1,2]. Wnt signals have pleiotropic functions; with effects that are important for controlling cell proliferation, stem cell maintenance, and cell fate decision, as well as organizing cell movements and establishing tissue polarity [3]. Over the past few decades, numerous studies have shown that Wnt signaling is frequently dysregulated in human cancer and degenerative diseases[4, 5]. Thus, the Wnt signaling pathway is an attractive target for therapeutic intervention, and potentially a vital key for stem cell and regenerative medicine.

1.1 History and Nomenclature of Wnt ligand

Wnt protein was first discovered and studied in the late 1980s and early 1990s when the gene products of *Drosophila wingless* (*wg*) and vertebrate *integration 1* (*int1*), which was subsequently renamed *wnt*, were found to belong to a large evolutionally conserved family of extracellular signaling molecules. The nomenclature of 'Wnt' derived from the combination of *wingless* and *int1*; i*nt1* was first identified as an oncogene which activates the formation of mammary carcinoma in mice[6]. Identification of *Drosophila wingless* showed it to be homologous to vertebrate *int1*. Further analysis in *Drosophila* demonstrated that disruption of Wingless signaling caused dramatic defects in segmentation during embryonic development and later numerous other developmental

defects were attributed to loss of Wingless signaling. Due to the involvement of these genes in cancer and embryonic development, the interest prompted an exhaustive search for additional Wnt homologs in eukaryotes [7].

Wnt ligands are a family of secreted molecules that are cysteine-rich proteins consisting of 350-400 amino acids and an N-terminal peptide signal required for ER targeting and secretion. To date, nineteen Wnts have been found in mammals, seven in *Drosophila*, and five in *Caenorhabditis elegans*[8]. Primary sequence analysis of Wnts shows they share 23 highly organized cysteine (Cys) residues and several potential N-glycosylation sites. It has been speculated that the multiple Cys residues are involved in the formation of intramolecular disulfide bonding and are important for proper folding of Wnt protein[7]. Wnts are characterized as morphogens, or secreted signaling molecules that form a concentration gradient, ranging from high levels at the localized source of production to low levels at a distance from the source. This gives rise to differential cellular responses leading to the activation of short- and long-range targets in developing tissues. Many developmental processes are mediated by mechanisms involving morphogen cellular communication to provide positional information for surrounding cells. Wnts are essential regulators of developmental decisions and of homeostatic processes, such as maintaining stem cells population in the gut epithelia and colon crypt. Aberrant expression of Wnts or activation of its signal-transduction cascades has been linked to the formation of various human cancers[9].

1.2 Canonical Wnt signaling transduction

Wnt-receptor interactions elicit a variety of intracellular signaling responses. The first to be elucidated was the canonical Wnt pathway in which Wnts mediate the stability

of cytosolic β-catenin (Figure 1-1). Previous studies have demonstrated that Frizzled (Fz) receptor proteins are the primary receptors that Wnt ligands bind[10]. Fz are a family of seven pass transmembrane serpentine receptors, which have a long Cysteine-rich domain at N-terminus to which Wnts directly binds [11]. In the absence of Wnt, Fz is inactive; this suggests that Fz activation is Wnt ligand-dependent [11]. The mechanism of Fz activation by Wnt binding is not fully understood. However, it is believed that Fzs are reconfigured by Wnt binding in a similar fashion to other heptahelical receptors. In addition to Wnt/Fz interaction, a low density-lipoprotein receptor protein (LRP) is also required to transduce the signal. LRP contains a cytoplasmic tail that has a motif consisting of several Pro-Pro-Pro-(Ser-Trp)-Pro that become phosphorylated in response to Wnt signaling [11]. The phosphorylation of LRP motif causes recruitment of Axin, a component of β-catenin degradation complex. In addition to Axin recruitment, the interactions between Wnt, Fz and LRP produce a receptor trimeric complex whose interactions cause the activation of an inhibitor protein Disheveled (Dsh) [12].

dsh is expressed ubiquitously and is present in the cytoplasm. Dsh directly binds to Fz through a C-terminal cytoplasmic Lys-Thr-X-X-X-Trp motif that allows for transduction of the Wnt signal. The activation of Dsh blocks its antagonistic activity on Glycogen Synthase Kinase 3β (GSK3β), an important cytoplasmic Wnt transducer protein [13]. Binding of Wnt to form the tripartite complex causes the inhibition of β-catenin degradation, increasing cytoplasmic level of β-catenin [4].

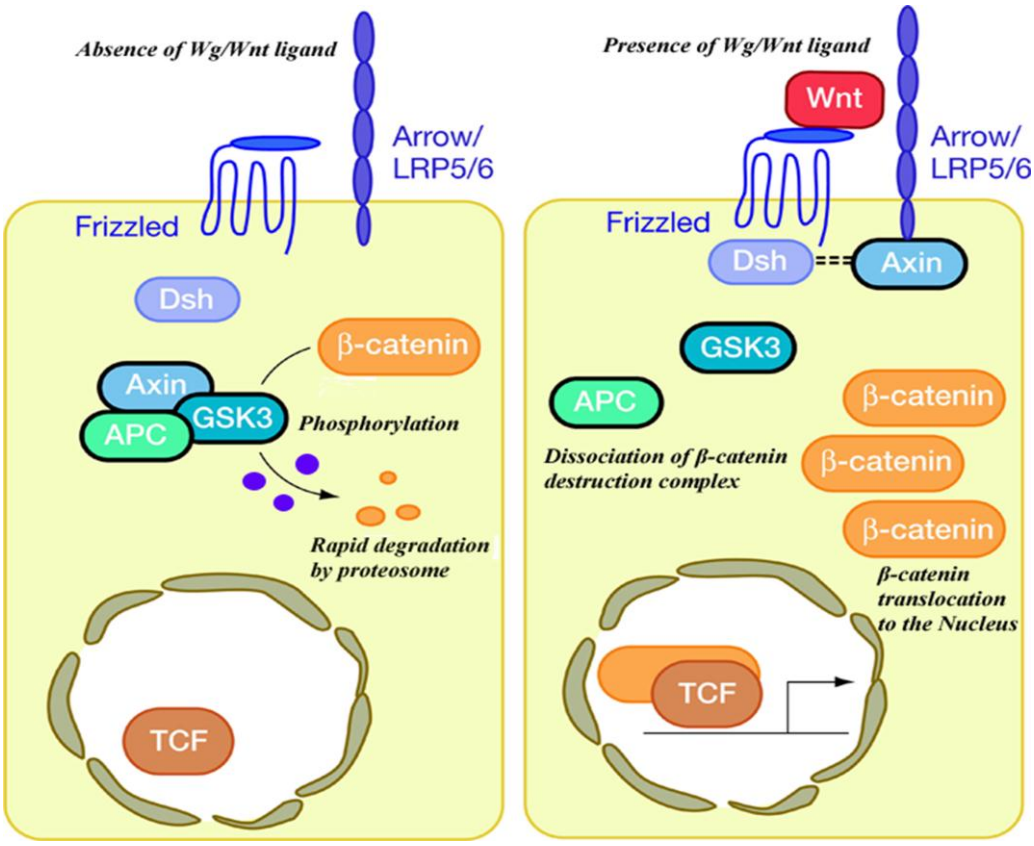

Figure 1-1 **The Canonical signaling transduction of Wg/Wnt ligand**. In the absence of Wnt, β-catenin is targeted for phosphorylation through its association with the Axin, APC, and GSK3β complex (left panel). The phosphorylation of β-catenin then targets it for degradation by proteasome. In the presence of Wg/Wnt, the ligand binds and activates the Frizzled-LRP receptor complex at the plasma membrane (right panel). These receptors transduce the signal through Dishevelled and Axin recruitment, thus dissociating the β-catenin destruction complex. This subsequently inhibits the degradation of β-catenin and stabilizes cytoplasmic β-catenin, which accumulates and translocates into the nucleus where it activates Wnt downstream target genes. Reproduced from Logan and Nusse, 2004.

When GSK3β is inhibited by the activation of Wnt signaling, cytosolic β-catenin is stabilized. Hypophosphorylated β-catenin accumulates in the cytoplasm and translocates

to the nucleus (Figure 1-1). Normally in absence of nuclear β-catenin, the activity of lymphoid enhancer factor 1 (LEF1)/T-cell factor (TCF) is inhibited by the transcriptional repressor Groucho and histone deacetylases, which prevents the transcription of Wnt target genes [14]. The interaction between β-catenin and LEF1/TCF, family of transcription factors, promotes DNA sequences specific binding of the complex to the regulatory region of Wnt-responsive gene to activate their transcription[15].

LEF1/TCF and Groucho are just two of the factors that are involved in directing the activation of Wnt target genes. There are other members of this activation complex, such as histone acetylase CBP/p300 and SWItch/Sucrose Non-Fermentable SWI/SNF which help remodel chromatin around TCF binding site to provide increased accessibility of β-catenin-TCF to cognate DNA binding sites [16]. Furthermore, Wnt signaling exhibits positive feedback control, with many Wnt target genes encoding components of Wnt signal transduction pathway itself. Together these factors provide and regulate proper canonical Wnt signal transduction. Nevertheless there is more than one way in which Wnt signals elicit downstream affects.

In the absence of Wnt signaling, the unstimulated state, β-catenin is phosphorylated by the Serine/Threonine kinases, casein kinase I α and GSK3β [11]. Adenomatous Polyposis Coli (APC) and Axin facilitate the phosphorylation of β-catenin by GSK3β. Together these proteins form the β-catenin degradation complex. This complex also allows phosphorylated β-catenin to be recognized by the ubiquitin protein ligase complex, β-TrCP. The ubiquitination of β-catenin then targets it for rapid degradation by proteasome, which maintains low level of β-catenin[17].

The Wnt pathway described conforms to simple scheme of signal, receptor and transduction cascade, which is much the same as other signaling pathways (Figure 1-1). However, the functional branching of its components complicates the Wnt pathway. Most Wnt components are not only involved in transduction of Wnt signaling; they are also involved in other cellular processes. The change in these components' concentrations through Wnt signaling can lead to diverse responses [18]. It is believed that there are two pools of β-catenin; one pool is bound at the cell membrane to the cell adhesion molecule E-Cadherin and provides the link to actin cytoskeleton; while a second pool in the cytoplasm binds to APC and GSK-3β [19]. A stable balance in these β-catenin pools is crucial for Wnt signaling transduction and dynamic cellular maintenance.

Wnt signaling can also influence the cytoplasmic proteins that then regulate β-catenin stability through several mechanisms. Receptions of Wnt signals trigger the recruitment of Axin to LRP, as well as Fz binding to Dsh, effectively inhibiting the formation of β-catenin destruction complex and promoting the stability of β-catenin. It has also been suggested that the protein phosphatase (PP2A) is associated to Axin and required in Wnt-dependent elevation of β-catenin levels which further regulates β-catenin stability [20, 21]. This suggests that PP2A can function to dephosphorylate GSK-3β substrates. However, the mechanism by which Wnt signaling regulates PP2A remains unclear. Dsh also interacts with the destruction complex through GSK-3 binding protein, GBP/Frat [22]. GSK-3β binding protein can promote the dissociation of β-catenin from the destruction complex and prevent phosphorylation of β-catenin.

Notably however, research over the past few decades has shown Wnts activate other intracellular messengers independent of β-catenin which are termed non-

canonical Wnt pathways [3]. The planar cell polarity (PCP) pathway and Wnt- Calcium (Wnt/Ca2+) pathway are two non-canonical Wnt pathways which are essential to morphogenetic cell movement, but do not signal through GSK3 or β-catenin, and do not generally regulate cell fate determination. As its name implies, PCPs' function is to establish cell polarity and is essential for movements in cells that requires polarity guidance. In contrast, the Wnt/Ca2+ pathway mediates cytoskeletal structure and cell adhesion by regulating intracellular calcium level [7].

1.3 Wnt target genes and the development of Cancer

In vertebrate development, the loss of a single copy of a *wnt* gene can produce detrimental phenotypes ranging from embryonic lethality, abnormalities in central nervous system development and organ or limbs defects [11]. Given the critical roles of Wnt signaling, it cannot be seen as a surprise that mutation in Wnt pathway components are associated with many hereditary disorders, cancer, and other diseases. The dysregulation of Wnt signaling has been well documented to be one of the leading causative factor in the development of cancer, particularly in colorectal cancer [23].

Wnt signaling is mobilized to drive numerous developmental events during embryogenesis, a function that is conserved from *Drosophila* to vertebrates and appears to be vital for maintaining adult tissue homeostasis. Mutational analysis of *wnt* genes shows that Wnt signaling controls a wide range of biological processes and failure in its regulation can affect a wide variety of organs and tissues. The loss of Wnt or any of its pathway components can be detrimental for development and cellular maintenance. Among Wnt pathway components, the *APC* gene encodes a tumor suppressor (section 1-2). The mutation in this particular gene causes a hereditary cancer syndrome known as

Familiar Adenomatous Polyposis (FAP) [5]. Inheriting only one defective APC allele causes FAP. Further studies of FAP patients suggests that the mutation of *APC* causes inappropriate stabilization of cytoplasmic β-catenin[24]. Implying that Wnt cascade regulation by APC is vital to growth control of epithelial cells in the colon. Among other Wnt regulated targets, Tcf-β-catenin activation complex targets the expression of *c-Myc* and *cyclin D1,* which have been shown to be important components for proliferating epithelial cells in the colon [25]. Once the Wnt cascade is mutationally activated, these cells continue to proliferate indefinitely, which then lead to the accumulation of additional mutations. These individuals develop large numbers of colon adenomas, or polyps, during early adulthood. The individual polyps are clonal outgrowths of epithelial cells that have undergone inactivation of the second *APC* allele [5, 24]. Loss of APC function has also been shown to occur in most sporadic colorectal cancer, as well.

Due to the broad impact of Wnt signaling on many areas of research ranging from cancer to development, intensive study has identified many Wnt pathway components acting in receiving cells. While we know the maturation of Wnts are complex, key pathway components crucial for regulating the production, maturation and release of Wnts are less understood. Recently studies have focused on understanding the complex molecular mechanisms required for Wnt secretion. The logic in these studies is based on the promise that understanding secretion mechanism will lead to identification of important components that can be targeted for prevention of misregulation or disruption of Wnt signaling. As a signaling molecule, Wnts need to be able to migrate from producing cells to a target signal-receiving cell. Thus, release, transport, and receipt of the Wnt signaling ligand must be tightly regulated to ensure proper cellular communication.

1.4 Secretion of Wnt

Wnt proteins are defined by sequence similarities rather than by functional properties[6]. In fact many of the Wnts found in both *Drosophila* and humans are non-functional. All Wnts contain a signal sequence and a highly conserved distribution of cysteines [7]. Due to the complexity of the protein, characterization of Wnt has been very difficult. Although Wnts are secreted proteins, it is difficult to isolate soluble active Wnt molecules since most Wnts isolated are insoluble. It has been recently shown that Wnt proteins are palmitoylated, addition of fatty acids, a post-translational modification that renders them hydrophobic[26]. This finding supports the idea that as a signaling morphogens, Wnts need a vehicle to reach long-range target cells. The enzymes that palmitoylates Wnt were found earlier in *Drosophila* and encoded by *porcupine* (*por*) gene [27].

The majority of our understanding of the Wnt secretory pathway and Wnts themselves were derived from *in vivo* studies of *Drosophila wingless* (*wg*) [28]. In developing *Drosophila*, *wg* is expressed throughout development, from early embryogenesis through to fully mature adults. The secretion of the Wg morphogen is vital to numerous developmental events from embryonic and larval patterning to synaptic differentiation[29]. In the embryo, Wg acts as a short-range morphogens that patterns the epidermis. Wg is secreted by a subpopulation of cells within the posterior compartment of parasegments and is required for proper cell fate determination in the receiving cells. These receiving cells adopt an epithelial cell fate and at the end of embryogenesis they secrete cuticle that lack denticle giving rise to “naked region”. These epithelial cells alternate those that secrete cuticle with denticles to give the embryo its characteristic pattern at the end of embryogenesis [30, 31]. It has been shown that loss of

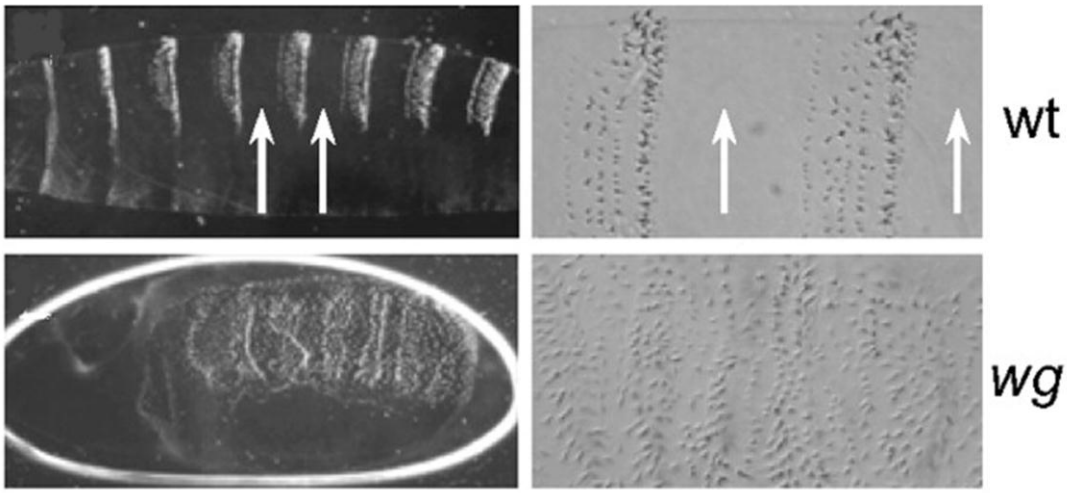

Figure 1-2 Loss of Wingless (Wg) signaling during embryonic development cause a "Lawn of Denticles" phenotype. Wg is expressed through embryonic and adulthood in *Drosophila*. The loss of Wg signaling causes embryonic lethality due to improper regulation of segmentation. Reproduced from Mieszcanek, 2008**.**

Wg signal transduction during embryogenesis causes segmental polarity phenotype in which the larval epidermis forms a 'lawn of ventral denticles' that lacks naked cuticle between the segmental denticles (Figure 1-2) [32]. The absence of epithelial cells that secrete naked cuticle to yield a lawn of denticles phenotype causes lethality in the developing organism.

During larval development, Wg can also act in long-range signaling in a concentration-dependent gradient. In the wing imaginal disc, Wg is produced by a population of cells primarily along the dorsal ventral boundary and migrates symmetrically throughout the dorsoventral compartment[33] (Figure 1-3). In 1993, van

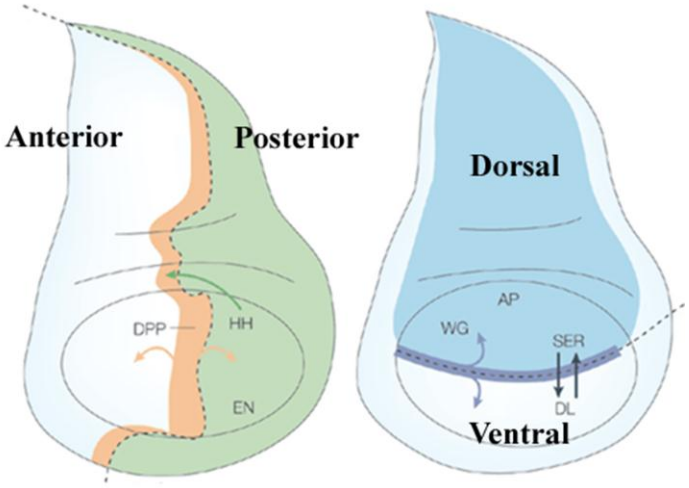

Figure 1-3 **Wing imaginal discs orientation and signaling ligands.** Wing imaginal discs image shows posterior is right and anterior is left, while dorsal is up and ventral is down. Hedgehog (Hh) and engrailed (En) are expressed in the posterior compartment and create a signaling gradient from posterior to anterior. Wg is expressed at the dorsal-ventral boundary and migrates dorsally and ventrally. Reproduce from Kiecket and Lumsden, 2005.

den Heuvel *et al.* found that embryo mutant for another segment polarity gene *por* showed a Wg accumulation phenotype in which Wg is retained in cells that produce it [34]. It was shown later by Kadowaki *et al.* 1996 in *Drosophila*, that Por is one of the key players in Wg secretion [27]. *Por* is ubiquitously expressed and acts as an upstream regulator of Wnt/Wg glycosylation and lipid modification. Interestingly, the expression of Por is essential only in the Wnt secreting cells, but not in the receiving cells. Por is required for the lipid modification of Wnts; however, the exact mechanism is still to be determined. Lipid modification is important for both Wnt long range signaling and for ligand-receptor interaction and internalization [35]. It has been

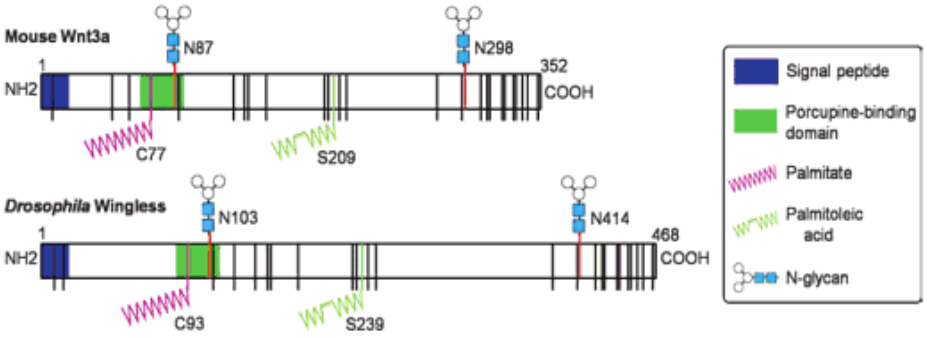

Figure 1-4 **Illustration of mouse Wnt3a and Drosophila Wingless protein demonstrating the approximation of cysteine residues in black vertical lines.** Shown above are locations in which Wnt/Wg are palmitoylated by Por. Two lipid modifications, one palmitate at the N-terminal cysteine 77 follow by one palmitoleic acid at serine 209. Finally indicated above are potential N-linked glycosylation sites. Reproduced from Goss *et al.*, 2011.

suggested that palmitoylation may also play an important role in Wg targeting to lipid raft membrane microdomains that form in Golgi and may help in trafficking Wg to the plasma membrane [36]. Although not evident in early primary sequencing, it seems that the mature, insoluble Wnt/Wg has two lipid modifications.

The first palmitate group added to the conserved Cys 77 in vertebrate Wnt3A was identified by Willert *et al.* in 2003. This Cys site was in fact shown to be conserved in *Drosophila* Wg (Figure 1-4). Por binds to the N-terminal 24 amino acid domain at residue 83-106 of Wg protein, which is known to be highly conserved in the Wg/Wnt family. This binding of Por to Wnt is important for the palmitoylation of Wg, as well as N-linked

glycosylation[37]. However, mutations of this residue do not necessarily result in the loss of Wnt signaling. A second lipid modification was reported by Takada *et al.* in 2006. The lipid moiety, an unsaturated fatty acid, palmitoleic acid, is also added to another conserved residue, Ser 209 in vertebrate Wnt3A[38].

Through bioinformatics studies it was suggested that *porcupine* encodes a putative multi-pass transmembrane protein belonging to the membrane-associated *O*-acyltransferase superfamily[27, 39] . *Por* homologs have been identified in *Xenopus*, mouse, human, and *C. elegans*[37, 40, 41] . It has been shown that Por is required for Wingless activity. Genetic and immunohistochemistry studies suggest that Por is required for the secretion of active Wingless ligand. *Por* functions upstream and is required by Wingless expressing cells. Mutation in *por* prevents the palmitoylation of Wnt, leading to the loss of Wnt signaling [42]. Por deficiency results in Wg/Wnt3A accumulation in the endoplasmic reticulum (ER) and loss of palmitoylated Serine 209, suggesting that Por is also responsible for lipid modification of Wg/Wnt proteins at this conserved amino acid [38].

Although palmitoylation is important to Wg signaling, the exact function is still not fully understood. It has been demonstrated that the over-expression of Wg in *Drosophila* can overcome the block caused by dysfunctional *por* [43]. One possible explanation for this observation is that the lipid moiety targets Wg to the membranes, but its absence can be overcome by high concentrations of Wg protein [27]. Studies in *Drosophila* have suggested that Wg protein could be secreted bound to lipoprotein particles[44, 45]. These particles could serve as vehicles for the movement of lipid modified ligands and facilitate long-range signaling [38]. An alternative suggestion was that Wnt proteins form a multimeric complex and through the lipid moieties they overcome the

hydrophobicity that allows them to move freely through the extracellular matrix. This suggests that palmitoylation of Wnt could play an important role for multimerization or lipoprotein particle association of Wnts [36]. However, there has been little to no data supporting these hypotheses. It still unclear how Wg is transported to receiving cells [8].

In addition to palmitoylation, Por has also been shown to be important for the N-glycosylation of Wg [37]. It has been demonstrated that in the absence of *por,* N-glycosylation of Wg is impaired, and that ectopic expression of *por* can stimulate N-linked glycosylation in both exogenous and endogenous Wg ligands [37]. As previously mentioned, Por binding to the N-terminal 24 amino acid-long domain in Wg is crucial not only for the palmitoylation of Wg, but also for its proper glycosylation [37]. Thus, it has been suggested that Por plays an important role in Wg maturation by tethering Wg to the ER where Wg is allowed time for proper folding and for the addition of sugars.

Two additional molecules are required for proper secretion of Wg/Wnt; Wntless (Wls) and the retromer complex. Wls, also known as Evenness interrupted (Evi) and Sprinter (Srt), is a multi-pass transmembrane protein that has been identified to be segment polarity gene in *Drosophila*, and is shown to be required for Wg signaling throughout development [31, 46, 47]. Genetic mapping by Bänziger, 2006,

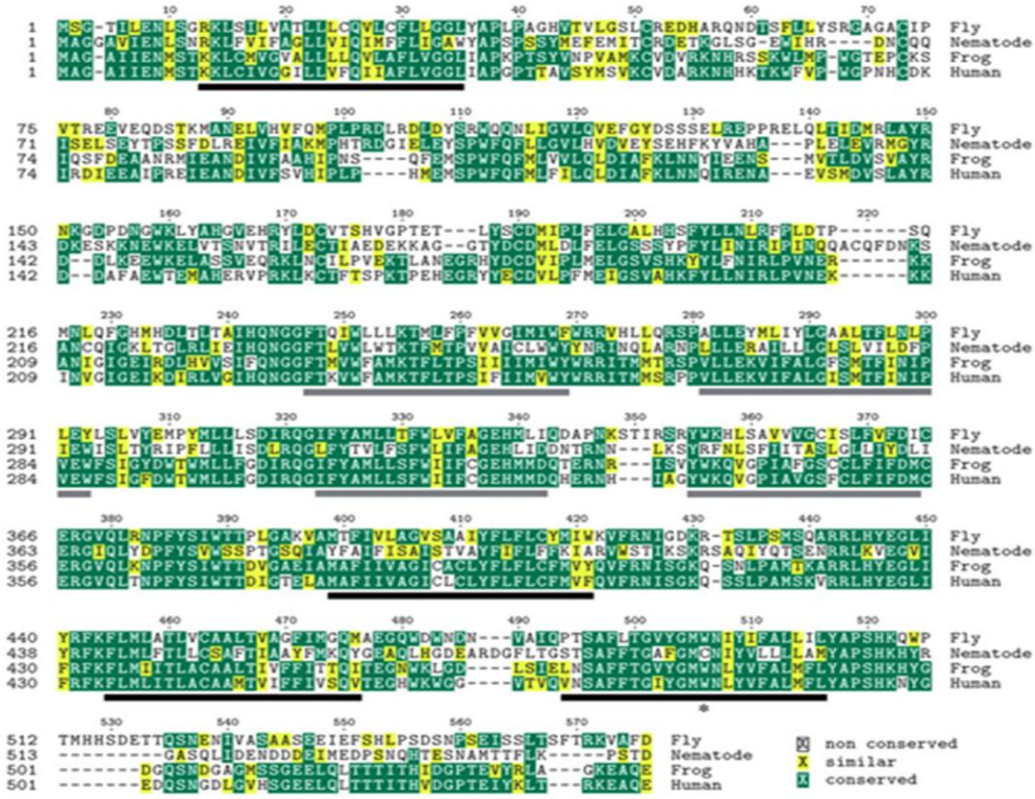

Figure 1-5 Comparison of Wls amino acid sequence between organisms from *Drosophila* to Human. Wls is a highly conserved protein from *Drosophila* to human, as suggested by above amino acid sequence comparison. Analysis shows overall 43% sequence identity and 62% similarity of *Drosophila* Wls to human. Black lines denote probable transmembrane helices, while gray bars are possible transmembrane regions, Reproduced from Goodman *et al*., 2006.

indicated that the *wls* genomic locus is composed of three exons with two possible splice variants encoding presumptive 594 (isoform A) and 562 (isoform B) amino acid residue proteins with an N-terminal signal sequence [47]. Orthologs of this gene are conserved from *Drosophila* to vertebrates. Sequence alignment of the *Drosophila* Wls isoform A relative to human reveals 43% sequence identity and 62% similarity with human Wls

(hWls, Figure 1-5) [31, 47]. Whereas some regions in the N-terminus and the majority of C-terminal regions of Wls diverge from vertebrate Wls, there is a high level of conservation that extends throughout the central region of Wls [47].

Analysis of the amino acid sequence predicts that Wls is composed of four to eight transmembrane spanning domains [47,48]. Much of the topology of Wls has been constructed from earlier sequence analysis, but has not been confirmed experimentally. The signal sequence is believed to be the first transmembrane domain because it does not have a good consensus signal peptidase cleavage site [49]. There are three highly hydrophobic regions, which are probable transmembrane regions. Another four hydrophobic regions are potential transmembrane domains, but they are either too short or weakly hydrophobic to be certain they are actual transmembrane regions (Figure 1-5). Based upon these observations, it is believed that Wls has four transmembrane domains with a large N-terminal globular extracellular/luminal domain that has two potential N-linked-glycosylation sites; however, the topology of Wls remains controversial due to the fact that there could be several other models depending upon how any transmembrane domains Wls possesses (Figure 1-6).

The primary function of Wls in the Wg pathway is still unclear; however, it is believed that Wls plays an important role in regulating the maturation of Wg ligand and maintaining proper Wg secretion. Wnt secretion is tightly regulated by physical interaction with Wls[31, 46]. Much like Por, *wls* mutation only affects the Wg pathway. It has been shown that Wg is retained within the Wg-producing cells in the absence of Wls, resulting in Wg signaling loss of function phenotypes [47].

During wing development, *hedgehog* (*Hh*) is expressed in the posterior compartment and moves anterior to activate targets in the anterior compartment and promote cell growth and wing pattering. Analysis of Hh demonstrated null mutant *wls* plays no role in Hh signaling, suggesting that Wls is specific only to the Wg secretory pathway [47]. How exactly Wls regulates the Wg ligand for proper secretion requires more research before it is fully understood.

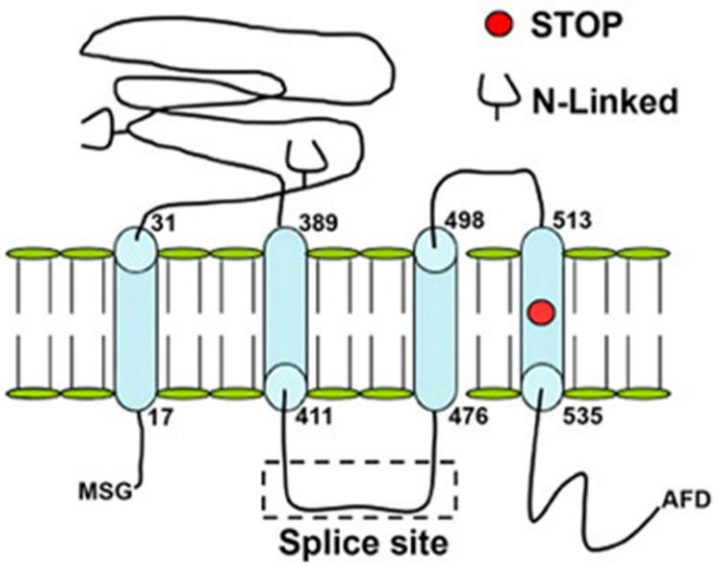

Figure 1-6 **Predicated Wls topology.** Analysis of Wls amino acid sequence suggests that Wls is a multi-transmembrane protein with N-linked glycosylation. However, there are other sites shown to be potential transmembrane region and other topologies for Wls are possible. Reproduced from Goodman *et al*., 2006.

It has been suggested that one possible role that Wls plays in the Wg pathway might mimic that of Por in Wg post-translational modification. Mutations of *por* have

similar Wg retention phenotypes as mutation in *wls*, which suggests that Wls could function to further post-translationally modify Wg ligand and target Wg to the plasma membrane. In this proposed role, Wls participates in known post-translational modification of Wg proteins, such as glycosylation or palmitoylation, which are both required for proper maturation.

The function of Wntless has only begun to be explored. A possible alternative function of Wls could be that it serves as a chaperone protein to promote proper folding and shuttling of the Wg ligand through the secretory pathway. There is an analogous precedent mechanism in which chaperone proteins could escort secreting proteins to the plasma membrane; *Drosophil*a Arrow protein, the Wg low density lipoprotein co-receptor (LRP in vertebrate), has been shown to reach the plasma membrane only in the presence of its specific chaperone protein, Boca [50]. Wls may act as a chaperone protein to Wg ligand in the same way by escorting Wg to the plasma membrane for proper intercellular trafficking. Furthermore, previous studies suggest that some Wg protein is loaded into lipoprotein particles during larval development, which may be required for the movement of lipid-modified Wg in the extracellular space to establish its morphogenetic gradient in the wing [44]. These lipoprotein particles are exogenously synthesized in the fat body and may be loaded with their lipid-modified cargo in the cells that produce Wg ligand. Wls may catalyze the loading of Wg into these lipoprotein particles, allowing it to be secreted from the cell surface [47]. Indeed, more recent experiments support the idea that Wls serves as a Wg molecular chaperone.

1.5 Retromer complex maintains Wls concentration in Wg secreting cells

Another essential Wg secretory factor is the retromer complex. The retromer complex is composed of five subunits first identified in yeast that mediates membrane protein trafficking between endosome and the Golgi apparatus[51]. Its importance in endosome to trans-Golgi-network trafficking has been implicated for a wide range of intercellular signaling including Wg signaling activities, bacterial toxin import and delivery and regulation of neurogically diseases such as Alzheimer [51]. Studies examining the role of retromer complex have also shown that the retromer is vital for maintaining Wls levels in Wg secreting cells[52].

The process of an endomembrane-targeted recycling by the retromer complex begins at the plasma membrane where membrane proteins are sorted for recycling. The sorting protein family is comprised of various proteins. Several of these proteins have been shown to regulate trafficking steps in endocytic processing. These sorting proteins usually possess a highly conserved protein dimerization domain Bin–Amphiphysin–Rvs (BAR) which is sensitive to membrane curvature and is able to remodel membranes in order to drive endocytosis[51]. The curvature of the membrane is then recognized by the retromer complex, which is made of Vps35, Vps26, and Vps 29 subunits. These subunits of retromer have the capability of detecting membrane deformation which allow them to bind and target the cargo to the Golgi compartment[52].

In the Wg secretory pathway, it has been shown that the retromer complex plays an important role in maintaining Wls concentration. In 2008, Belenkaya *et al.* examined the role of Vps35, an essential component of retromer complex, in Wg signaling in *Drosophila* and mammalian HEK293T cells. This study showed compelling evidence that the retromer complex is required for Wg secretion. In the

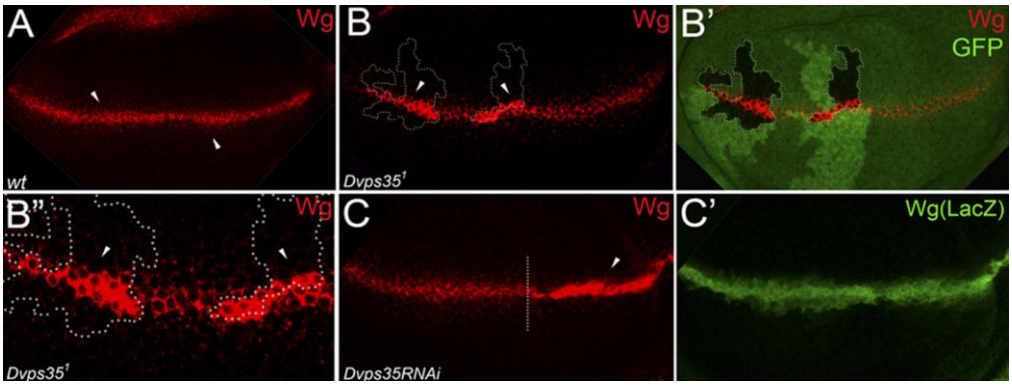

Figure 1-7 **Retromer is required for proper Wg secretion.** Top panel shows wild type (A) and mosaic analysis of mutant *vps35* retromer complex component (B), which demonstrates that there is a high retention of Wg ligand (red) in *vps35* mutant cells and further enlarged in (B''). Cells that are not expressing GFP identify *vps35* mutant tissues (B'). In the bottom panel, RNAi against the retromer component *vps35* in the posterior compartment indicated by the white arrow caused high retention of Wg protein. (C') shows *lacZ* expression under control of the *wg* promoter, which demonstrates the high levels of Wg in (C) is not due to increased *wg* expression in the posterior compartments. Reproduced from Belenkaya *et al.*, 2008.

absence of Vps35 retromer complex component, like *wls* loss of function mutant, Wg accumulates in secreting cells (Figure 1-7, B-B'' and C), which blocks downstream Wg signaling [52]. Additionally, examinations of null retromer mutant and RNAi knockdown in *Drosophila* showed Wls is targeted to the lysosome for degradation (Figure 1-8, E-E'''). It has also been demonstrated that in the background of retromer RNAi, the over-expression of *wls* rescued Wg retention (Figure 1-8, G). Compared to high Wg retention

due to retromer RNAi expression in the posterior compartment of the wing imaginal disc (Figure 1-7, C), when *wls* was over-expressed in the same

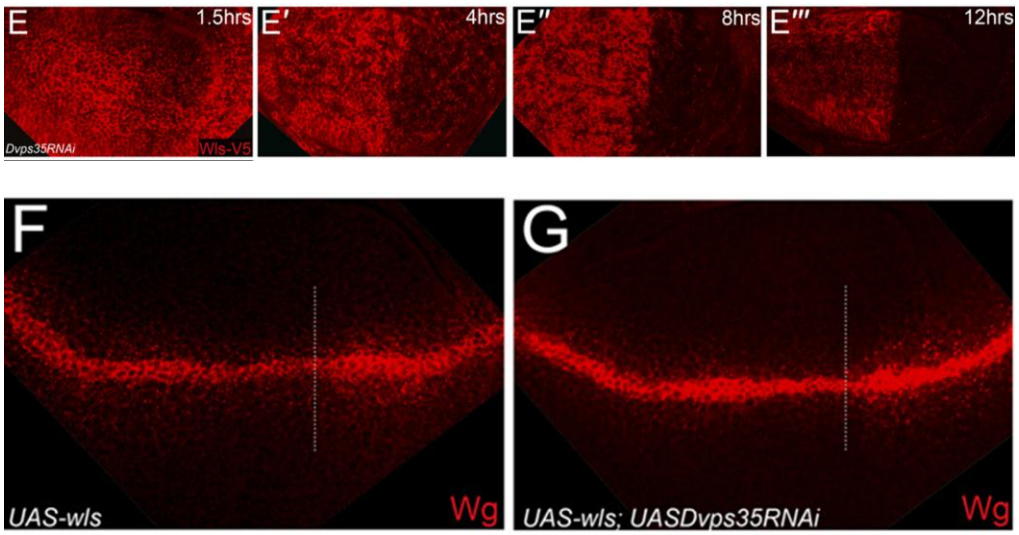

Figure 1-8 Wls is degraded in retromer knockdown and the over-expression of Wls rescues Wg retention. Top panel, RNAi to *vps35* is expressed in the posterior compartment of the wing imaginal disc (E-E'''). Over 12 hours, Wls (red) is dramatically depleted in the absence of retromer. Over-expression of *wls* (G) in the background of retromer RNAi, rescues Wg retention. Reproduced from Belenkaya *et al.*, 2008.

background (Figure 1-8, G), there's a definite rescue of Wg retention phenotype. These findings suggest a link between Wls and the retromer in the Wg secretion pathway. It was proposed that upon Wls dissociation from Wg, Wls is internalized and returns to the Golgi apparatus in a retromer-dependent manner [53]. Additionally, these data support the idea that the function of the retromer is to influence Wg secretion by recycling and maintaining the Wls concentration inside Wg secreting cells [52, 53].

1.6 Wls localization implicates its functionality in Wg secretion

Studies on the role of retromer in Wg biosynthesis suggested a model, in which Wg and Por interact in the ER where Por then post-translationally modifies Wg. Following Por catalyzed lipidation, Wg is trafficked to the Golgi where it is engaged by Wls. Wls then escorts Wg to the plasma membrane where the two proteins dissociate. Following dissociation, Wg is secreted, whereas Wls is internalized and returns to the Golgi apparatus in a retromer-dependent manner to support additional rounds of Wg secretion. Without the retromer, Wg secretion is impaired because Wls is diverted to the lysosome for destruction, thus reducing Wls levels necessary to support Wg secretion [53]. Although this seems to be a widely accepted model for the secretory pathway for Wg ligand, is has not be experimentally examined and therefore, the underlying mechanism is still unknown.

Due to the dogmatic function of the retromer complex, which recycles plasma membrane proteins back to the Golgi, it has been suggested that Wls should be located largely be in the Golgi in Wg producing cells [52]. However, Wls is found in multiple locations throughout the secretory pathway in Wg producing cells. In addition to the Golgi apparatus, Wls can be detected at the plasma membrane and the endosome, and the ER [46, 47]. Due to the controversial issue of Wls localization, the function of Wls in Wg secretion is not yet clear. Including the possible functions of Wls mentioned previously, Wls could act as a cargo recognition protein that directs Wg to its dedicated secretion track. Wls localization, and thus the initial site of Wls-Wg interaction, can determine Wls functionality. Wls localization in the lipid rafts at the plasma membrane would suggest its involvement in generating Wg-loaded lipoprotein particles. Additionally, Wls

localization at the ER or the Golgi could indicate its role in Wg maturation prior to Golgi trafficking.

1.7 Preliminary data suggests Wls and Wg initial interactions occur in the endoplasmic reticulum

Recent observation in *wls* mutant tissues by clonal analysis shows Wg retained at the basolateral surface of *Drosophila* wing imaginal discs without strict Golgi colocalization or disruption of Golgi structure or intracellular concentration (Figure 1-9) [54]. If the site of Wg and Wls engagement is in the Golgi, Wg accumulation caused by *wls* mutation should occur within the Golgi, as was observed with the yeast secretory (*sec*) mutants. Secretory mutant accumulated the organelle in which the mutated gene product was required. However, Wg retention was observed in the absence of strong Golgi colocalization or a change in Golgi structure in *wls* mutant cells. This suggests Wg-Wls engagement may not occur in the Golgi. Analysis of Wg and Golgi specific staining markers also suggests minimal colocalization between the two markers (Selva, unpublished data, Figure 1-9).

Together these data strongly argue that initial site of Wls and Wg engagement is not at the Golgi. Additional analysis of homozygous *wls* mutant wing imaginal discs showed stronger colocalization of Wg with an ER compartment marker than a Golgi marker and this result was statistically significant relative to Wg to Golgi colocalization (Figure 1-10). In this analysis Wg colocalization to a Golgi specific

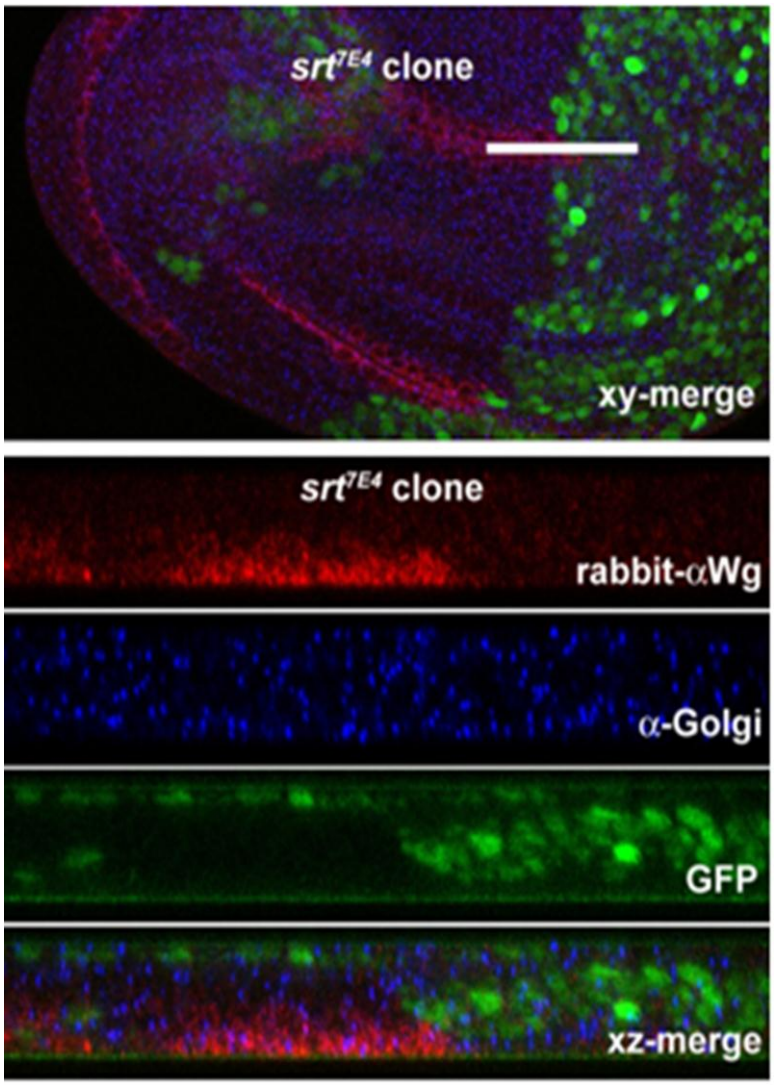

Figure 1-9 ***Drosophila*** **wing imaginal disc homozygous mutant for** ***wls*** **showed retained Wg does not colocalize with the Golgi.** Top panel shows xy-merge of *wls*^{7E4} mutant clones in the wing discs stained for Wg (red), Golgi (blue) and GFP (Green), Absence of GFP identifies *wls*^{7E4} mutant clones. White bar identifies xz sections taken of clones that cross the D/V boundary. Bottom panel shows xz-section of *wls*^{7E4} for all individual markers and the merge.

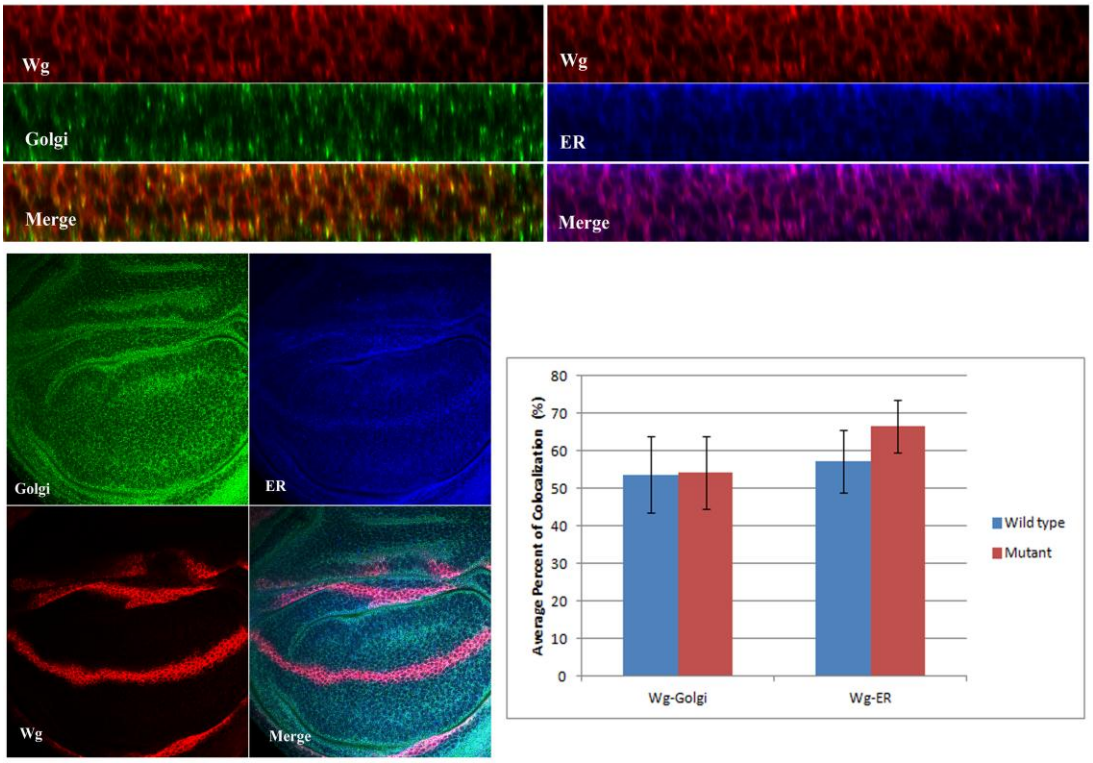

Figure 1-10 *Drosophila* wing imaginal disc homozygous mutant for *wls* showed Wg colocalization to the ER. An xz image taken through the Wg expressing cells in *wls* mutant wing discs to look at the colocalization (top). Colocalization of Wg (red) to ER (BiP, blue) and Wg to Golgi (GM130, green) was measured as a percentage (bottom right panel red bars), and student t- tests were used to determine if the difference between the two were statistically significant ($P < 0.0001$, $N=20$ bottom right). The same comparison was made in wild type wing discs (blue bars). Additionally, increased BiP-ER staining shows Wg accumulation induces ER membrane stress response suggesting this is the compartment of Wg retention.

marker and an ER specific marker was examined. Comparative study of these compartmental markers shows that the colocalization of Wg and the Golgi

specific marker GM130, showed approximately 55% colocalization, while the colocalization of Wg and ER specific marker Binding immunoglobulin protein (BiP), showed approximately 65% colocalization. Statistical analyses of these data suggest that in fact Wg and ER colocalization is significantly higher than Wg colocalization to Golgi. Furthermore, comparison of the wild type tissues in Wg-ER colocalization shows significantly less colocalization versus *wls* mutant tissues (57%, $P< 0.034$, $N=10$). However, there was no difference in the colocalization of Wg to the Golgi marker in WT as compared to *wls* mutant tissues ($P<0.277$, $N=10$). Due to the nature of these data, it was difficult to conclude that the ER is the site where Wls and Wg engage. Preliminary data from homozygous *wls* mutants also suggests accumulation of Wg in *wls* mutant tissues causes ER protein, BiP, accumulation, which is indicative of ER stress response (Figure 1-10, bottom left panel, blue)[55, 56]. High accumulation of Wg to the ER caused by improper escorting of Wg by Wls from the ER to the plasma membrane could suggests a stress response in the ER, which supports the hypothesis Wls and Wg engagement occurs in the ER. This ER stress response is shown more clearly when the dominant negative Wls (Wls-NHA) is ectopically expressed in the posterior compartment of the wing discs, which will be described later in Section 3.3 (Figure 3-10).

To further probe the previous results, Wg ligands generated in *wls* mutant wing imaginal discs were examined for structural modifications. Unlike Wg ligand obtained from wild type tissues, Wg from *wls* mutant tissue was found to be hyperglycosylated (Figure 1-11, red arrow). EndoH treatment marked in (+) column (Figure 1-11) suggests no structural modification of Wg proteins in the mutant tissues other than the additional glycosylation. As compared to the mutant, the wild type has two sugars added; in the mutant tissue there are three sugars added, where a third cryptic site within Wg is being

utilized in the Wls mutant tissue. This preliminary data suggests Wg protein is being retained in the ER, allowing time for the

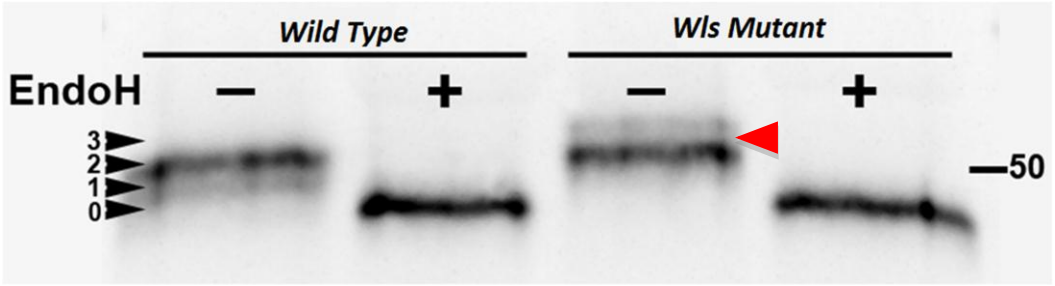

Figure 1-11 EndoH assay and Western blot analysis of Wg glycoproteins isolated from *wls* mutant wing imaginal discs shows hyperglycosylation at a site of Wg absent in wild type. Wg generated in *wls* mutant wing imaginal discs showed glycosylation of a third site (right, red arrow). This additional glycosylation site is not normally used in wild type (left), suggesting that Wg is retained in the ER in *wls* mutant discs, which provided time for the extra glycosylation to occur. Sharma and Selva unpublished data.

oligosaccharyltransferase to add on the extra sugar to the cryptic N-glycosylation consensus site that is never modified in the wild type Wg-producing tissues. This data, in addition to evidence that Wg colocalized with the ER in *wls* mutant wing discs, further supports the conclusion that Wg and Wls are engaging one another in the ER.

1.8 Proposed role of Golgi to ER retrograde transport in maintaining stable Wnt secretion

Anterograde transport of ER resident proteins from ER to Golgi is offset by its opposite retrograde transport from Golgi to ER. Through constant recycling, retrograde transport balances the out-flow of lipid membranes, as well as maintaining the steady

state of protein distribution needed in various compartments throughout the secretory pathway [57]. To facilitate proper cyclical pathway, residential ER proteins utilize sorting signals motif, such as KDEL and KKXX, for mediating Golgi to ER retrograde-transport [58]**.** Coatomer protein complex (COPI) is a cytoplasmic membrane coat complex binds specifically to cytoplasmic protein domain with ER retention such as KKXX or similar motifs[57]. This recognition and binding mediates the formation of retrograde vesicles. Retrograde transport from the Golgi to the ER has been known for quite some time; however, the recycling of endogenous protein from the plasma membrane back to the ER has not been rigorously demonstrated. Exogenous proteins like Cholera toxin and *Pseudomonas* exotoxin both have been shown to traverse the secretory pathway from the plasma membrane to the ER by retrograde transport and co-opting the host's pre-existing mechanisms [57, 59]. A lesser known retrograde transport COPI-independent mechanism, has been shown to be utilized by Shiga toxin to traffick from the plasma membrane to the ER [60]. YiP1A, a highly conserved multi-spanning membrane protein, regulates COPI-independent retrograde transport from plasma membrane to ER [61]. How this mechanism is exactly regulated is still unclear.

Due to their function, which is to target proteins for the ER membrane, it is reasonable to believe that the retrograde transport would be important for recycling of Wls from Golgi to ER in order to maintain proper concentration of Wls for Wg secretion. Additionally, although the recycling of endogenously produced protein from the plasma member to the ER has never been rigorously demonstrated, it has been shown that such pathway exists for exotoxin en route to the cytoplasm where they exert their toxic effects. Therefore, if Wls is targeted to the ER membrane for recycling, the existence of a

Wls recycling pathway would further support the hypothesis that Wls and Wg initial site of engagement is at the ER.

1.9 Specific Aims

The dogmatic function of the retromer complex suggested the initial interaction between Wls and Wg occurs at the Golgi [62]. However, *wls* mutant data strongly indicates that the Wg secretory block is to be in the ER, not the Golgi. The focus of this research is to determine the site where Wg and Wls initial engagement occurs and to elucidate the recycling mechanism of Wls from its initial interaction with Wg in the ER and its return upon release of its Wg cargo. We hypothesize that Wg initially engages Wls in the ER where Wg requires Wls and Por for proper maturation. With Wls as its partner, Wg goes to the Golgi compartment for subsequent modification. Wls then dissociates from Wg at the plasma membrane prior to Wls shuttling back into the cell to the Golgi via retromer-mediated transport. Finally, Wls is trafficked from the Golgi to ER via retrograde transport (Figure 1-12).

We approach this global hypothesis by addressing three specific aims. The first was to demonstrate that Wls recycles to the ER through fluorescently labeled Wls in $S2R^+$ cells. Furthermore, we isolated plasma membrane biotinylated Wls to demonstrate that surface Wls is recycled to the ER. The second aim of this project was to demonstrate the expression of an ER restricted form of Wls (Wls-NHA) that can still interact with Wg act as a dominant negative. Finally, the third aim focuses on the role of retrograde transport from Golgi to ER in maintaining ER levels of Wls. Retrograde transport has been shown to be a conserved mechanism from yeast to vertebrates [62]. We aim to demonstrate that the retrograde transport components, β-

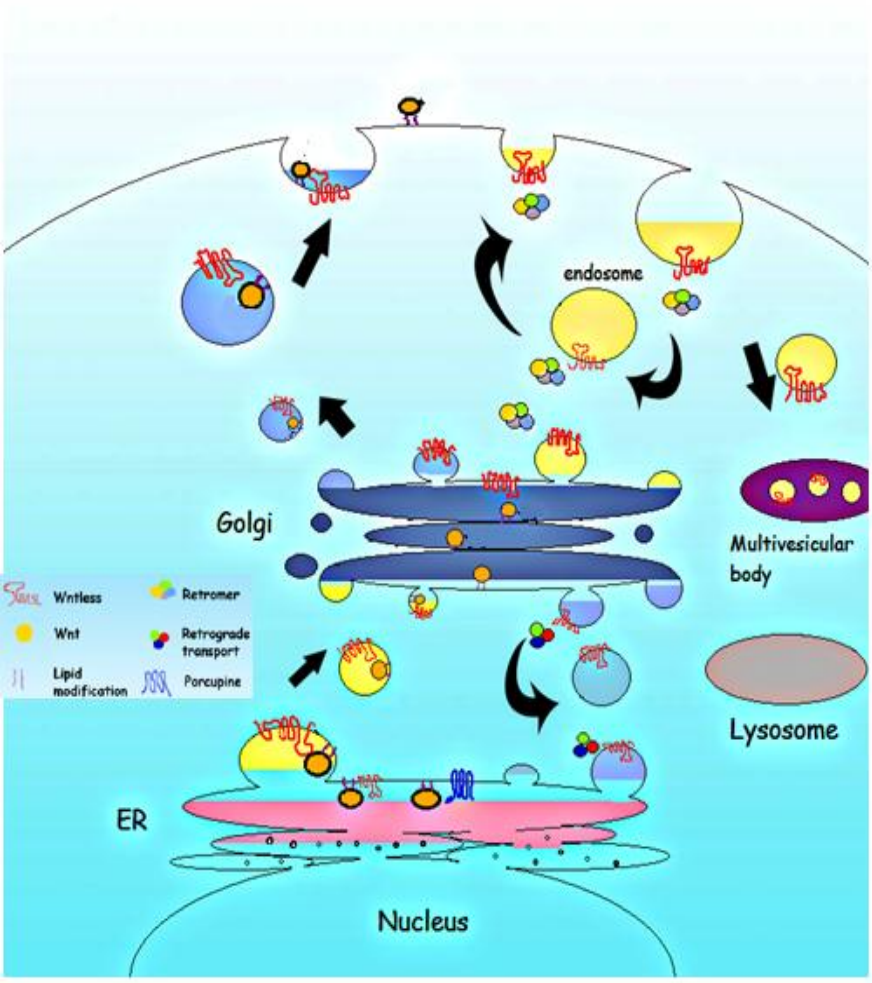

Figure 1-12 Proposed recycling mechanism of Wls in Wg secretion. From previous studies on Wg secretion, it has shown that Wg engages Por in the ER and was thought to engage Wls in the Golgi to facilitate proper Wg secretion. However, analysis of *wls* mutant tissues suggests the initial site of Wls and Wg engagement occurs in the ER. Thus, it is essential that Wls is recycled back to the ER where it would then interact with newly synthesized Wg ligand to maintain proper Wg secretion.

COP and Yip1A, are vital to maintaining high levels of Wls in Wg producing cells, similar to the function of the retromer. Furthermore, we hope to demonstrate that the over

expression of *wls*, in the absence of the retrograde transport, can overcome the Wg secretion block. With these approaches, we strive to demonstrate our global hypothesis that Wls and Wg initial engagement occurs at the ER and Wls is required to be transport back to the ER from the plasma membrane where it can engage with newly synthesized Wg for an additional round of Wg secretion.

Chapter 2

MATERIALS AND METHODS

2.1 Fly husbandry

Fly stocks, either obtained from Vienna Fly center, Bloomington Fly center or the Selva laboratory collection, were generally maintained at 20-25°Celcius (°C) and maintained on Carolina blue food mixture supplemented with baker's yeast. Experimental stocks were transferred into new vials every 4 days for expansion. Crosses were maintained in the same condition with exception to Wls-NHA stocks, which were maintained at 29 °C for some experiments (Section 3.3). True breeding stocks used in this study were maintained by transferring the flies to vials with fresh media once every two weeks and kept at 18°C. Adult flies were disposed of after 18-25 days maximum. Virgin females were collected twice each day within 4 hours after the adult flies emerge from the pupa case or 'eclosured'. Virgin females were inspected for proper phenotypes and distinctive abdominal spot in the intestine, which marks recent eclosure of female and thus their virginity. Males for experimental crosses were collected at any time between 2-10 days after eclosure. CO_2 was used to anesthetize the flies for both virgin and male collections.

2.2 Gal4-UAS system and fly stocks

Gal4 encodes a protein of 881 amino acids first identified in yeast as a regulator of genes induced by galactose. Gal4 regulates the transcription of the other genes by

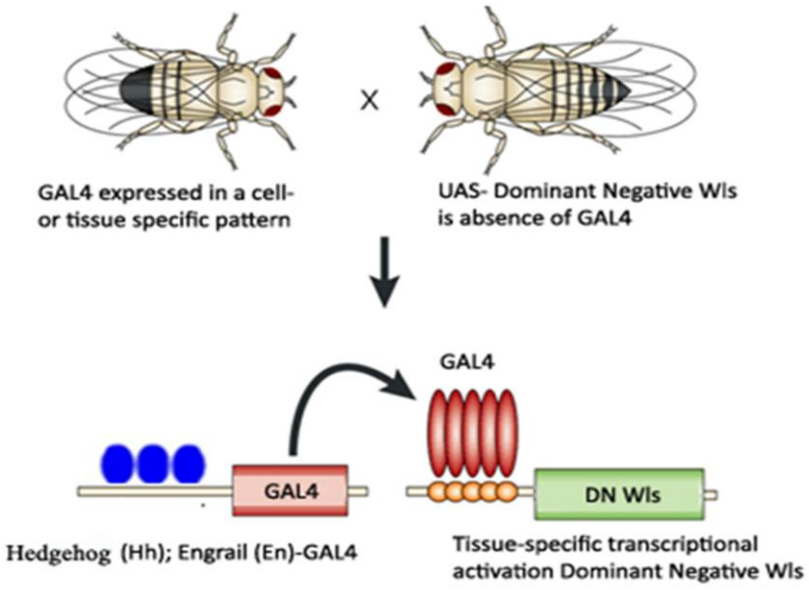

Figure 2-1 **Gal4-UAS transgene expression system.** The Gal4-UAS system was used to control the express *wls-NHA* (Dominant negative Wls), as well as *β-COP RNAi* and *Yip1A RNAi*. In this diagram, Gal4 is only expressed in *hh* and *en* expressing cells, thus limiting the *Gal4* expression to the posterior compartment. *UAS wls-NHA* expression does not occur in the absent of Gal4. In the progeny, Gal4 dictates the expression of *UAS-wls-NHA*. Reproduced from Muqit and Feany, 2002.

directly binding to four related 17 basepairs (bp) sites. These sites are defined as the Upstream Activating Sequences (UAS) elements, similar to enhancer element in mammals, which are essential for transcriptional activation of Gal4-regulated genes [63]. Following early work in yeast, it was demonstrated that *Gal4* could drive the expression of any genes under UAS control in *Drosophila* (Figure 2-1)[64]. Using this Gal4-UAS system, ectopic expression of *β-COP* or

Cg 6223 Beta COP crosses		
Bloomingdale stock number	Genotype	Phenotype Observed
1533	*w[*]; wg[Sp-1]/CyO; P{w[+mW.hs]=GAL4 dpp.blk1}40C.6TM6B, Tb[1]*	Major defect in the legs, wings, and lost of aristal on the antanae.
3045	*P{w[+mW.hs]=GawB}bi[md653], y[1] w[1118]/FM7a*	Late pupal lethal
5818	*w[*]; P{w[+mW.hs]=GawB}459.2*	1st-2nd in star lethal
6354	*w[*]; P{GAL4}bs[1348]*	Development pause at late 3rd in star
6791	*w[*]; P{w[+mC]=Ser-GAL4.GF}1 P{Ser-GAL4.GF}2*	late pupal lethal
8222	*y[1] w[1118]; P{w[+mC]=vgM-GAL4.Exel}2*	Burnt wing nicks, necrotic wings
8230	*y[1] w[1118]; P{w[+mC]=vgMQ-GAL4.Exel}2*	No profound phenotype
8696	*w[1118] P{GawB-DeltaKE}Bx[MS1096-KE]*	Only female wing lost of function
8761	*P{w[+m*]=GAL4}A9, w[*]*	Lethal
8860	*w[1118] P{w[+mW.hs]=GawB}Bx[MS1096]*	female wing lost of function
25083	*w[*]; P{w[+mW.hs]=GawB}dpr[PGawJ/CyO*	No profound phenotype
25676	*w[*]; P{w[+m*]=GAL4}zfh2[MS209]/In(4)ci[D], ci[D] pan[ciD]*	All adult have ci[D] parental phenotype; GAL4 driver is lethal
25754	*P{w[+mC]=UAS-Dcr-2.D}1, w[1118]; P{w[+mW.hs]=GawB}nubbin-4C-62*	Major defects in the leg development, No wing
25755	*P{w[+mC]=UAS-Dcr-2.D}1, w[1118]; P{w[+mW.hs]=GawB}salm[LP39]*	1st-2nd in star lethal
25757	*P{w[+mC]=UAS-Dcr-2.D}1, w[1118]; P{w[+mW.hs]=GawB}bbg[C96]*	Wing nicks
26662	*y[1] w[*]; P{w[+mW.hs]=GawB}vsh[MD751]*	No profound phenotype
27327	*w[*]; P{w[+m*]=cut-GAL4.E}3*	1st-2nd in star lethal
30806	*P{w[+mW.hs]=GawB}Bx[MS1096]; P{w[+mC]=UAS-jub.RNAi.22.5}3*	Lost of wing function
Prd-Gal4	*Paired*	Embryonic lethal
p{GawB}Ap544	*Apterous/Cyo*	Embryo/larval lethality
E15a	*later pattern Cyo/antena*	Late pupal lethal
Ci-Gal4 on 3	*cubitis interrupted*	Early larval lethal
Ci-Gal4 on 2	*Ci/Cyo*	Late pupla lethal
Wg-Gal 4	*Wg-Gal4; delta src/TM6C*	Late pupal lethal
UAS GFP AP-GAL4/cyo	*UAS GFP AP-GAL4/cyo*	Late larval lethal
Cg 12404 YiP1A		
Bloomingdale stock number	Genotype	Phenotype Observed
1533	*w[*]; wg[Sp-1]/CyO; P{w[+mW.hs]=GAL4 dpp.blk1}40C.6TM6B, Tb[1]*	Disrupt in Hh signaling, short aristal on antenae
3045	*P{w[+mW.hs]=GawB}bi[md653], y[1] w[1118]/FM7a*	Unstable stock
5818	*w[*]; P{w[+mW.hs]=GawB}459.2*	2nd to 3rd in star lethal
6354	*w[*]; P{GAL4}bs[1348]*	No profound phenotype observed
6791	*w[*]; P{w[+mC]=Ser-GAL4.GF}1 P{Ser-GAL4.GF}2*	Late pupal lethal
8222	*y[1] w[1118]; P{w[+mC]=vgM-GAL4.Exel}2*	Wings collapse, and deterioration, burnt wings
8230	*y[1] w[1118]; P{w[+mC]=vgMQ-GAL4.Exel}2*	No profound phenotype
8696	*w[1118] P{GawB-DeltaKE}Bx[MS1096-KE]*	Not fully penetrant, Wg lost of function*
8761	*P{w[+m*]=GAL4}A9, w[*]*	Lost of Wg function
8860	*w[1118] P{w[+mW.hs]=GawB}Bx[MS1096]*	Lost of Wg function
25083	*w[*]; P{w[+mW.hs]=GawB}dpr[PGawJ/CyO*	Late pupal lethal
25676	*w[*]; P{w[+m*]=GAL4}zfh2[MS209]/In(4)ci[D], ci[D] pan[ciD]*	Lethal phenotype
25754	*P{w[+mC]=UAS-Dcr-2.D}1, w[1118]; P{w[+mW.hs]=GawB}nubbin-4C-62*	Cubitis interrupted [ci] phenotype
25755	*P{w[+mC]=UAS-Dcr-2.D}1, w[1118]; P{w[+mW.hs]=GawB}salm[LP39]*	1st-2nd in star lethal
25757	*P{w[+mC]=UAS-Dcr-2.D}1, w[1118]; P{w[+mW.hs]=GawB}bbg[C96]*	Loss of Wg function
26662	*y[1] w[*]; P{w[+mW.hs]=GawB}vsh[MD751]*	No profound phenotype
27327	*w[*]; P{w[+m*]=cut-GAL4.E}3*	1st-2nd in star lethal
30806	*P{w[+mW.hs]=GawB}Bx[MS1096]; P{w[+mC]=UAS-jub.RNAi.22.5}3*	Lethal in female
Prd-Gal4	*Paired*	No profound phenotype
p{GawB}Ap544	*Apterous/Cyo*	Embryo to larval lethality
E15a	*later pattern Cyo/antena*	No profound phenotype
Ci-Gal4 on 3	*cubitis interrupted*	Late pupal lethal
Ci-Gal4 on 2	*Ci/Cyo*	Larva lethal
Wg-Gal 4	*Wg-Gal4; delta src/TM6C*	Loss of Wg function
UAS GFP AP-GAL4/cyo	*UAS GFP AP-GAL4/cyo*	Late larval lethal

Figure 2-2 Retrograde components knockdown by expressing *β-COP RNAi* or *Yip1A RNAi* using various Gal4 drivers results in adult defects or lethality. Virgin females carrying *UAS-β-COP RNAi* or *UAS-Yip1A RNAi* constructs were crossed to males harboring many different Gal4 drivers to induce the expression of the dsRNAi targeted to the retrograde components. Out of all the drivers tested, only two were selected. C96-Gal4 and Wg-Gal4 were chosen because both express in cells where Wingless ligand is produced. Knockdown of retrograde components using these drivers shows dramatic loss of Wg signaling phenotypes. Figure was generated using Bloomington fly center information sheet.

Yip1A RNAi was achieved by crossing *UAS-β-COP* and *UAS-Yip1A* RNAi lines (Vienna Stock Center) to multiple Gal4 specific driver lines (Bloomington Fly stock center). Gal4 drivers for these β-COP and Yip1A RNAi stocks were selected based on the progeny phenotypes. From the 34 listed Gal4 stocks tested, approximately twenty-seven displayed phenotype ranging from lethality to developmental defects, when crossed to *UAS-β-COP* and *UAS-Yip1A* RNAi lines (Figure 2-2). Wg-Gal4 and C96-Gal4 showed a strong phenotype known to be associated to loss of Wg signal transduction.

In the non-rescue/rescue experiments the following strains were used: *UAS-βCOPI RNAi*, *UAS-Yip1ARNAi*, *UAS-wls*, *wg-Gal4/CyO*, *C96-Gal4*. With the exception of Wg-Gal4, which is homozygous lethal, the fly stocks used in crosses were homozygous and thus, all progeny expresses the RNAi to either β-COP or Yip1A. To demonstrate that each progeny is truly expressing RNAi to the retrograde proteins, UAS-GFP was placed on the third chromosome in Wg-Gal4 fly strain and second chromosome in C96-Gal4 fly strain.

For the dominant negative experiments stable e*n-Gal4/en-Gal4 ; hh-Gal4/TM6C* male flies were crossed to *UAS-wls-NHA* virgin flies to drive the expression of Wls-NHA in the posterior compartment. Non-tubby third *in star* larva, which carry both *en-Gal4* and *hh-Gal4,* and *UAS-wls-NHA* were dissected for wing imaginal discs then stained for HA, ER marker, and Wg. Progeny with wing nicks were counted. *Apterus-Gal4/ CyO* male flies were crossed to *UAS-wls-NHA* to drive the expression of Wls-NHA in the dorsal compartment. Fifty percent of all progeny would carry both the *Apterus-Gal4* and *UAS-wls-NHA*. Third instar larva were dissected for wing discs and stained for HA, Achaetes, and Senseless.

RNAi to β-COP and Yip1A were designed to co-express *UAS-wls* in the rescue experiment. Each stock was created by crossing each strain to strain harboring stable balancer, to produce the following strains: *UAS-RNAi/CyO; UAS-Wls/TM6C*. UAS-RNAi and UAS-*wls* inserts are homozygous viable on the second and third chromosome, respectively. Homozygous females were crossed to *Wg-Gal4/CyO; UAS GFP* or *UAS GFP; C96 Gal4/TM6C*. Progeny expressing *GFP* carry the Gal4 driver, the RNAi to retrograde transport and over-express *wls*.

2.3 Wing imaginal disc dissection and immunohistochemistry

Wild type (w^{1118}) *Drosophila* third instar larvae were harvested into a dissecting petri dish in phosphate buffer saline (PBS) approximately 8-9 days after the eggs were laid. Primary dissections were done to expose and fix wing imaginal discs and remove fat body for antibody staining. Using two forceps the anterior portion of the larvae were gently separated and the posterior portion, which was discarded. The anterior portion, which has the wing imaginal discs, was inverted. Fat body and other internal structures were gently separated away the larval carcass and discarded.

The dissected sample was placed into an Eppendorf tube with PBS on ice. The primary dissected tissues were then washed with ice cold PBS three times. Samples were fixed with 4% formaldehyde in PBS for 20 minutes then washed with PBT (PBS with 0.1% TritonX-100) three times for 5 minutes. After the washes, the samples were blocked in PBT with 5% normal horse serum (NHS) for 30 minutes at room

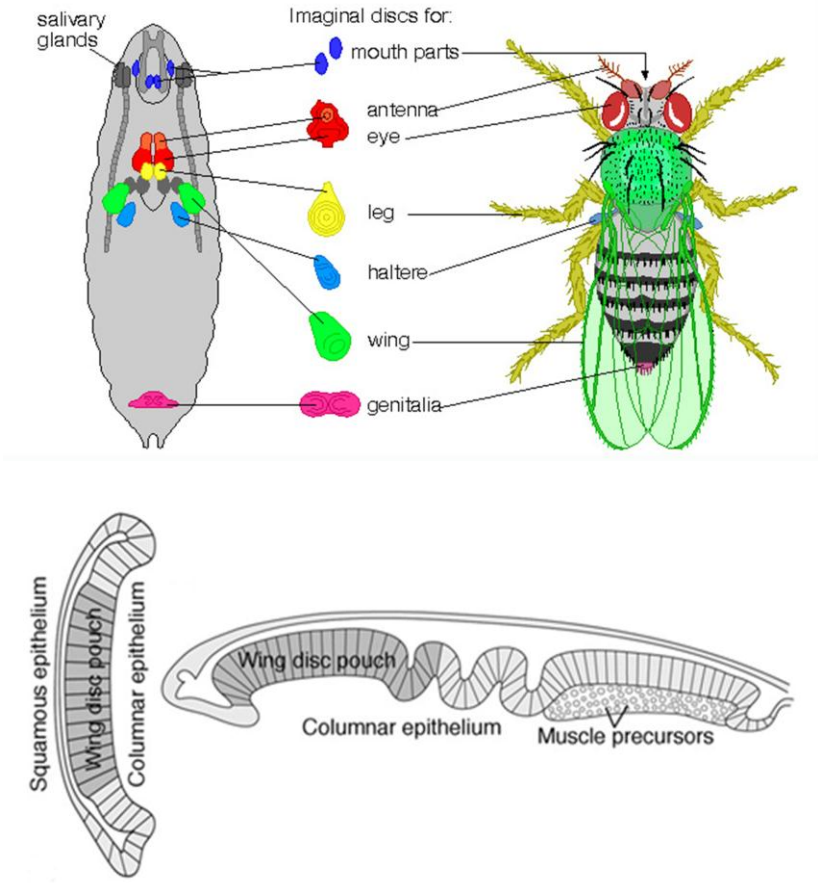

Figure 2-3 ***Drosophila*** **larval wing imaginal discs.** The first panel is a diagram of the localized areas of imaginal discs within the larvae, which differentiate during pupation to become distinctive organs in adult flies (top). Wing imaginal discs in the larva, bottom panel, are composed of two epithelial cell sheets; a squamous epithelium and the columnar epithelium, which later develops into the adult flies wings (bottom). Reproduced from Brian E. Staveley, Ph.D. (top) and Clemens *et al*., 2008 (bottom).

temperature and then stained with primary antibodies, which are listed in figure 2-4, in PBTN for 2 hours at room temperature or overnight at 4°C. The primary antibody was saved and the tissues were washed with PBT three times for 5 minutes and blocked

again PBTN for 30 minutes. After blocking, secondary antibody in PBTN against the primary antibodies were added and incubated for 2 hours at room temperature. Secondary antibodies were then removed and tissues were washed three more times with PBT for 5 minutes each.

The samples were then placed in a 35x10 mm Falcon™ Petri dish in PBT for a secondary dissection. In the secondary dissection, the wing imaginal discs are completely isolated from the trachea located approximately one-third of the way down from the mouth. The imaginal discs are located above the smaller haltere discs and below the leg discs. Imaginal discs are generally identified by size. Unlike the rest of the imaginal discs, wing discs are usually the largest and are mostly flat. After the discs were isolated, a micropipette was used to place each disc on a slide mounted in 70% glyceraldehyde mounting medium. A cover slip is placed and sealed with nail polish. Images of the wing imaginal discs were taken in the similar condition with Zeiss LSM confocal microscope 780 using a 40x objective at 1x zoom unless mentioned otherwise. The xz images were taken from the dorsal-ventral boundary by manually drawing a straight line though Wg expressing cells, which was identified by Wg staining. Due to the varying curvature of wing discs where Wg was expressed each individual line drawn varied in size, which changes the zoom for xz images. Furthermore, the depth of these wing imaginal discs also varies from one disc to another. Nevertheless, xz images were taken with these factors in mind and were taken at an approximate 2x-3x zoom.

This protocol was slightly modified later to improve ER staining in certain experiments. Instead of using TritonX-100, the detergent used was NP40 at 0.1% in PBS or PEM (0.1M Pipes, 2mM EGTA, and 1mM $MgCl_2$, pH 7) with 4% formaldehyde was used

to fix the tissues. Primary staining for these experiments was also done at 4°C for 48 hours incubation.

Antibody	Dilution	Source	Primary(P)/Secondary (S)	Used
Mouse α Wg	1/500	Hybridoma bank	P	In this work
Rat α BiP	1/500	Hybridoma bank	P	In this work
Rabbit α GM130	1/100	AbCam	P	In this work
Rabbit α PDI	1/100	AbCam	P	For Optimization
Rabbit α Syntaxin	1/100	AbCam	P	For Optimization
Guinea pig α HSC (BiP)	1/100	Babraham	P	In this work
Rabbit α Senseless	1/1000	HugoVelen	P	In this work
Rabbit α E-Cadherin	1/10	AbCam	P	In this work
Rat α KDEL	1/100	AbCam	P	In this work
Mouse α Acheates	1/10	Hybridoma bank	P	In this work
Mouse α Alpha 5	1/100	Hybridoma bank	P	For Optimization
Mouse α Delta	1/10	Hybridoma bank	P	For Optimization
Rabbit α HA	1/100	Invitrogen	P	In this work
Mouse α Srt	1/100	Konrad Basler lab	P	In this work
Mouse α biotin	1/500	Invitrogen	P	In this work
Goat α Mouse 568	1/500	Invitrogen	S	In this work
Goat α Mouse 647	1/500	Invitrogen	S	In this work
Goat α Rabbit 488	1/500	Invitrogen	S	In this work
Goat α Guinea pig 549	1/500	Invitrogen?	S	In this work
Goat α rat 647	1/500	invitrogen	S	In this work
Rhodamine Donkey α Rat	1/500	Jackson Lab	S	In this work

Figure 2-4 List of antibody used in this work. Listed above are antibodies used throughout this study. Note that some antibodies were not shown in this thesis but were used for optimization. Next to each antibody are the dilution and source corresponding to the antibodies.

2.4 Tracking subcellular location of inducible Wntless in S2R+ cells

2.4.1 Optimization of Metallothionein promoter in S2R+ cells

Cultured S2R+ cells were first incubated for 24 hrs in 6 well Petri dishes containing GIBCO® Schneider's *Drosophila* medium supplemented with 10% fetal

Bovine Serum (*Invitrogen*) and 1% Streptomycin/Penicillin (Thermo Scientific®) at 25°C. Post incubation, $S2R^+$ cells were harvested and transiently transfected with a metallothionine-Gal4 plasmid (*Drosophila* Genomics Resources Center) and pUAST GFP using Qiagen Effectene (Qiagen) transfection kit at a concentration of 0.2 micrograms/microliter according to the manufacturer's instructions. The pActin-GAL4 driver was transfected into a separate well with pUAST GFP a positive GFP transfection control. Experiments were initiated 24 hours post-transfection. Prior to each experiment, expression of GFP was checked for transfection efficiency.

After optimizations for transfection efficiency and metallothionine activation, it was determined that the most effective concentration of copper sulfate [$Cu(II)SO_4$)] was 1.5mM with a 1-3 hour incubation period. Transfected cell cultures were introduced to $CuSO_4$ solution at 1.5mM for 1 hour exposure period. After 1 hour induction period in $CuSO_4$, cell cultures were washed with media containing 0.5mM EDTA metal chelating reagent to eliminate the $CuSO_4$ and replaced with fresh medium. Multiple wells on the 8-well plates were used to transfect with MT-Gal4 and pUAST-GFP for additional data collections. Induced, transfected cell cultures were imaged overnight for over 12 hours on Zeiss LSM 510 confocal microscope in a time-lapse with a 20x objective. Fluorescent data were recorded and measured for peaked intensity.

2.4.2 Fluorescent Recovery after Photobleaching

After examining the data collected, it was determined that the expression of *GFP* reporter showed consistent peak intensity five hours post induction and washed out period. Furthermore, the expression of *GFP* did not deteriorate over time, which was not expected; this is further discussed in Section 3.1. The stability of GFP protein was tested

using Fluorescent Recovery after Photobleaching (FRAP). S2R^{+} cells that were transfected with the MT-GAL4 and UAS-GFP constructs were exposed to optimal concentration of Cu(II)SO_4, washed with EDTA, and incubated for 5 hours post exposure at 25°C. The selected cells were photobleached to approximately 50% of the normal intensity. Data were collected from the samples over a 13 hour period and measured for intensity. Fluorescence in the region of interest was collected for analysis.

2.4.3 Subcellular trafficking of Wls-CHA using a heat shock promoter

S2R^{+} cells were transfected with heat shock promoter expressing *wls-CHA* plasmid (See 2.4.1). 24 hours post transfection the cells were placed on a cover-slip and left for another 12 hours to adhere. After the incubation, cells were transferred into 37°C for a 1 hour heat shock to induce the expression of *wls*-CHA in fresh Schiender's media. Multiple samples were used to test optimal heat shock induction times prior to fixing the cells. Each cover-slip containing the cells was then fixed with 4% formaldehyde in phosphate buffered saline (PBS) for 10 minutes. The cells were gently washed three times for 5 minutes with phosphate buffered saline containing 0.2% Triton X-100 (PBT). Next, the cells were blocked with PBT containing 5% normal horse serum (NHS) for 20 minutes at room temperature. The cells were then stained for mouse anti-Wingless (1:10), and rabbit anti-HA (1:500) for 2 hours then washed again with PBT. Lastly, the cells were treated with secondary antibody generated in donkey (as listed in figure 2-4). Phalloidin with conjugated fluorochrome was used in some experiments to stain filamentous actin. Secondary antibodies were always used at a 1:500 dilution in PBTN and incubated for 2 hours at room temperature. Following secondary antibodies, cells were washed 3 times with PBT for 5 minutes each wash. Anti-fade/glycerol (70% in

PBS) was placed on sample slides and the cells on the cover slips were then inverted and gently placed on each slide. The slides were sealed with nail polish and visualized using a Zeiss LSM 510 confocal laser microscope.

2.4.4 Cellular Cholera Toxin uptake in S2R$^+$ cells

S2R$^+$ cells were transferred into 6-wells plates with cover slips at the bottom of each well. 12 hours post incubation the cells were washed with fresh Schneider's medium and placed on ice for 30 minutes prior to each experiment. Schneider's medium was removed and Cholera Toxin-Alexa568 fluorochrome conjugate (CT) was added at 1:500 with fresh cold medium. The cells were left to on ice for 5 minutes before they were transferred to 4°C for 30 minutes to allow CT and membrane protein binding.

The cells were washed with fresh medium three times and then incubated at room temperature for various induction periods. After each induction period the cells were washed with PBS and fixed with 4% formaldehyde (in PBS) for 10 minutes and blocked (See 2.2.1). Membrane compartment stainings were done using rat anti-BiP (ER marker, Babraham) at 1:20 and rabbit anti-Rab5 (early endosomal marker, Abcam) at 1:100 and incubated overnight at 4°C. After exposure to primary antibody, cells were washed, and the samples were stained with secondary antibodies and mounted, as described. Slides were then visualized with a Zeiss LSM 510 confocal microscope.

2.4.5 *Drosophila* wing imaginal discs surface biotinylation and uptake

Primary wing imaginal tissues were dissected, as described above (See 2.3). Dissected tissues were surface biotinylated with NHS-SS-biotin at 100 mM in PBS for 30 minutes on ice. Excessive biotin was removed by washing with PBS. The tissues were

then transferred in PBS to 4°C for a 30 minute incubation to allow the biotin cross link reaction and activation. The reaction was quenched with 125 mM glycine at room temperature for 15 minutes.

The tissues were washed again with PBS three times before incubation for 45 minutes at room temperature to allow for uptake. Post-incubation, the tissues were fixed with 4% formaldehyde-PBS for 30 minutes, washed with PBT three times for five minutes, and then blocked with PBNT for 20 minutes at room temperature. After blocking, the wing discs were stained with mouse anti-Biotin (1:500), rat anti-BiP (1:500), and rabbit anti-GM130 Golgi marker (1:100) and incubated overnight at 4°C. The samples were washed and secondary antibodies were added, as described. Samples were subsequently examined on a Zeiss LSM 710 confocal microscope.

2.5 Whole mount embryo staining

Embryos from experimental crosses were collected at 0-6 hours on apple juice agar plates and transferred to collection baskets with distilled water. Embryos were rinsed with distilled water and incubated in 50% bleach for 5 minutes to dissolve the chorion layer. Post-dechorination, embryos were washed thoroughly with distilled water and fixed for 20 minutes on a shaker in PEM-FA: Heptane solution (1:1). PEM-FA consisted of PEM (0.1M Pipes, 2mM EGTA, 1mM MgSO4, pH 6.95), and 4% Formaldehyde.

After fixation, the bottom layer containing PEM-FA was removed slowly with a glass pipette and discarded. An equal volume of methanol was added before the samples were vortexed for 1 minute to remove the vitelline membrane. The top heptane layer was removed along with any embryos that were not devitellinized. The devitellinized

embryos were washed with methanol for 3 times 5 minutes each before PBT buffer exchange and staining (See 2.3).

2.6 Optimization of ER membrane isolation by Opti-prep gradient

S2R+ cells were harvested 24 hours after seeding into 15 ml conical vial and spun down for 2 minutes at 2000xg at 18°C. After the Schneider's medium was removed, the mass of cells in each samples were measured before they were lysed using a homogenizing reagent consisting of 10 mM Tris pH 7.5, 5 mM EDTA, 0.25 M sucrose, and protease inhibitor cocktail and a glass dounce homogenizer with 15-20 strokes. Potassium chloride (KCl) was added to the homogenized cells at a final concentration of 100mM. The solution was then centrifuged at low speed at 3000xg (5400 rpm Beckman) for 10 minutes to remove nuclei and cellular debris at 4°C. The pellets were saved for control (Figure 3-4 and 3-5, P1), the supernatants were isolated (S1) and further centrifuged at a high-speed spin of 10,000xg (48,000 rpm TLA 120.2 rotor) for 1 hour at 4°C. After the second spin, the supernatant was saved for centrifugation control (S2). The pellet was thoroughly resuspended in Golgi buffer (P2) consisting of 10mM Tris pH7.5, 5mM EDTA, 50mM KCl, and 0.25M Sucrose with addition of protease inhibitor. The samples were kept on ice while preparing the Opti-Prep™ gradient. Gradients consisted of four layers with different Opti-Prep™ concentrations: 5%, 10%, 20%, and 30%. Each concentration was made by a mixture

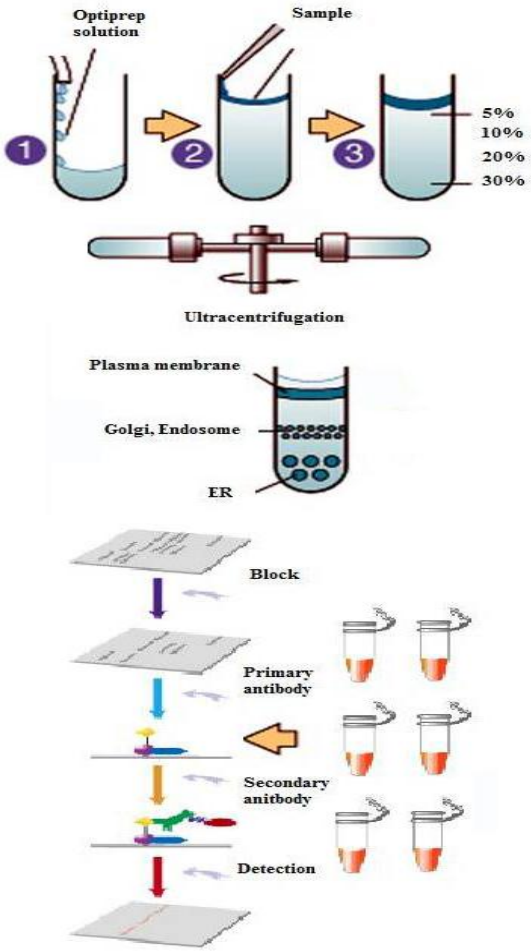

Figure 2-5 Membrane isolation by Opti-prep ™ and detection by Western blotting. Samples are loaded onto Opti-prep gradient and centifugated. Membrane compartments are separated by lipid content. The gradient was fractionated and fractions were run on SDS-PAGE, blotted to membranes and probed for compartmental markers. Modified from Ltaing, 2011

of 60% Opti-Prep™ solution with Golgi buffer and protease inhibitor. The resuspended pellet (P2) was slowly pipetted on top of the gradient and centrifuged at 60,000rpm using NVT65 Beckman rotor for 1 hour at 4°C (Figure 2-5). The gradient was fractionated into microcentrifuge tubes. Each of the samples from the gradient was run

on 10% SDS- PAGE, blotted to membranes and probed with rat anti-BiP antibody, which was detected by chemiluminescence from donkey anti-rat HRP secondary antibody on a chemiluminescent imager (ECL Advance, GE Healthcare). The blot was then stripped with Stripping Reagent (Qiagen™) for 15 minutes and blotted with rabbit anti-Golgi marker130, and visualized with donkey anti-rabbit HRP secondary antibody. To optimize the ER isolation protocol, multiple isolations of ER membrane were done from cell cultures, wing imaginal discs, and whole larva.

2.7 Surface biotinylation and subcellular fractionation of ER membrane in wing imaginal discs

Primary dissection of third *instar* larva was first done on ice in PBS (Section 2.3). Approximately 150 discs were dissected from wild type larva and placed into microcentrifuge tubes in PBS. The discs were carefully washed with cold PBS and incubated with NHS-SS-biotin at 100 mM for one hour on ice. The samples were then placed into 4°C incubation for one hour to allow biotin binding. Post incubation, the samples were moved to room temperature for 45 minutes for biotin uptake. The samples were then quenched and washed to remove residual biotin. After quenching and washing, the samples were homogenized and fractionation of membrane was done according to steps described previously (Section 2.6). Each fraction was run on SDS-PAGE gel and stained for ER membrane. The blot was then stripped and stained for biotin.

Chapter 3

RESULTS

3.1 Subcellular localization of Wls in S2R+ cells

Preliminary data strongly suggested that the site of Wg-Wls engagement was in the ER. Since Wls needs to be recycled to maintain sufficient levels to support continuous Wg secretion, we hypothesize Wls must traffic from the ER with its Wg cargo to the plasma membrane for release and return to the ER for subsequent rounds of Wg secretion. In order to demonstrate this experimentally tagged Wls could be transiently expressed and its movement tracked as it cycles through the secretory pathway over time. If our hypothesis is correct then, the pulse expressed Wls would transit to the plasma membrane and then return to the ER as a function of time.

In order to subcellularly track Wls, two pulsatile expression methods were tested. The first system examined was a metallothionine-Gal4 inducible promoter, which was used to drive a pulse of Wls with an HA tag expressed from *UAS-wls-CHA*. The metallothinonine inducible system was used because it was accessible and easily activated with low concentration of heavy metal. In order to optimize *wls* expression in *Drosophila* S2R+ cells, several issues needed to be addressed; such as concentration of heavy metal substrate, activation period, and its ability turn off *wls* expression in a controlled manner (Section 3.1.1). The second expression system that was tested was to place *wls-CHA* under the control of a heat-shock promoter. For this experiment, pCaSpeR-hs-wls-CHA transfected cells would be shifted to heat-shock conditions for a

short time period to pulse Wls-CHA expression and then Wls-CHA could be subcellularly tracked as a function of time following the pulse (Section 3.13). While both approaches showed some promise for technical reasons described below neither yielded the intended results.

3.1.1 Copper Sulfate inducing the expression of *UAS-GFP*

In order to use metallothionine (MT) induction to control the expression of Wls-CHA in cells, the timing of induced expression for Wls needed to be determined prior to implementing subcellular tracking. Ideally the promoter used to induce *wls* expression must possess rapid on/off kinetics such that *wls* is transiently expressed for a brief time period. To optimize the condition and timing of *wls* expression, S2R$^+$ cells were transfected with Metallothionine (MT)-GAL4, which has a copper sulfate inducible promoter, and UAS-GFP plasmids (MT-GFP). In order to activate the metallothionine promoter, the presence of heavy metal is needed. Therefore, it is also necessary to optimize the concentration of inducing metals, which allows high-level induction while preserving cell viability. The optimal concentration of Copper (II) Sulfate ($CuSO_4$) was experimentally determined to be 1.5 mM (data not shown). At this concentration of heavy metal, it was found that transfected cells efficiently express *GFP* when under the control of MT-GAL4 (Figure 3-1). Time lapse analysis shows that the expression of *GFP* has a lag time of 4-5 hours post introduction of $CuSO_4$ to the cells. This suggests that the activation time of MT is approximately 3-4 hours. Prolonged expression of *GFP* suggests that the removal of $CuSO_4$ by EDTA chelation did not effectively stop GFP expression. In order to track *wls* subcellularly in these S2R$^+$ cells, the expression *wls* needed to be controlled pulse. The reason for the

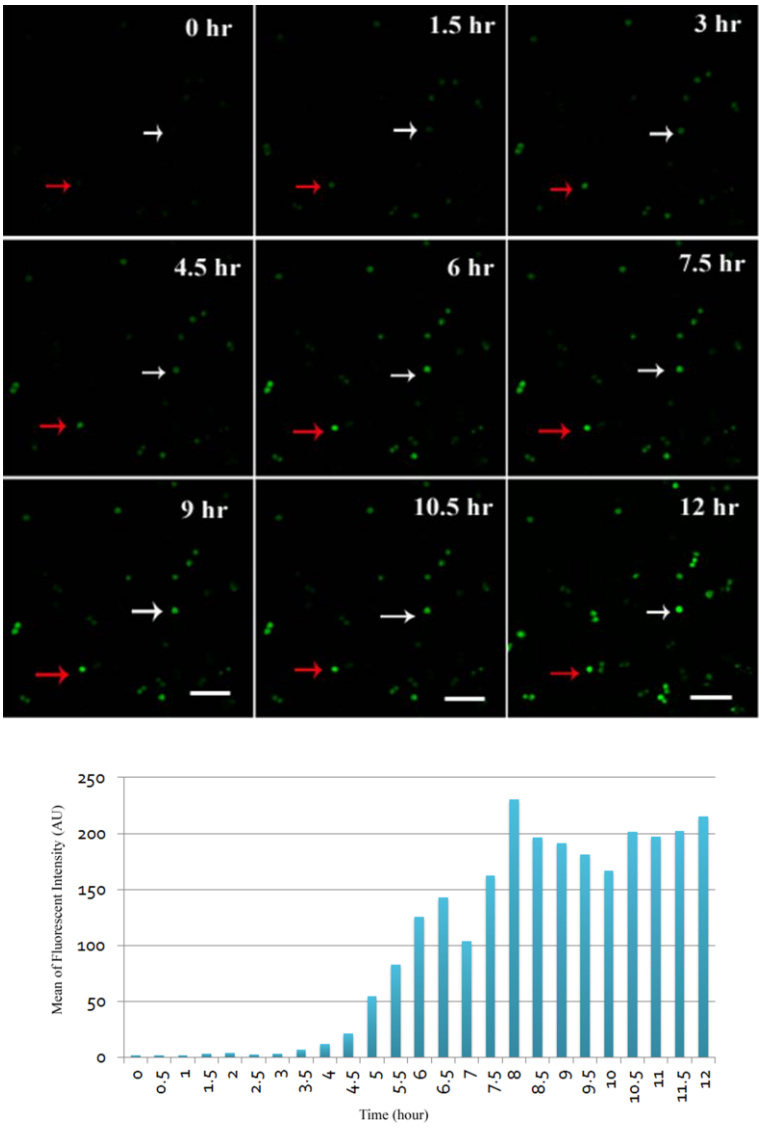

Figure 3-1 Subcellular time lapse of S2R+ suggests MT-Gal4 induce UAS- GFP expression at 4-5 hours post $CuSO_4$ introduction. Upper panels show induction of the same field every 1.5 hours 48 hours post-transfection S2R+ cells were treated with 1.5 mM $CuSO_4$ for 1 hour cells and then washed with PBS containing EDTA to remove residual inducer. Lower panel show the mean florescent intensity of all the cells within this fields taken at 30 min intervals. This time lapse was done using LSM Zeiss 510 time lapse with 20X objective, (Scale bar: 50 μm). S2R+ cells begin expressing GFP (green) 4-5 hours post introduction of CuSO4, and reached a maximum threshold at 7-8 hours.

prolonged expression of GFP could either be due to GFP possessing a long half-life or washing out the $CuSO_4$ did not stop metallothionine promoter activity. If prolonged GFP expression is due to an inability to tightly control the MT promoter, this experimental design would not work.

3.1.2 Optimization targeted MT promoter induction

Interestingly, the expression of GFP was found to persist for over 22 hours when transfected cells were pulsed with 1.5 mM $CuSO_4$ for 1 hour (data not shown). Multiple low concentrations of $CuSO_4$ and chelating reagent were used to show that this phenomenon is not due to the amount of heavy metal present in the cell cultures. Furthermore, shorter time periods were used along with lower concentration of $CuSO_4$; however, shorter incubation time only led to smaller numbers of cells expressing the GFP. This suggested that either metallothionein proteins have a high affinity for $CuSO_4$ and remain highly active once bound to the inducer or GFP could have a long half-life, either would explain the prolonged fluorescence after removal of the inducer (Figure 3-1). If GFP has a prolonged half-life, then the destabilization of GFP should prevent new fluorescence. However, if GFP expression recovers after GFP destabilization this would suggest that the MT promoter remains active long after the inducer is removed. To address this question a photobleaching experiment was performed.

However, after performing fluorescent recovery after photobleaching (FRAP), we demonstrated that GFP expression recovered. Post chelation of $CuSO_4$ and photobleaching, the expression of GFP continued to elevate towards fluorescent thresholds similar to cell that were continuously exposed to $CuSO_4$ (Figure 3-2).

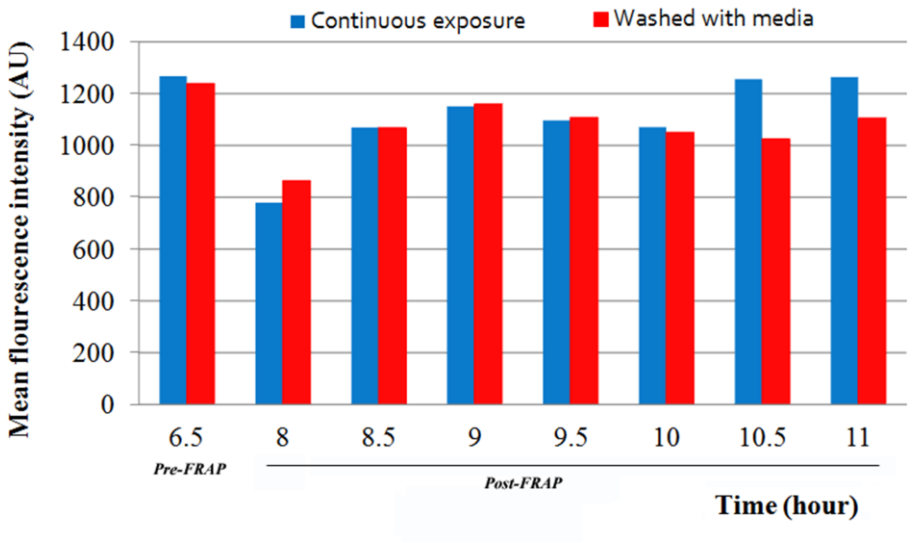

Figure 3-2 **Fluorescent Recovery After Photo-bleaching.** S2R+ cells were incubated for 1 hour in $CuSO_4$ then chelated before partial photobleaching at 6 hours post treatment where expression of GFP reaches threshold. It was observed that the fluorescent intensity elevated back to threshold just half an hour after photo-bleaching.

Therefore, it was concluded that the prolonged GFP expression was due to persistent MT protein activation. To track the trafficking of Wls, the expression of *wls* needs to be tightly controlled. Thus, this approach could not be used, as it did not meet the required parameter to pulse *wls* expression.

3.1.3 Heat shock induction of *wls-CHA* and subcellular localization of S2R$^+$ cells

As an alternative to the metallothionein promoter, the heat shock promoter was used to drive the expression of *wls*-with a carboxyl terminal HA tag. S2R$^+$ cells were transfected with pCaSpeR-hs-wls-CHA. Two days post transfection, S2R$^+$ cells were then

heat shocked at 37° C for 1 hour then incubated at room temperature for 1 hour. Samples were fixed and stained with phalloidin-A643, anti-Wg and anti-HA (Figure 3-3). Phalloidin stains F-actin (Figure 3-3, blue) and was used to demarcate cell

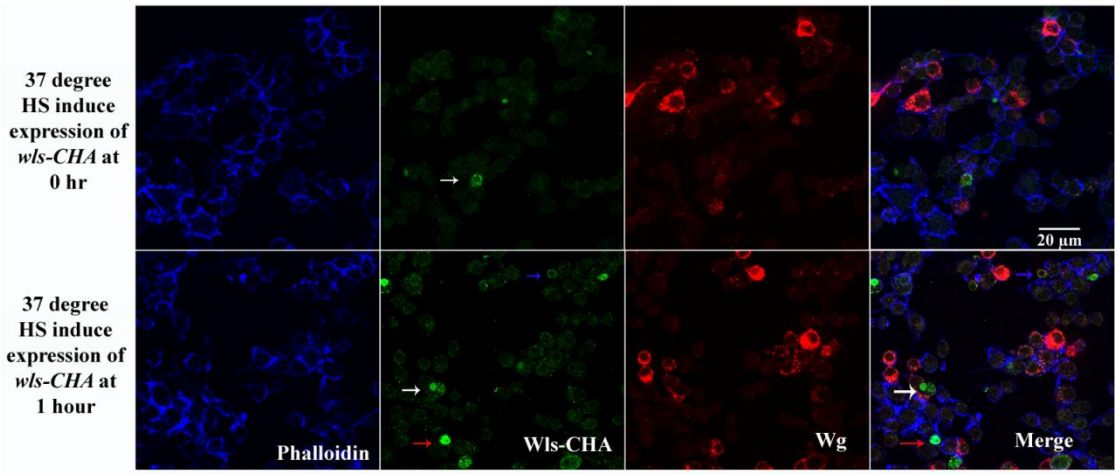

Figure 3-3 Induction of *wls-CHA* ectopic expression by heat shocking at 37°C shows marginal Wls-CHA expression. Shown are S2R+ cells cotransfected with pCaSpeR-hs-wls-CHA and a Wg expression plasmid before (upper panel) and after a 1h heat shock at 37°C. Cells were stained for Phalloidin (blue), Wls-CHA (green) and Wg (red). Image taken by Zeiss LSM 510 with 40x objective at 1x zoom. The partial colocalization of Wg and Wls-CHA at the membrane suggests that our incubation period was too short.

outlines. Wg staining (red) and Wls-CHA (green) showed some colocalization, suggesting an interaction between Wls and Wg. However, due to low transfection efficiency of pCaSpeR-hs-wls-CHA in S2R+ cells, it was difficult to determine if this technique would be effective and was therefore not pursued.

3.2 Subcellular localization of Wls by surface biotinylation and lipid membrane fractionation assay

To further approach our global hypothesis that Wls and Wg engagement occurs in the ER, we implemented a different technique. Plasma membrane biotinylation Wls could be tracked back to the ER following a chase period. Biotinylation assay has been shown to be a valuable technique for examining endocytosed proteins from extracellular matrix into the cell [65]. This technique, some optimization steps in which Cholera toxin was used to determine the optimal uptake and the trafficking time of surface biotinylated proteins to the ER.

3.2.1 Cholera toxin uptake into S2R+ cells for biotinylation assay optimization

To optimize surface biotinylation assay, the time in which a surface protein recycles to the ER was determined. Cholera toxin was used for this purpose, as it is one of few proteins known to traffic from the plasma membrane to the ER and is commercially available with a fluorescent label (Invitrogen™). Cholera toxin (CT) is composed of a pentameric β-subunit and an enzymatic active A-subunit with a KDEL signaling motif [66]. The pentameric β-subunit of the toxin has the ability to co-opt the host ganglioside GM1, a plasma membrane glycolipid, which facilitates transports of toxin from the plasma membrane to the ER [67]. $S2R^{+}$ cells were incubated with CT at room temperature and after thorough washing, cells were fixed and stained (Figure 3-4) for rat anti-BiP (blue) and CT-β-A594 (red). Preliminary experiments demonstrated that CT traverses from the plasma membrane to the ER within 30-45 minutes. Colocalization of Cholera toxin to the ER marker suggested that this surface membrane protein is trafficking to the ER (Figure 3-4). However, due to difficulties in optimizing Cholera toxin concentration and staining issues, it was difficult to

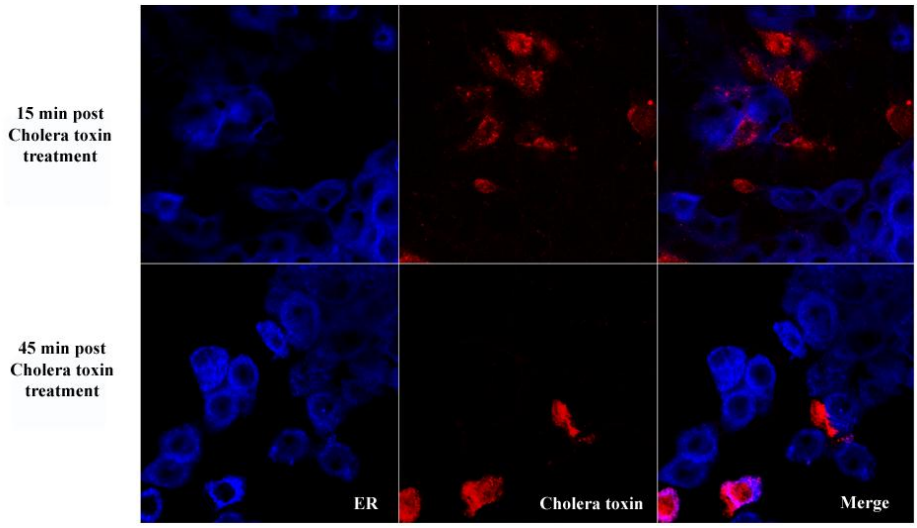

Figure 3-4 Cholera toxin uptake experiment indicates that optimal PM to ER trafficking occurs within 30-45 minutes. S2R+ cells were treated with CTβ-A594 (red). Cells were fixed and stained with anti-BiP, an ER marker (blue) after the indicated incubation times. Colocalization between these markers indicated plasma membrane CT traversed to the ER within 30-45 minutes after CT is introduced. Image taken by Zeiss LSM 510 with 63x objective at 2x zoom.

determine whether Wls trafficking to the ER could be monitored in transfected S2R+ cells.

Due to uptake efficiency of CT in S2R+ cells, it was suggested that *Drosophila* cells may not share a PM to ER trafficing mechanism found in mammalian cells. The Cholera toxin uptake experiment was then repeated in wing imaginal disc tissues to demonstrate that CT uptake mechanim is truly conserved from vertebrate to *Drosophila*. *Hedgehog-Gal4* and *Engrailed-Gal4* were used to drive the ectopic expression of *UAS-wls-CHA* in the posterior compartment of the wing imaginal disc. Wing discs were dissected from the third *instar* larva and CT was introduced (Section

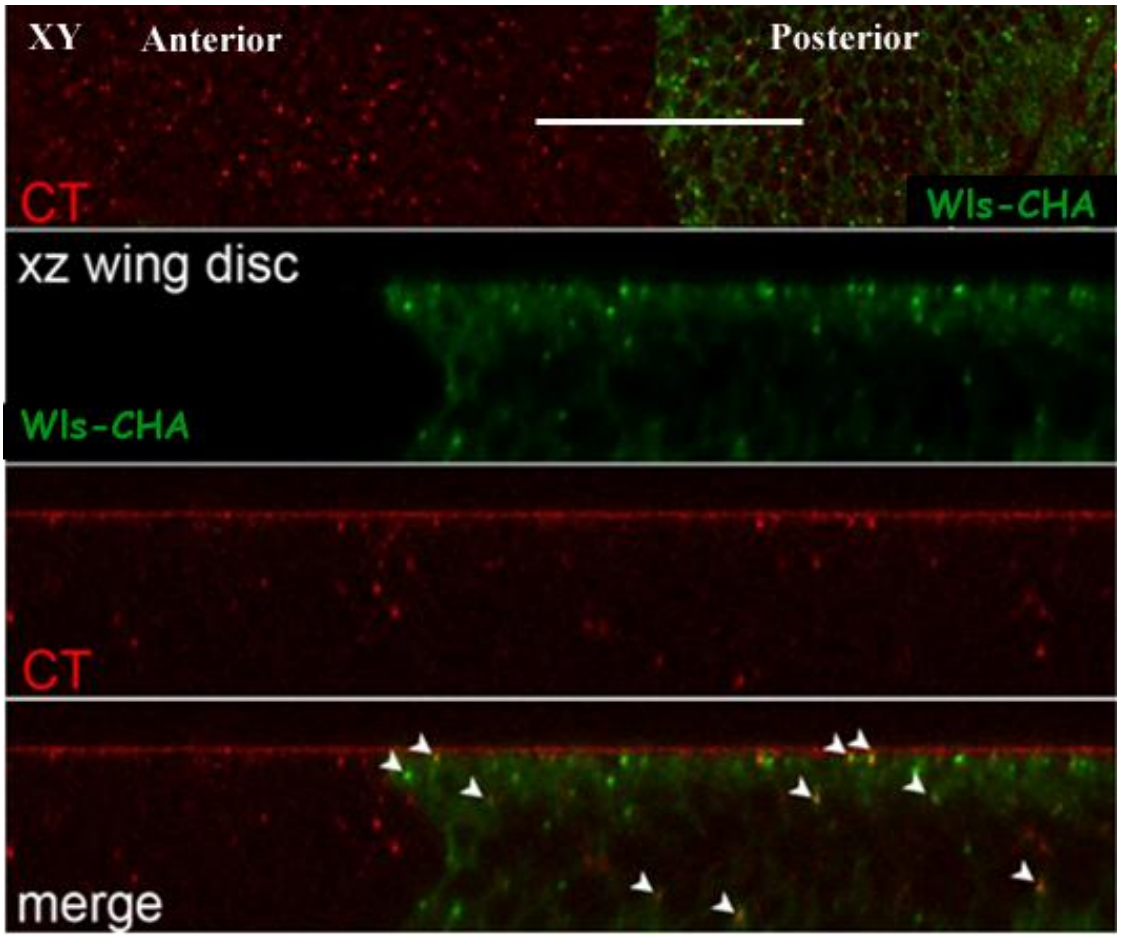

Figure 3-5 **Wls-CHA colocalization with Cholera toxin suggests that both utilize similar recycling mechanism.** The expression of *wls-CHA* was driven by *Hedgehog-* and *Engrailed-Gal4*, which drives expression only in the posterior compartment. Wing discs expressing Wls-CHA were dissected and treated with CT. Above are xz images taken from the dorsoventral boundary which shows CT (red) uptake after 30 minutes incubation and colocalization with Wls-CHA (green). This colocalization suggests that both Wls (green) and CT (red) utilize the same endocytosis mechanism as shown by overlapping intercellular punctate localization (white arrows). Furthermore, no difference in the concentration and distribution of CT uptake in anterior versus posterior compartment where Wls-CHA is expressed suggests that this form of Wls does not inhibit cellular endocytosis. Reproduced from Rich Wittmeyer, unpublished data 2009.

2.4.5) before fixing and staining (Figure 3-5). An xz section was taken in the wing pouch demarcated by white bar (Figure 3-5). Clearly shown, only at the posterior compartment, Wls-CHA is epxressed as demonstrated by HA staining in punctate vesicles (Figure 3-5, green). The distibution of CT (Figure 3-5, red) throughout both anterior and posterior compartments suggest that CT uptake is not hindered by the ectopic expression of Wls-CHA. In the posterior compartment, Wls-CHA punctate vesicles (green) seems to strongly colocalization with CT shown by the white arrows. This suggests that CT and Wls might be utilizing similar endocytic pathway, supporting the notion that Wls could be targeted to ER compartment. However, since we did not stain for any specific compartments, this result (Figure 3-5) only gives a suggestive support that Wls might be recycling to the ER in similar retrograde trafficking pathway as CT. Several attempts were made to figure out exactly what compartment the Wls punctate vesicles were within; however, nothing really conclusive was determined. Staining of early endosome marker such as Rab5 (data not shown) showed marginal colocalization to CT and Wls-CHA. Furthermore, inconsistent ER and Golgi membrane staining proved to further thwart success.

3.2.2 Membrane isolation for Opti-Prep™ gradient separation

Opti-Prep™ gradient (Sigma-Aldrich®), a sucrose-like substance, is a ready-made solution that simulates the viscosity of sucrose. Opti-Prep™ was used to separate intracellular lipid membrane compartments based on their density. Opti-Prep™ is easier to use than sucrose because it has a self-forming gradient. The density of each intracellular compartment is determined by its lipid content. The plasma membrane is composed largely of sphingolipids and sterols that make them the least

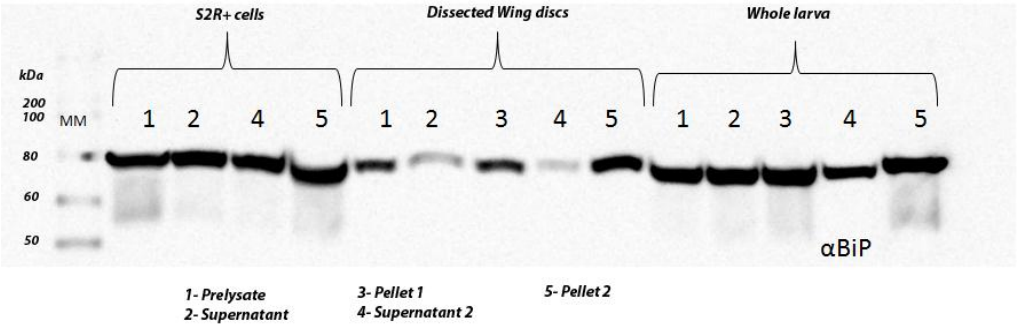

Figure 3-6 Western Blot comparison of membranes isolated from different sources. Shown in lane 1 are total homogenates from S2R+ cells, wing imaginal discs and whole larva. Lanes 2 and 4 are the soluble supernatant and lanes 3 and 5 are membrane pellets following two consecutive rounds of centrifugation. Much of the BiP is found in the soluble fraction for S2R+ cells and whole larvae samples, indicating there is a problem with the integrity of these membranes.

dense membrane while the ER is the most dense lipid membrane because it is the site where most of the structural phospholipids and cholesterol synthesis. Rough ER is especially dense due to the associated ribosomal proteins.

Before performing the Opti-Prep™ separation, membrane isolation was optimized. It was important to determine the quality and quantity of ER membrane isolated from different tissues. The amount of membrane present is correlated to the amount of resident protein present. BiP is an ER resident protein. Therefore, the amount of BiP indicates the amount of ER membrane present in total membrane preparations. Figure 3-6 shows a Western blot for isolated total membrane fractions comparing S2R+ cells, wing imaginal discs, and whole larva.

Drosophila cells are significantly smaller than those in vertebrates, thus membrane isolation was difficult. Our data suggested that dissected wing imaginal discs were best for ER membrane isolation (Figure 3-6). However, ER membrane isolation, from wing imaginal discs is extremely difficult and time consuming, as it requires dissection of individual wing discs.

3.2.3 Optimization of surface biotinylated wing imaginal discs and ER membrane isolation by Opti-Prep™ gradient

The optimal time period post biotinylation for membrane isolation were determined based upon Cholera toxin (CT) uptake in S2R$^+$ cells experiments (Figure 3-4) and results from CT uptake in wing imaginal discs, which showed a relatively similar PM to ER trafficking period (Figure 3-5). Membrane isolation from wing discs showed cleaner isolation of membranes in this tissue. Therefore, most Opti-Prep™ membrane separation experiments were performed using wing imaginal discs (Figure 3-5). Following activation and cross-linking surface biotin at 4°C for 30 minutes, biotinylated wing imaginal discs were washed and quenched. This deactivates residual uncross-linked biotin present so surface proteins are not continually biotinylated, and prevents biotinylation of internal membrane protein post homogenization. Wing imaginal discs were then incubated at room temperature for one hour to allow intracellular trafficking of surface biotinylated proteins. Several wing discs were removed for immune-fluorescent experiments where they were incubated with rat anti-BiP antibody for ER membrane staining and mouse anti-biotin antibody. Confocal analysis indicates that a high concentration of biotin still persists at the apical and basal membranes of the disc (Figure 3-7).

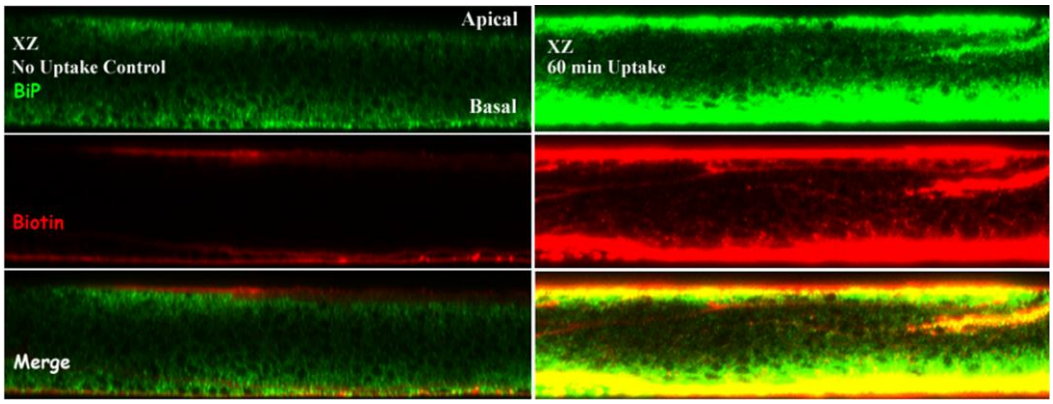

Figure 3-7 Biotinylation assay of wing imaginal discs demonstrates uptake of biotinylated membrane proteins after 1 hour incubation period. Wild type third instar larva were dissected for wing imaginal discs. The tissues were then incubated with biotin and allowed proper activation and uptake period. Shown above are xz images taken at the dorso-ventral boundary where Wg is produced. No uptake control (left) shows marginal biotin (red) uptake at the apical or basal surface of the wing disc. After 60 minutes incubation (right) xz image shows biotin uptake throughout the wing disc. However, due to the intensity of biotin staining at the apical and basal surface, colocalization of biotin and ER marker BiP (green) weren't able to be determined.

Most of the dissected wing imaginal discs post biotinylation were subjected to Opti-Prep™ gradient (see protocol in Section 2.7). Opti-Prep™ gradient separation of the biotinylated wing imaginal discs showed that the biotin was predominately found in the ER fraction and unexpectedly showed marginal biotin at the plasma membrane. (Figure 3-8). It was originally expected that biotinylated proteins would be present throughout the intramembrane compartments. These results suggest that either the quenching

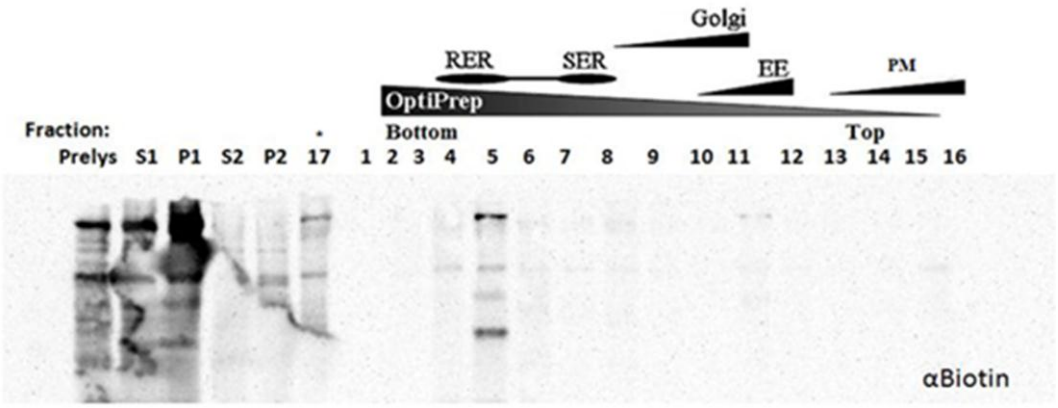

Figure 3-8 Intracellular membrane separation by Opti-Prep™. Wing imaginal discs were isolated by dissection, homogenized (pre-lysis) and subject to centrifugation. Lanes S1 and S2 are the soluble supernatants and lanes P1 and P2 are membrane pellets following two consecutive rounds of centrifugation. Lanes 1-16 are Opti-Prep™ fractions from the bottom and top of the gradient as indicated. Shown above are the intracellular compartments expected in the different fractions. RER is rough endoplasmic reticulum (ER); SER is smooth ER; RE is recycling endosome; EE is early endosome, PM is plasma membrane. Samples were separated by SDS-PAGE and blotted to nitrocellulose membranes, which were probed with anti-biotin antibody.

methods needed to be further optimized, or there was a collapse in the Opti-Prep™ gradient during the high speed spin. Both would require significant optimization prior to continuing this experimental approach. Due to the fact that this optimization could be quite time consuming, this approach was abandoned in favor of other approaches that were shown to be more fruitful and efficient.

3.3 ER localized *wls*-NHA indicates it acts as dominant negative

Previous preliminary data from the direct approaches to determine the recycling behavior of Wls encountered with numerous technical problems. Therefore, alternative

methods were explored. Two forms of Hemagglutinin (HA) tagged Wls proteins were developed in the Selva lab; a carboxyl-terminal HA tagged (Wls-CHA) and an amino-terminal HA tagged Wls (Wls-NHA) (Figure 3-9). Ectopic expression of both Wls-CHA and Wls-NHA in wing imaginal discs showed they behave quite differently from one another. Wls-CHA, much like the endogenous wild type Wls, showed normal intracellular trafficking as demonstrated by the punctate vesicles

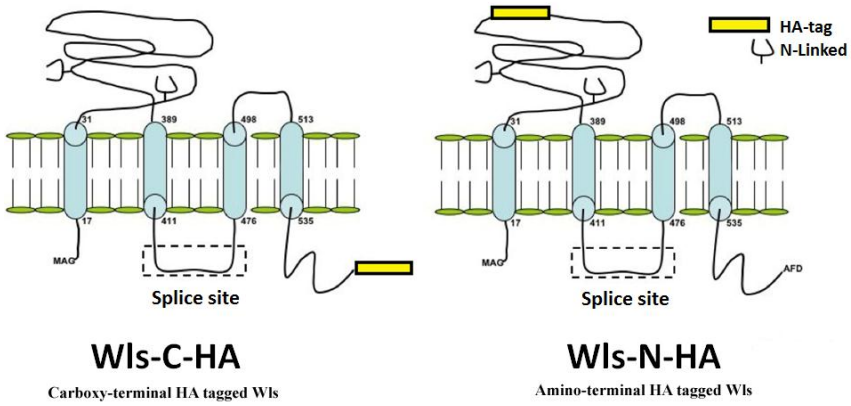

Figure 3-9 **Two forms of Wntless proteins with HA epitope tags.** The Selva lab developed two forms of Wls proteins with HA tags. Above is the cartoon illustration of the two forms of Wls constructs where on the left is the carboxyl terminal HA tagged Wls, and on the right is the amino-terminal HA tag.

throughout the peripodial cells, or the squamous epithelial cells at apical surface of the wing imaginal disc (Figure 3-10, top panel). Colocalization analysis of Wls-CHA to ER membrane showed low percentage of colocalization with 39% overlap between the two. Whereas Wls-CHA is distributed throughout the endomembrane

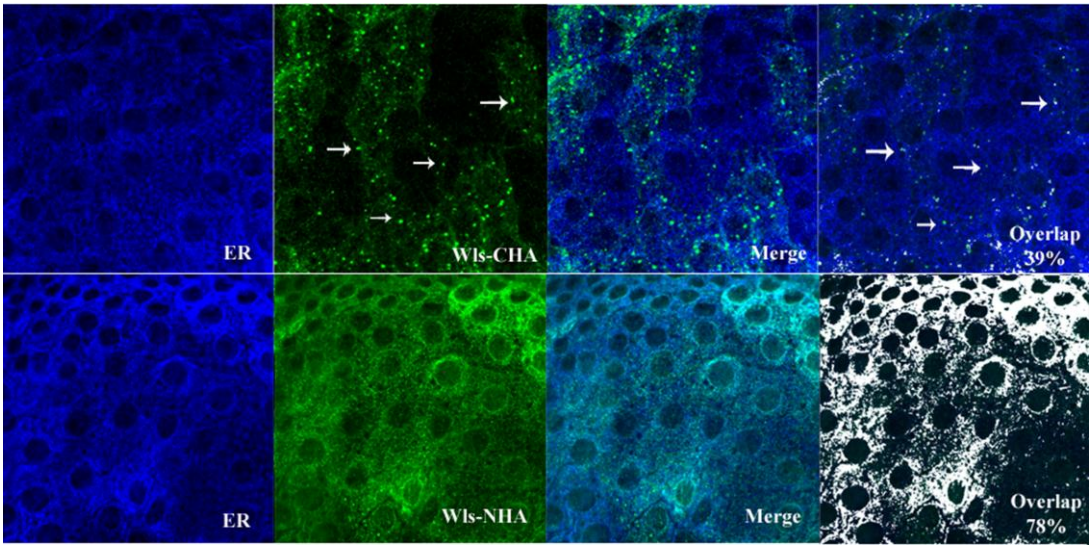

Figure 3-10 ER localization of Wls-CHA and -NHA in the posterior wing disc peripodial cells. Wls-NHA was expressed in the posterior compartment of the wing disc using *en-Gal4* and *hh-Gal4*. Discs were stained with an ER compartment marker (anti-BiP, blue) and anti-HA to detect Wls-NHA (green). Confocal images were taken with an LSM Zeiss 780 focusing on the peripodial squamous epithelium expressing Wls-NHA because of their spread out morphology, which allows for easier colocalization comparison. Much like the wild-type, staining of Wls-CHA demonstrated by the punctate vesicles (white arrow) to be evenly distributed and has only 39% colocalization with the ER membrane. Whereas colocalization of ER compartment marker and Wls-NHA showed over 78% colocalization, indicating that unlike the wild-type Wls and Wls-CHA, Wls-NHA is predominantly localizes to the ER.

compartment, Wls-NHA is almost entirely confined to the ER membrane (Figure 3-10, bottom panel). Wls-NHA staining in the peripodial cells suggests Wls-NHA accumulates within the ER membrane. Additionally, colocalization analysis showed Wls-NHA colocalized with an ER marker protein at 78% overlap (Figure 3-10, bottom

panel). The colocalization assays of Wls-CHA and Wls-NHA to the ER membrane was done in the peripodial cells of the wing imaginal discs because of their spread morphology at the apical surface, which allowed us to perform the colocalization analysis.

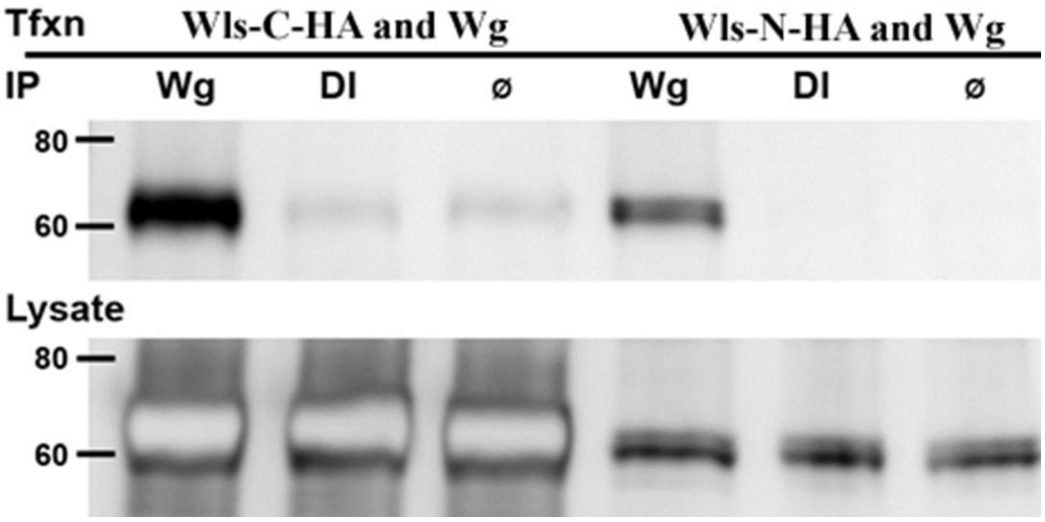

Figure 3-11 Co-immunoprecipitation shows Wls-NHA efficiently binds to Wg. Like Wls-Carboxyl terminal HA tag (top left), which acts similarly to the wild type of Wls, Wls-NHA co-immunoprecipitates with Wg (top panel right) as compared to non-specific antibody Delta (Dl) and the no antibody control. Cell lysates (bottom) shows the presence of Wls in all samples. Reproduced from Harmen, 2008

Interestingly however, both Wls-CHA as well as Wls-NHA, were shown to have high affinity to Wg protein. Due to its confined localization to the ER, it was believed that Wls-NHA would not bind to Wg protein; however, as shown by the co-

immunoprecipitation with Wg protein this is not the case (Figure 3-11). Wls-CHA, much like the wild type Wls, showed strong affinity for Wg protein as demonstrated by the co-immunoprecipitation. Assay where we pulled down for Wls-CHA was pulled down when anti-Wg was used for immunoprecipitation. Wls-CHA can effectively binding to Wg protein as compared to non- specific antibody Delta (Dl) and no antibody controls (Ø) where Wls-CHA showed little weak or no affinity. Surprisingly, Wls-NHA was also demonstrated to have a similar binding affinity for Wg protein. These results suggested that if Wls-NHA is localized to only the ER and effectively binds Wg, then the ectopic expression of Wls-NHA within Wg producing cells would be predicted to act as a dominant negative and cause accumulation of Wg if Wls engages Wg in the ER.

To test this hypothesis, Wls-NHA was expressed in the posterior compartment of the developing wing disc. Wls-NHA would be expected to bind Wg and prevent its intracellular transport. If the predictions were correct, then expression of *UAS-wls-NHA* in the posterior compartment of the wing disc would be expected to block Wg secretion and its downstream signaling. To test this prediction, *wls-NHA* was expressed in developing wing discs using the Gal4-UAS technique specific to the posterior compartment (Figure 2-1).

Adult flies that harbor promoter specific Gal4 drivers were crossed to adults with *UAS-wls-NHA*. The presence of both Gal4 and UAS drives the expression of the gene of interest. When *wls- NHA* was expressed using the double Gal4 driver line *en-Gal4* and *hh-Gal4*, as predicted, caused Wg accumulation (Figure 3-12, in red) in the posterior compartment when compared to the adjacent anterior cells expressing endogenous levels of wild type *wls*. Analysis of adult *Drosophila* wings obtained from the same cross showed a wing nick phenotype, which is indicative of a loss of Wg signaling specific to

the posterior compartment (Figure 3-12). This phenotype was shown to be completely penetrant at 29°C (n= 41). In addition to Wg retention and wing nicks phenotypes, the expression of *wls-NHA* not only hinders Wg secretion, but

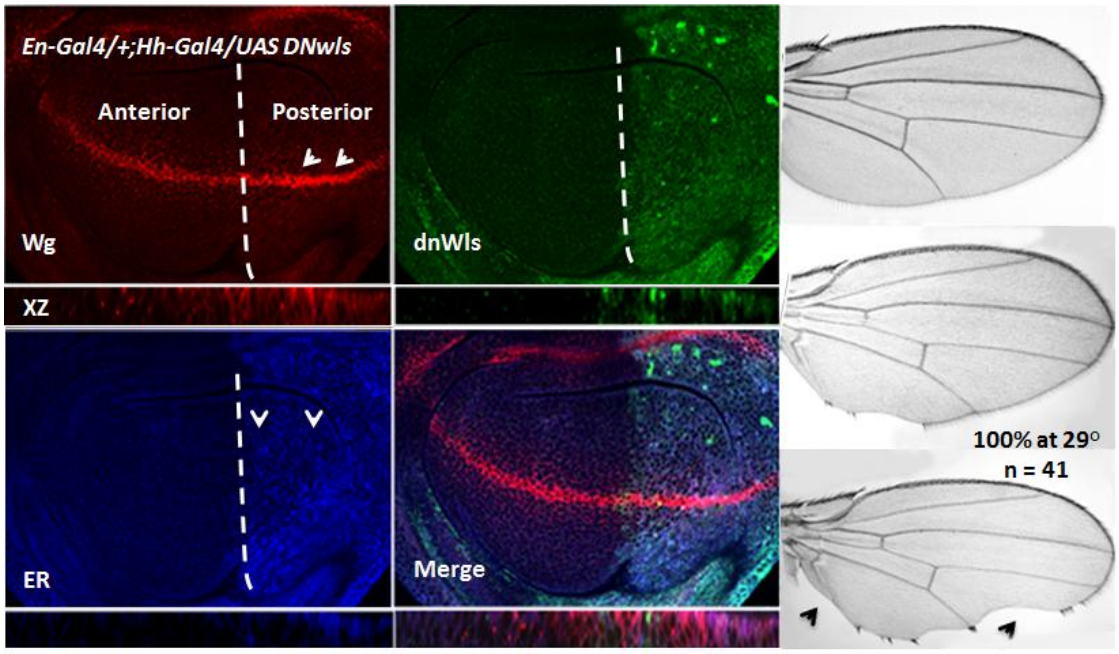

Figure 3-12 Expression of *wls-NHA* in the posterior compartment of the wing imaginal discs shows Wg retention only at the posterior compartment. Wing nick phenotype in adult flies further indicates loss of Wg signaling. The expression of *wls-NHA* in the posterior compartment causes dramatic retention of Wg ligand (red) with the accumulation seen clearly in the xz image beneath. Furthermore, increased BiP staining indicated ER stress. These phenotypes were observed to be 100% penetrant at 29 degrees.

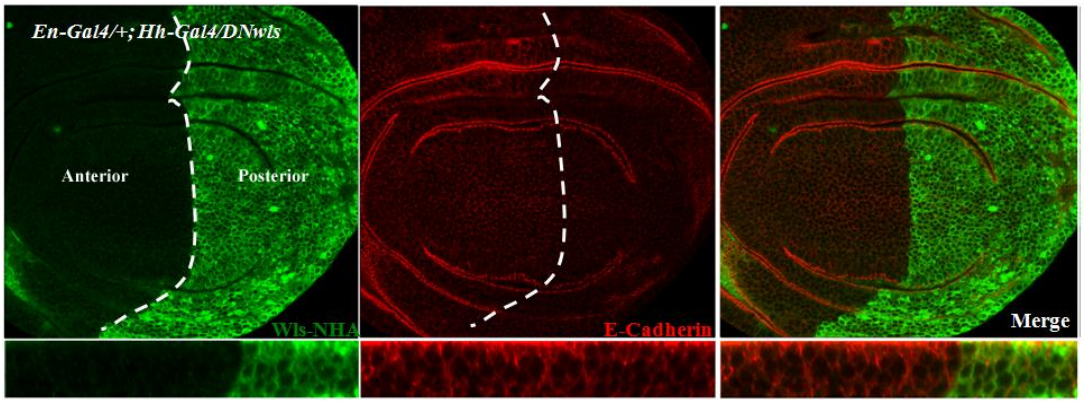

Figure 3-13 E-Cadherin distribution and concentration is not changed when *wls-NHA* is expressed in the posterior compartment compared to the adjacent anterior compartment that expresses the wild type form of Wls. The expression of *wls-NHA* has been shown to elicit BiP (ER marker) accumulation in the posterior compartment (fig. 3-9, blue), which is an indication of ER stress response. E-Cadherin, a plasma membrane transmembrane protein, staining (red) suggests that the expression of *wls-NHA* does not hinder other secretory proteins. Thus, this ER stress response is specifically due to ectopic expression of *wls-NHA*.

the expression of Wls-NHA also caused a corresponding increase in BiP concentration, an indication of an ER stress response (Figure 3-12, blue). This provides further evidence that Wls-NHA is confined to the ER, and that the site where Wls and Wg initially interact is in the ER.

Increased BiP in the posterior compartment, where the *wls-NHA* was expressed, further suggests that Wls-NHA accumulates within the ER membrane causing the ER stress. To confirm Wls-NHA specifically caused Wg accumulation and the ER stress response did not result in the non-specific retention proteins that pass through the secretory pathway we examined another ER-targeted protein. E-Cadherin is a well-known transmembrane protein and targeted for anterograde trafficking to the plasma

membrane. E-Cadherin staining in the anterior and posterior compartment of the wing disc where Wls-NHA was expressed showed no difference in levels or apparent change in localization (Figure 3-13). This suggests that Wls-NHA expression in the posterior compartment and ER protein accumulation does not hinder bulk anterograde trafficking of other protein that pass through the secretory pathway (Figure 3-13). Notably, further analysis is needed to confirm that Wls-NHA does not hinder secretion of other *Drosophila* Wnts that would then cause the observed ER stress. Together, these data suggests that Wls-NHA accumulates in the ER resulted in the high colocalization of Wls-NHA staining with ER marker and acts as a dominant negative in Wg producing cells, causing Wg retention. In addition to what is known about the function of Wls in Wg anterograde transport, this provides further evidence to support the hypothesis that the site of Wg and Wls initial engagement is at the ER and not the Golgi.

wg expression at the dorsoventral border of the wing disc provides both short-range and long-range signaling activity in the wing pouch. Short-range Wg signaling results in specification of the cell that gives rise to the wing margin. The wing margin is amassed by the development of distinct bristles and the sensory organ which are specified in response to Wg signal transduction [68, 69]. Therefore, if Wg secretion is blocked, the response in the receiving cells should also be disrupted. Thus, wing nicks present in the progeny are indicative of an inability to signal brought about by Wg retention (Figure 3-12). Indicated by the dark arrows are locations within the posterior compartment where the loss of Wg signaling caused the wing margins to improperly develop.

In the dorsal compartment of *Drosophila* wing imaginal discs, Wg signaling is required for regulating the expression of sensory precursor organs that ultimately gives rise to adult thorax bristle [69]. Among other tasks, Wg in the dorsal compartment is

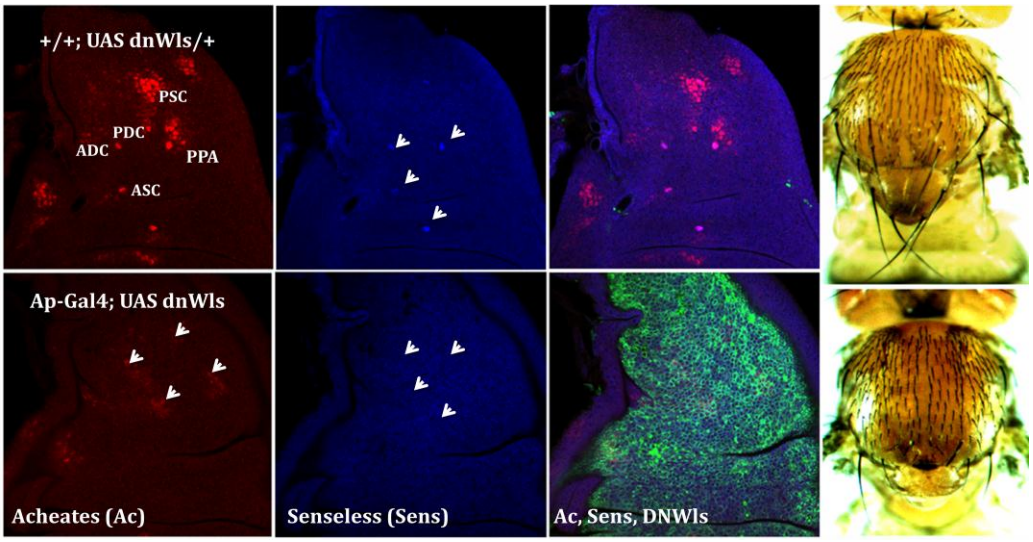

Figure 3-14 Expression Wls-NHA in the dorsal compartment of the wing imaginal discs blocks Wg signaling. Wild type wing discs expressing endogenous Wls (top panel), shows normal activation of downstream Wg targets in the dorsal compartment. Both Ac (red) and Sen (blue) are expressed in SOPs. However, expression of Wls-NHA (green, bottom panel) in the dorsal compartment using *ap-Gal4* blocks Wg signaling, as SOP markers Ac and Sen are not expressed (red and blue, bottom panel). There is also a corresponding loss dorsal thoracic bristles in *ap-Gal4; UA- wls-NHA* adults (lower right) as compared the full complement thorax bristles in adults when Wls-NHA was not expressed (upper right).

responsible for sensory organ development. *Achaete-scute* (*ac*) is a direct target of Wg signaling in this tissue. In the wing imaginal disc, *ac* is expressed in multiple clusters of

proneural cells, arranged along the proximal-distal axis. The dorsal clusters of Achaete (Ac) become the long, widely spaced chemosensory thoracic bristles while ventral clusters become mechanosensory bristles [70]. Along the proximal-distal axis of the wing disc, Wg also regulates the expression of *senseless* (*sen*) in the dorsal compartment of the wing disc. Sen plays two roles in sensory organ development; first, *sen* functions as a proneural gene in mechanosensory bristle formation and specifies sensory organ precursors (SOPs) independent of Achaete and Scute proteins, and second, Sen functions downstream of Ac and Scute in chemosensory bristle development where it specifies SOP within the group of As-c proneural cells [71]. The presence of Ac and Sen suggests normal Wg signaling. To further examine the dominant negative nature of Wls-NHA, the Gal4-UAS technique was again used to express w*ls-NHA* in the dorsal compartment using *apterous-Gal4* (*ap-Gal4*). In the absence of the dominant negative-w*ls* expression, sensory organ precursor cells are detected by Ac and Sen staining (Figure 3-14 top panel, red and blue), and all the thorax bristles are present (Figure 3-14, top right). However, when *wls-NHA* was expressed, these sensory precursor cells were lost, as shown by the absence of Ac and Sen staining (Figure 3-14, bottom panel, red and blue). There is a corresponding loss of thorax bristles in *ap-wls-NHA* adults. This phenotype was completely penetrant at 29°C (n=59). These results suggest that Wls-NHA expression in the dorsal wing disc dominantly blocked Wg signaling presumably by preventing normal Wg secretion.

These results show expression of Wls-NHA in the wing disc dominantly blocks Wg secretion and downstream signal transduction. Given Wls-NHA shows strong colocalization to the ER compartment (Figure 3-10), and high affinity for Wg (Figure 3-11), these results indicate expressed Wls-NHA binds Wg in the ER and prevents its

proper secretion. These results suggest a model in which Wls engages Wg in the ER and escorts Wg to the surface for release and downstream signaling.

Preliminary studies of homozygous *wls* mutant wing tissues showed that Wg is more closely localized to the ER than the Golgi and is hyperglycosylated, lending additional support to this model. Requirement of the retromer, a multi-protein complex that mediates recycling of proteins from the endosomal compartment to the Golgi, for Wg secretion lead to the hypothesis that Wls must be recycled from the plasma membrane to the Golgi in Wg producing cells in order to maintain sufficient levels of Wls to support subsequent rounds of Wg secretion. If Wls-Wg engagement occurs in the ER, as these results have suggested, it is logical that Wls must be recycled back from the plasma membrane to the ER where it can bind Wg and participate in further rounds of Wg transport.

3.4 Retrograde transport from Golgi to ER is vital for Wg secretion

The final aim of this project was to determine if Wls is recycled back to the ER and if so, to determine if that recycling is important in maintaining proper Wg secretion. To achieve this goal, retrograde transport components were knocked-down using a tissue specific RNA interference (RNAi) technique. RNAi is a method used to reduce or prevent the expression of a target gene by the presence of double stranded RNA with sequence identity to the target. The double-stranded (ds) RNAs cause either degradation of the mRNA target or block its translation through a cellular process that is conserved in all eukaryotes from yeast to vertebrates. RNAi has been shown to be a powerful gene silencing technique in *Drosophila* [72].

As mentioned in the introduction, two known component of the retrograde transport from Golgi to ER are β-COP and Yip1A (Sec. 1.9). RNAi fly stocks that harbor dsRNAs to β-COP and Yip1A that are expressed under the control of a UAS promoter were obtained from the Vienna Stock Center. In the wing disc, Wg protein is produced at the dorsoventral boundary and forms a ligand gradient towards the dorsal and ventral axis. Multiple Gal4 promoter specific driver lines that expressed in the different patterns in the wing disc were crossed to *UAS-β-COP* RNAi and *UAS-Yip1A* RNAi. Most produced a lethal phenotype, but among the thirty-four Gal4 driver lines tested, two were selected for subsequent experiments. These drivers had restricted expression patterns that included the dorsoventral Wg expressing cells and yielded a similar Wg retention phenotype observed in retromer loss-of-function and mutant *wls* wing discs. C96-Gal4 and Wg-Gal4 expression patterns are shown by GFP (Figure 3-15 and 3-16, respectively).

For the purpose of these experiments, *UAS-GFP* chromosomes were incorporated into the *Wg-Gal4* and *C96-Gal4* backgrounds. Hence, GFP expression corresponds to the expression of the UAS-RNAi constructs, in all experimental progeny. Wg producing cells expressing *Yip1A* dsRNAs under the control of either *C96* or *Wg- Gal4* showed Wg accumulation as compared to wild type (Figure 3-15 and 3-16, red). Loss of Wg signaling is also detected in the adult progeny by the absence of bristles at the wing margin. Loss of Wg signaling and the absence of wing margin bristles were shown to be 100% penetrant in all progeny. Additionally, the absence of bristles in the progeny was consistently more dramatic when *Yip1A* dsRNAs were expressed using the *C96-Gal4* driver (compare Figure 3-15, *C96-Gal4* to Figure 3-16, *Wg-Gal4* wings). Yip1A knockdown through RNAi phenocopied

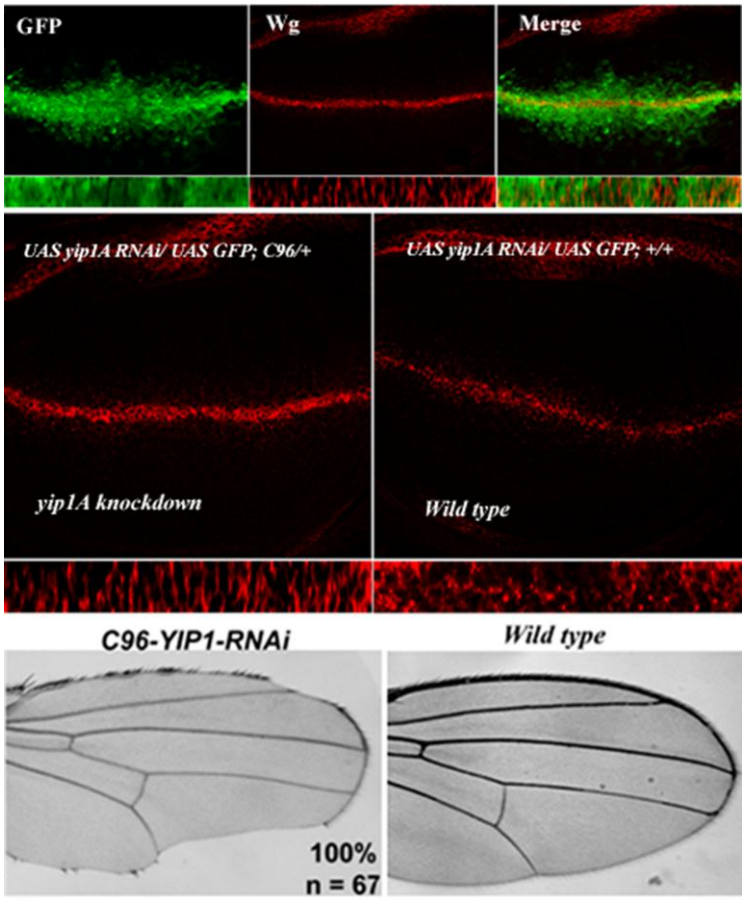

Figure 3-15 Expression of Yip1A RNAi under the control of C96-Gal4 results in Wg retention in Wg producing cells. C96-Gal4 expresses *UAS-Yip1A* RNAi in Wg producing cells, as well as surrounding cells that straddle the dorsal-ventral boundary. Retention of Wg was observed in cells that are expressing both Gal4 and *Yip1A RNAi*. Absence of wing margin in these progeny is also indicative of loss of Wg signaling.

retromer loss-of-function generated by the same method [52]. These results suggest that the retrograde transport from Golgi to the ER is essential for Wg secretion.

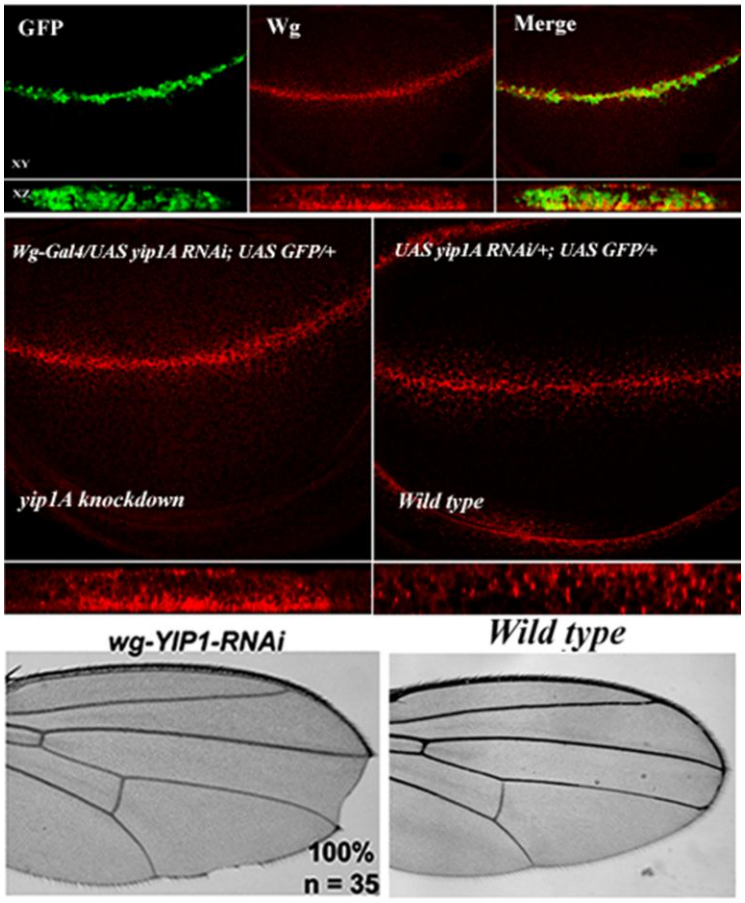

Figure 3-16 Yip1A Knockdown under Wg-Gal4 driver results in similar Wg retention in Wg producing cells but milder wing nick phenotype. *wg-Gal4* drives the expression of *UAS-Yip1A* RNAi only in cells that produces Wg ligand indicated by GFP expression (Top panel, green). The expression of *Yip1A RNAi* by *wg-Gal4* causes similar Wg retention (red) compared to wild type wing discs. Unlike, C96-Gal4 driver was used (Fig. 3-15), however, *wg- Yip1A RNAi* shows milder wing nick phenotypes (bottom left).

Expression of *UAS-β-COP* RNAi in Wg producing cells showed an even more dramatic Wg secretion defect phenotype. Ectopic expression of *β-COP* RNAi with the

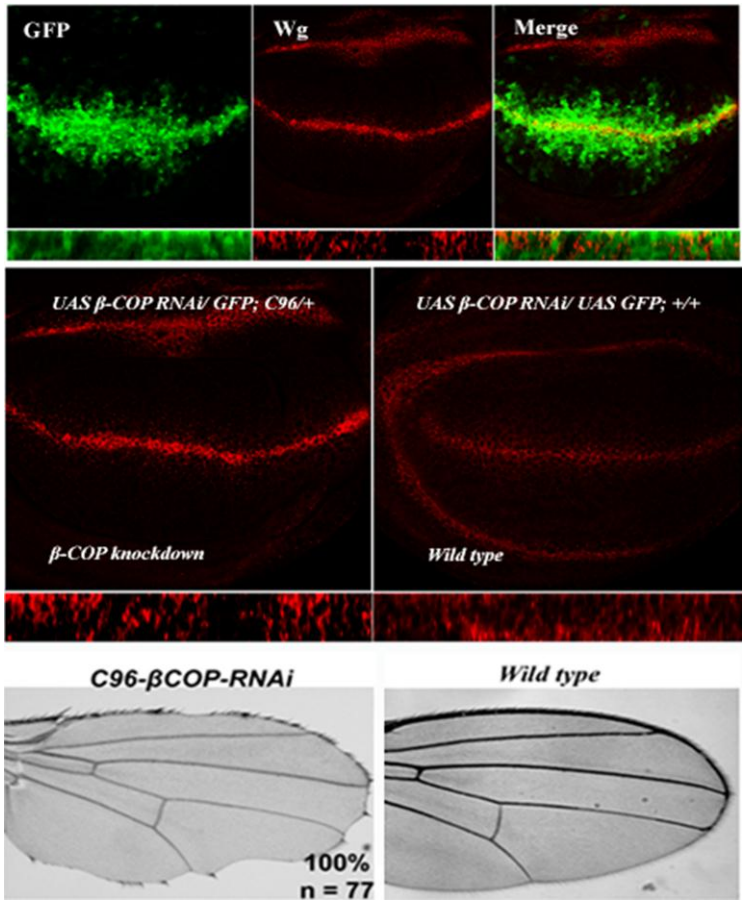

Figure 3-17 β-COP knockdown with Wg-Gal4 and C96-Gal4 driver causes more severe Wg retention phenotypes. Expression of *β-COP RNAi* with Wg-Gal4 driver caused lethality at late embryonic to early larvae stage. *β-COP* knockdown by *C96-Gal4* showed Wg retention (top panel, red), and severe loss of wing margin bristles (bottom right) consistent with Yip1A knockdown. The phenotype observed was fully penetrant in wing imaginal discs and adult wings in *C96-β-COP RNAi* progeny.

.

C96-Gal4 driver caused severe Wg retention and substantial loss of wing margin in adults (Figure 3-17). Furthermore, *Wg-Gal4* driven expression of *UAS-β-COP RNAi*

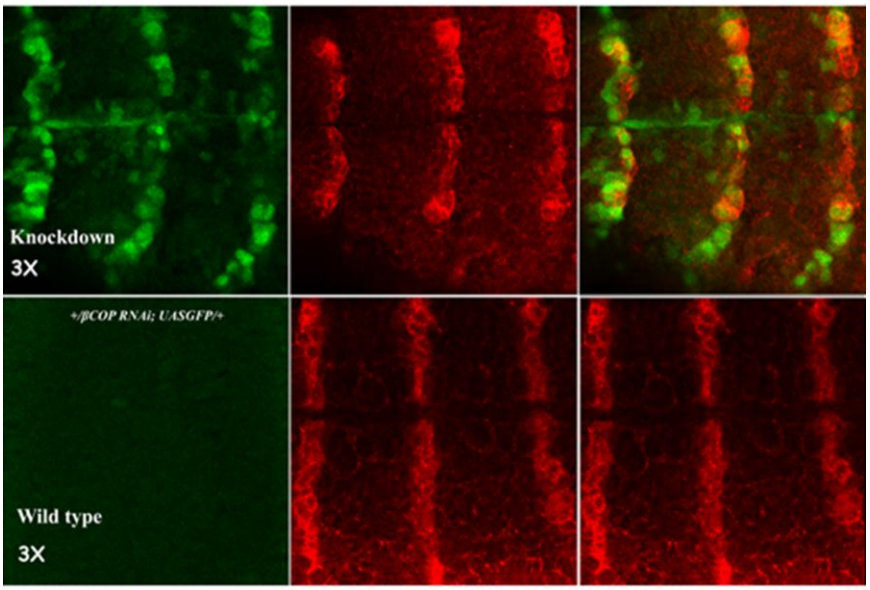

Figure 3-18 Expression of *βCOP* RNAi using Wg-Gal4 shows only marginal Wg accumulation in embryos at stage 9. The expression of *β-COP* RNAi with Wg-Gal4 causes lethality prior to third *instar*. Wg staining of early embryos at stage 9-10 suggests β-COP knockdown does not cause lethality until after germ band extension at stage 9-10. Top panel shows some Wg retention in cells that produce Wg (red), which correspond to the presence of GFP (green). To clearly see this accumulation, images were 3x zoomed to see three central lateral bands expressing the *β-COP* RNAi. Control embryos that did not express *β-COP* RNAi, identified by the absence of GFP, from similar stages (bottom panel, at 3X zoom) show normal Wg secretion compared the top panel images. This suggests that *wg-Gal4* driving the expression of *β-COP* RNAi causes lethality during late embryonic stages or early *instar* stages where retrograde transport might be more

leads to lethality in late embryonic and early larval stages. Embryos from the *wg-Gal4* crossed to *UAS-β-COP RNAi; UAS-GFP* were collected and stained for Wg (Figure 3-18). Staining of these embryos showed marginal retention of Wg in cells expressing *β- COP*

RNAi when compared the WT embryos of the same stage (Figure 3-18). However, inspection of the pupa and adults suggested that progeny expressing *β-COP* RNAi died prior to the third larva stage. We believe that this is due to the fact that Wg, and thus *wg-Gal4*, expresses throughout all stages of development. RNAi knockdown of *β-COP*, a vital component of the COPI coatomer vesicles, may cause Wg proteins to accumulate within Wg producing cells during late embryonic development which leads to the lethality. Taken together, the Yip1A and β-COP knockdown results suggest a model where the Wls concentration is maintained in Wg producing cells via COPI dependent and independent Golgi to ER transport.

3.5 Over-expression of *wls* overcomes retrograde transport requirement and rescues Wg retention

It has been established that the over-expression of *wls* can rescue the Wg retention phenotype in the absence of retromer function. This demonstrates that the role of the retromer is to maintain a high level of Wls inside Wg producing cells [52]. Previous experiments have shown Golgi to ER retrograde transport is crucial to support Wg secretion (Figures 3-15, -16 and -17). We hypothesize that the role of Golgi to ER retrograde transport in Wg secretion is to maintain proper ER levels of Wls needed for Wg ER export. Similar to prior experiments which showed retromer loss of function phenotypes can be rescued by over-expressing *wls,* if our hypothesis is correct the over-expression of *wls* in the retrograde knockdown backgrounds would be expected to rescue the Wg secretion defect (Figure 3-19). *wls* and *β*-COP or *Yip1A RNAi* were co-expressed using *Wg-Gal4* or *C96-Gal4* drivers. Wg secretion appeared to be normal as shown by a high amount of punctuated vesicles outside Wg-producing cells and no accumulation of Wg (Figure 3-20, 3-21 and 3-22). Although the rescue of

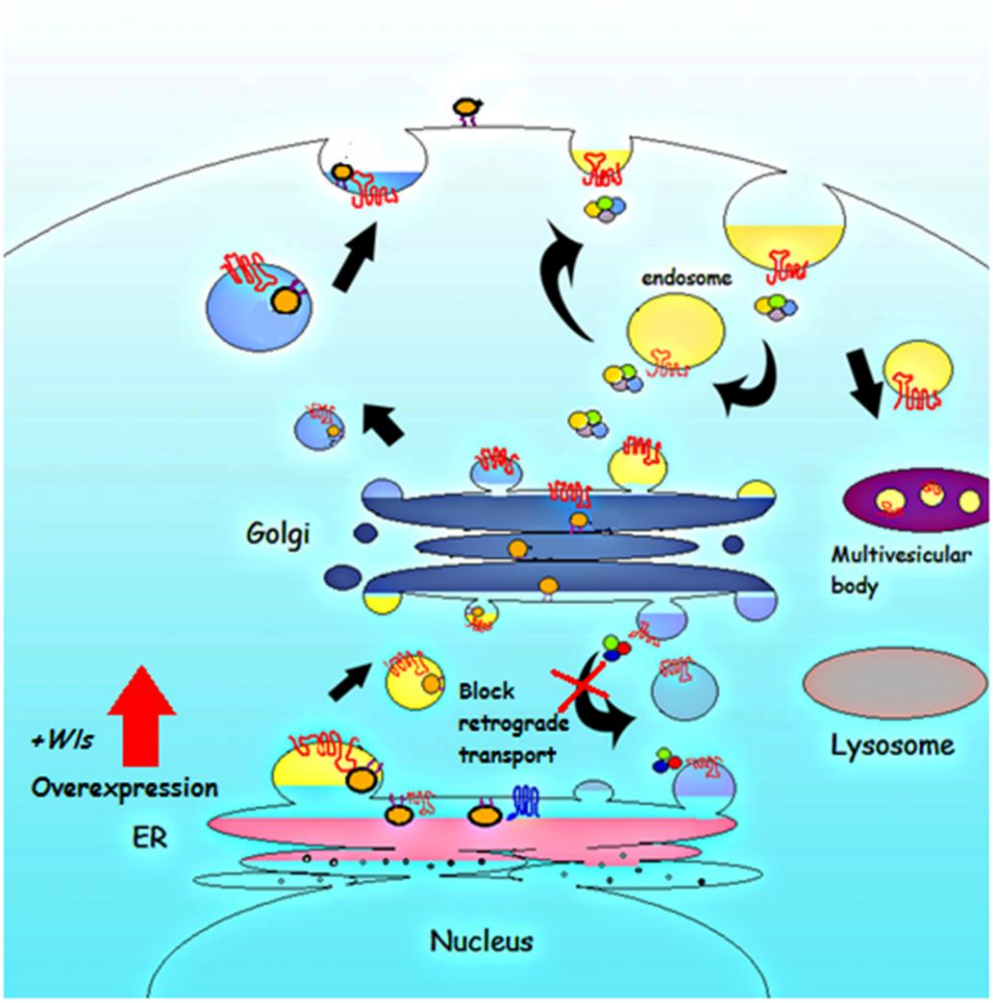

Figure 3-19 Schematic diagram showing co-expression of *wls* in retrograde RNAi knockdown backgrounds. Wg retention defect in retrograde trafficking knockdowns suggested Golgi to ER transport is vital for Wg secretion. If Wls is the component that is not able to reach the ER in the knockdowns, over-expression of *wls* in these backgrounds should rescue the Wg retention and wing nick phenotypes.

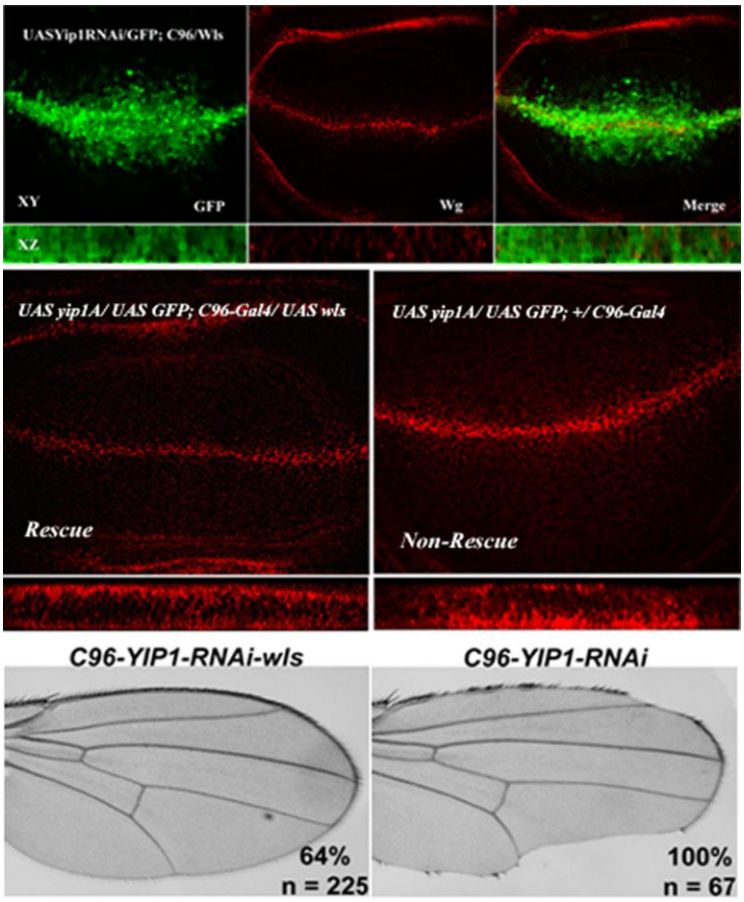

Figure 3-20 Over-expression of *wls* can rescue Wg secretion defect observed in Yip1A RNAi knockdown cells. *UAS-wls* and *UAS-Yip1A RNAi* were co-expressed using *C96-Gal4*. Wg retention shown in knockdown controls was drastically reduced when Wls was over-expressed (top panel, red). To clearly show this rescue, mid panel shows the side-by-side view of rescue (mid left) versus non-rescue (mid right) wing discs. Over-expression of *wls* also rescued loss of wing margin bristles which shows more than 64% of the progeny have complete wing margin rescues.

the Wg defect is not perfect and some residual cells still retained some Wg ligands,

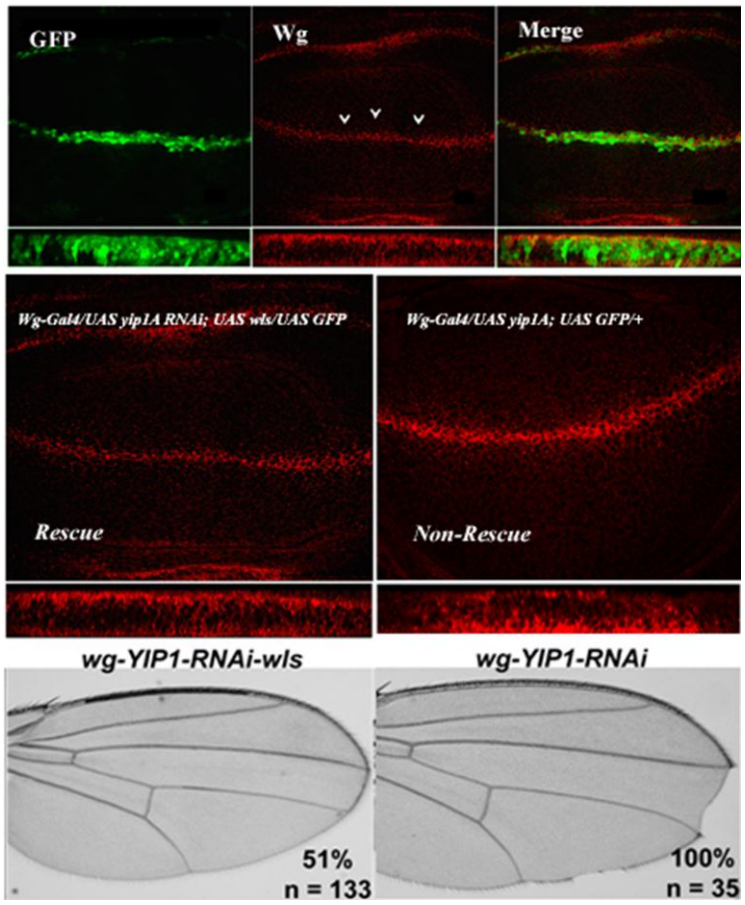

Figure 3-21 Over-expressions of *wls* in Yip1A knockdown using Wg-Gal4 rescues Wg retention. The over-expression of *wls* in Yip1A knockdown using Wg-Gal4 also showed rescues of Wg retention (top panel, red). Shown in a side-by-side view, the rescue of Wg retention (mid left) can be seen more clearly in comparison to the non-rescue wing disc tissue (mid right). The over-expression of *wls* rescued margin bristles at 51% of the progeny.

co-expression of *UAS-β-COPRNAi* or *UAS-Yip1A RNAi* with *UAS-wls* restored majority of Wg secretion.

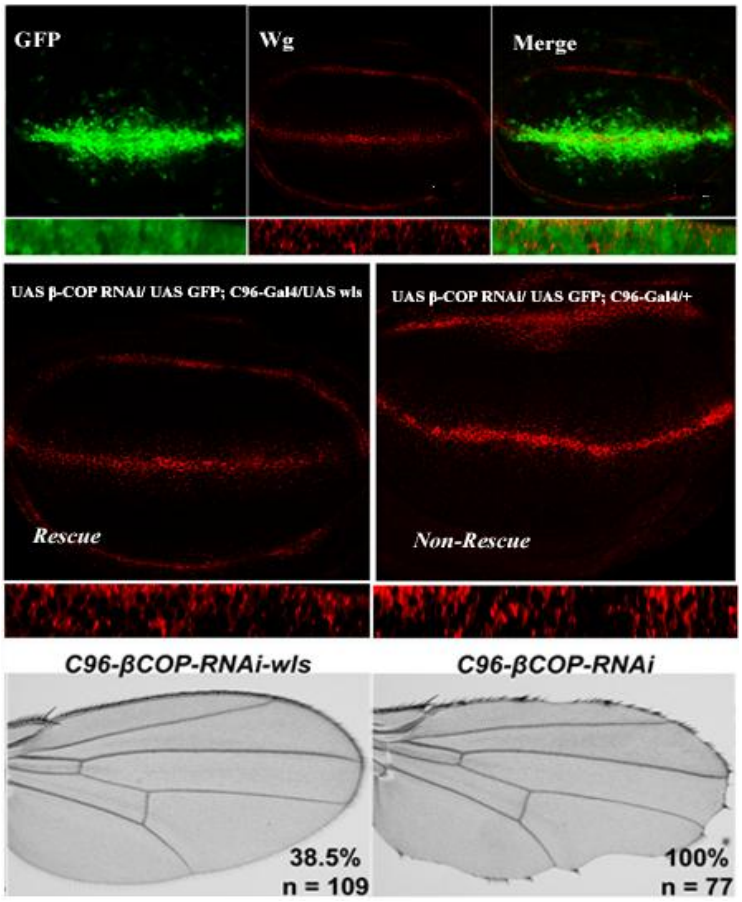

Figure 3-22 Over-expressions of *wls* in β-COP knockdown with C96-Gal4 rescues Wg retention. Similarly to Yip1A rescues, the over-expression of *wls* can rescue Wg retention phenotype. Wg (red) retention was drastically less, and wing margin bristle is present in adult progeny when *wls* is over-expressed the *C96-β-COP RNAi* background. However, the degree of rescue was observed to be much lower at 38% fully rescued adults.

While the expression of Wls in the β-COP or Yip1A knockdowns rescued the adult wing nick phenotype, the rescue was not fully penetrant in all backgrounds. Although adult wings devoid of wing nicks were found in all backgrounds they were found in vary

degrees depending upon the Gal4 driver (Figure 3-20 and 3-21). Each progeny shows consistent Wg retention in Yip1A RNAi control; however, in Wg rescued animals, the amount of Wg retention varies from one rescue to another. This is consistent with that fact that rescue to normal adult wing margins is not fully penetrant. The proportion of progeny with completely rescued wings was recorded, resulting in 64% rescue for C96-Gal4 and 51% for Wg-Gal4.

As a final control for these experiments Wg was co-expressed in the background of retrograde knockdown using *UAS-wg*. Previous experiments indicated Golgi to ER retrograde transport is vital to maintain a high enough level of Wls inside Wg producing cells to support its secretion. To confirm that Wls is the limiting factor, we co-expressed Wg in the retrograde knockdowns with *UAS-wg*. The co-expressions of *UAS-wg* in the background of *UAS-Yip1A* and *UAS-βCOP* knockdowns showed no rescue of the Wg retention phenotype (Figure 3-23). The expression of Wg in the retrograde knockdowns showed similar levels of Wg retention observed in previous knockdown experiments (Figure 3-15 and 3-17). Although the adult wings from the Wg expressing retrograde knockdowns all had wing nicks, there were signs of *wg* gain of function phenotype (Figure 3-24, bottom panel). One possible reason for this observed partial gain of function phenotype could be due to the C96-Gal4 driver itself.

Since the expression of *C96-Gal4* encompasses cells normally producing Wg protein, as well as adjacent cells, the effect of ectopic Wg expression in these cells

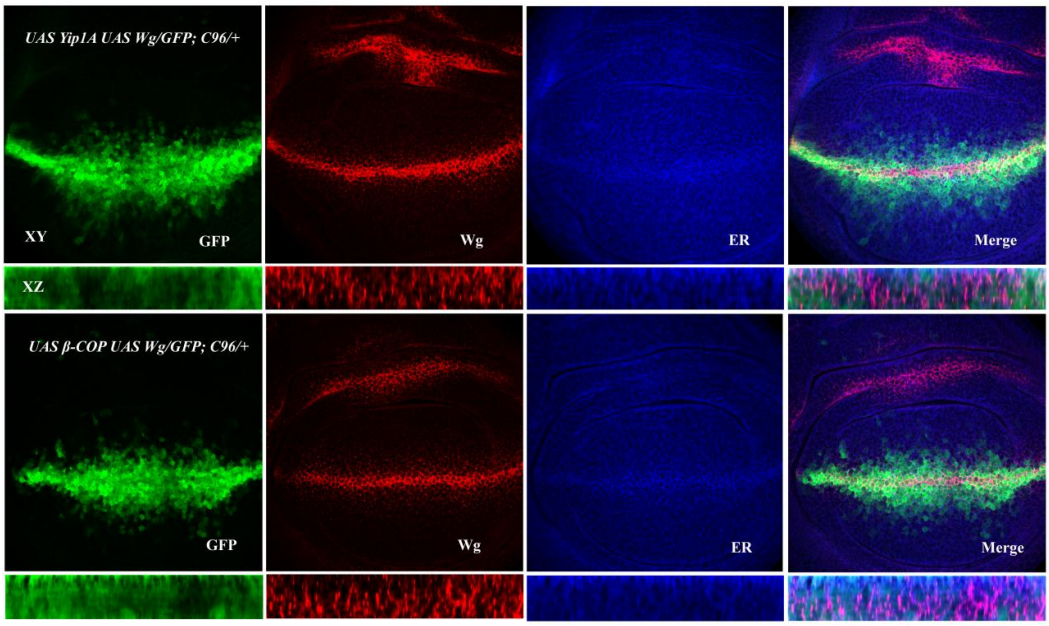

Figure 3-23 Co-expressions of Wg in β-COP and Yip1A knockdowns using C96-Gal4 shows retention of Wg in Wg producing cells. *C96-Gal4* driving the expression of Wg and retrograde knockdown did not rescue Wg retention (red) demonstrating retrograde trafficking of Wls is vital to maintain Wg secretion. Furthermore, high levels of Wg expression in retrograde blocked cells caused an increase BiP levels indicative of the induction of ER stress (blue).

could lead to the observed gain of function phenotype. Wg ligand may act as an autocrine signal in these adjacent cells and therefore retrograde transport may not be vital in this context. Ectopic over-expression of Wg may promote autocrine signaling in cells that do not normally produce Wg to yield gain of function phenotypes. Although the addition of Wg gain of function phenotypes were observed in *C96- Gal4*

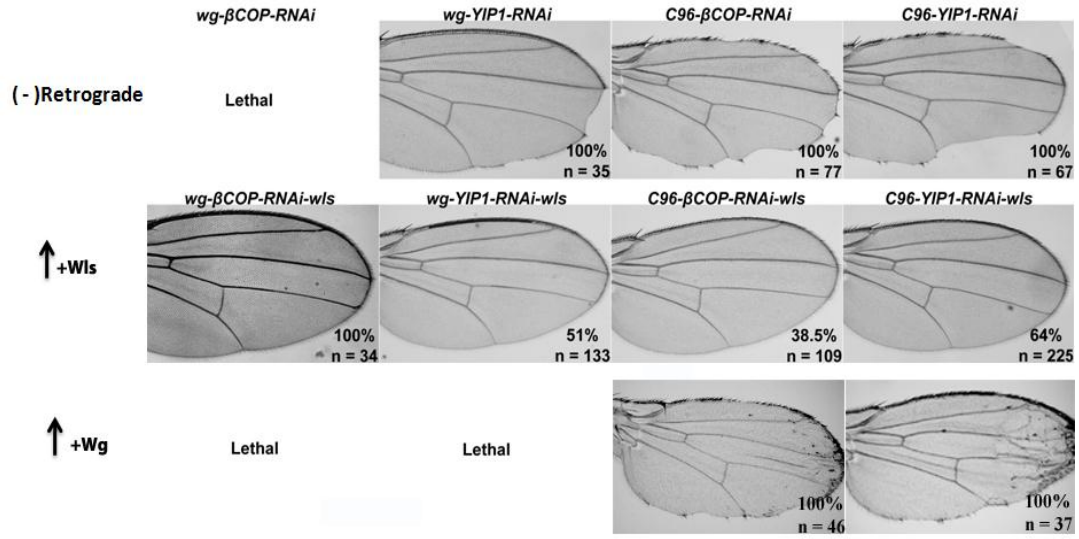

Figure 3-24 Summary of the adult *Drosophila* wing phenotypes. Top panel shows wing nick phenotypes obtained from adult progeny that express βCOP-RNAi or Yip1A RNAi using Wg-Gal4 or C96-Gal4 drivers. Other than lethality in the Wg-Gal4 and βCOP-RNAi cross, all progenies show similar wing nick phenotypes. Over-expression of Wls in these retrograde knockdowns background can rescue the wing nick phenotype (middle panel) with varying percent in adult flies with normal wings. Expression of Wls in the Wg-βCOP RNAi background restored viability to yield adults free of wing nicks. However, over-expression Wg in the background of retrograde knockdown does not rescue wing nick phenotypes or lethality (bottom panel). Over-expression of Wg with C96-Gal4 in the background of Yip1 knockdown demonstrates a Wg gain of function in the distal regions of the wings, as well as some anterior wing margin. This suggests that Wls recycling pathway may not be needed, especially through Yip, in these clusters of cells.

retrograde knockdowns that express Wg, wing nicks were still present in all flies suggesting the in cell that normally express Wg retrograde transport is required.

The expression of Wg in the *wg-Yip1A* RNAi background showed the same lethality as β-COP knockdown with the *wg* driver. This may be due to increased Wg accumulation within these cells. The combination of Wg and retrograde RNAi using the

wg-Gal4 driver did not rescue the lethality in *β-COP* RNAi expressing flies. This suggests that the over-expression of *wg* and knocking down retrograde transport in Wg producing cells during embryogenesis significantly affects *Drosophila* development at earlier stages. These data support the conclusion that it is Wls that is specifically limiting for Wg secretion. Taken together, these data demonstrate that Wls recycles to the ER through retrograde transport where it then engages Wg prior to Golgi targeted anterograde trafficking and secretion.

Chapter 4

DISCUSSION

4.1 Conclusion

Wnt/Wingless (Wg) signaling is important for many biological processes. Misregulation of this signal has been shown to lead to human cancers and other developmental diseases [5, 25]. Currently much of what is known about Wg has been focused on the processing Wg signaling in the receiving cells, but very little is known about the mechanism of Wg secretion itself. A number of proteins have been shown to be essential for the secretion of Wg ligands (Section 1-4). Among these proteins, Wntless (Wls) was shown to be a highly conserved multi-pass transmembrane protein vital for proper Wg secretion [31, 47]. Since the discovery of Wls, there have been several suggested mechanisms of Wg secretion based on the function of the retromer and Por [37, 52]. Additionally, analyses of Wls localization suggest multiple locations that Wls and Wg could initially engage. These locations included the endosomes, the Golgi apparatus, the plasma membrane, and the ER.

Due to the dogmatic function of the retromer, which recycles plasma membrane protein back to the Golgi, it was proposed that the site of Wg and Wls engagement is in the Golgi. Subsequently, *wls* RNAi knockdown studies showed Wls and Wg colocalize to the Golgi in this context within wing discs [46]. However, experiments in the Selva laboratory showed that in *wls* mutant wing discs Wg accumulates in the ER, strongly supporting the notion that the site of Wg and Wls initial engagement in the ER and not

the Golgi (see introduction). Results obtained in this study also support the hypothesis that the actual initial site of Wg and Wls engagement is in the ER: First, an N-terminal hemagglutinin (HA)-tag in Wls protein (Wls-NHA) caused it become an ER resident protein, unlike wild type Wls, which cycles throughout the secretory pathway. Wls-NHA still binds to Wg with high affinity and therefore it was hypothesized that Wls-NHA should act as dominate negative when over-expressed in the wing disc. This prediction was confirmed in this study. Second, since Wls was shown to engage Wg in the ER this suggested that Golgi to ER pathways would be required to maintain sufficient ER levels of Wls to support Wg secretion. As expected, knockdown of critical Golgi to ER retrograde components caused Wg-retention phenotypes as seen in *wls* mutant and retromer loss of function. These data suggest that the role of the retrograde transport is to maintain Wls levels in the ER of Wg producing cells for proper Wg secretion. Finally, the over-expression of *wls* in the Golgi to ER retrograde knockdown background rescued the Wg secretion defects. Furthermore, the rescue was specific as neither Wg nor Wls-NHA over-expression restored Wg secretion in this background. This indicates that the limiting factor needed for Wg section in the Golgi to ER retrograde knockdown backgrounds in Wls.

4.1.1 Expression of Wls-NHA in Wg producing cells acts as dominant negative

Wg proteins are secreted ligands that activate multiple targets in cells short- and long-distances from the secreted source. Similar to the role of Wnt in organ and limb development in vertebrates, Wg signaling in the wing imaginal disc is vital for the proper wing and thorax development flies [69]. In order to maintain constant Wg signaling, the secretion mechanism of Wg is highly regulated. Wg is palmitoylated by Por causing it to

be more lipophilic and requires Wls for transport to the plasma membrane for release into the extracellular space for signaling. Our results support the conclusion that proper Wg signaling, and thus proper development of the organism requires Wg to interact with Wls and this engagement occur initially in the ER.

Previous data obtained from homozygous *wls* mutant wing discs showed Wg significantly accumulates in Wg producing cells (Figure 1-9). These data further showed that the accumulation causes dramatic developmental defects similar to the loss of retromer function examined by Belenkaya *et al.*, 2008. Close examination of Wg localization within *wls* mutant wing discs did not conclusively determine the site of Wg accumulation. In this study we examined the effect of an HA-tagged form of Wls that is confined to the ER, but still binds Wg. Expression of Wls-NHA in wing discs acted as a dominant negative, which supports the hypothesis that Wls initially engages Wg in the ER.

Much like the wild type, Wls-CHA is distributed throughout the endomembrane system and showed only 39% colocalization to the ER compartment in the peripodial epithelial cells of the wing imaginal discs. Examination of Wls-CHA expression showed that this form of Wls does not hinder Wg was secretion, but rather increases it (Selva, unpublished data). In a similar experiment, it was demonstrated that unlike its counterpart Wls-NHA has over 78% colocalization to the ER membrane. Co-immunoprecipitation results suggest that both C-and -N-terminal HA tagged does not diminish their binding affinity for Wg protein. Expression of Wls-NHA in both the dorsal and posterior compartment of wing imaginal discs has a dominant negative effect in Wg secretion. Wls-NHA expression in the posterior compartment caused Wg retention similar to *wls* mutant[47] and retromer loss of function[52].

A wing nick phenotype is associated with loss of Wg signaling [73]. When Wls-NHA was expressed in the posterior wing disc compartment Wg was retained within those cells and100% of adult flies had wing nicks in the posterior compartment where Wls-NHA was expressed. Together these data support the conclusion that loss of Wg signaling only occurs when Wg producing cells express this form of Wls. Nevertheless, it is important to note that the wing nick phenotypes observed in these progeny are variable and are milder in comparison to other wing nick phenotypes like those observed in retrograde knockdown. Additionally, wing nicks were observed only when the crosses were reared at 29°C. Interestingly, expression of Wls-NHA by a single posterior driver, e*n*- or *hh-Gal4*, leads to no observable phenotype. Since additional drivers and increased temperature are expected to generate higher levels of the Gal4 transcription factor, these results suggest that the ectopic expression of Wls-NHA is competing with the endogenous wild type form of Wls. Thus, only one Gal4 was not sufficient to produce high enough levels of Wls-NHA to yield a dominant-negative effect.

In the dorsal compartment, Wg is known to induce the development of downstream sensory precursor cells. Ac and Sen are both activated by long range Wg signaling in this tissue [70]. Although it was impossible to compare side-by-side Wg expressing cells that were and were not expressing Wls-NHA with the *ap-Gal4* driver, we interpret these results in light of our other data. High-level expression of Wls-NHA in the dorsal compartment caused Wg retention in Wg producing cells and thus inhibited the expression of downstream target genes, such as *ac* and *sen*. Dramatic thoracic bristle loss in the progeny also suggests down-regulation of Ac and Sen. Ectopic expression of Wls-NHA demonstrated a dominant negative effect. However, since it is not completely lost, this suggests Wls-NHA is in competition with the wild type form of Wls in this tissue, as

well. Hence, some Wg ligand is still secreted properly with limited range signaling. Taken together these experiments demonstrate Wls-NHA localization in the ER has detrimentally effect on Wg secretion and downstream target activation of *sen* and *ac* vital for proper macrochaetae development. These results also illustrate the importance of Wls regulation, since in addition to effecting the activation of *sen* and *ac*, this block of Wg secretion can in turn potentially cause other developmental defects.

4.1.2 β -COP and Yip1A retrograde transport components are important to maintain Wg secretion

The retromer complex has been shown to target the recycling of plasma membrane proteins to the endomembrane compartment for recycling and proper sorting [51]. Retrograde transport proteins, such as β-COP and Yip1A, function to properly recycle proteins from the Golgi to the ER and have been long known to be essential for maintaining the balance of proteins distributed in these membrane compartments. However, there are few examples of retrograde recycling of protein from the plasma membrane to the ER. Exogenous proteins, such as Cholera toxin and Shiga toxin, have shown to follow the route for infections, but endogenously produced proteins that go from the plasma membrane to the ER have not been documented until this current study. If in fact this recycling exists, it could set a precedent for modeling other secretory pathways in *Drosophila* development and more importantly vertebrate development. Furthermore, this recycling mechanism can potentially be targeted to improve Wnt signaling and thus drug development.

The Wg retention observed in β-COP and Yip1A knockdown backgrounds demonstrates that retrograde transport from the Golgi apparatus to the ER is essential to

maintaining proper Wg secretion (Figure 3-13-15). Furthermore, rescue of the Wg retention phenotype by over-expressing Wls suggests that the knockdown of Yip1A and β-COP directly affects Wg secretion by limiting the concentration of Wls within the ER. Wg retention and wing nicks were consistent in flies with only marginal differences in phenotype for a given background. Wg protein and ER markers in these wing imaginal discs showed strong colocalization. However, due to high Wg retention within these Wg producing cells, there appears to be no way to unambiguously distinguish which membrane compartment Wg is retained within. Nevertheless, these data strongly suggest that Golgi to ER retrograde transport is important to maintain proper Wg secretion.

Prior to selecting *C96-Gal4* and *Wg-Gal4*, multiple lines of Gal4 driver lines were examined to identity, which was optimal for *β-COP* and *yip1A* RNAi expression. Most of these Gal4 lines had broader expression patterns and elicited phenotypes that ranged from lethality to severe tissue-specific defects. However, *C96* and *wg-Gal4* were chosen because their expression pattern closely followed the pattern of Wg expression. *wg-Gal4*, as the name suggests, expresses in all Wg secreting cells throughout the fly development. *C96-Gal4*, first identified as a *Gal4* enhancer trap expression pattern, but later classified as a gene *big bang* (*bbg*)[74], expresses in most Wg expressing cells at the dorsoventral boundary of the wing disc and in the cells that are straddling the dorsal-ventral line. Unlike *wg-Gal4*, *C96-Gal4* only expresses during the larval third instar and only in the wing imaginal disc. Preliminary data from these Gal4-drivers demonstrated that *β-COP* and *Yip1A* RNAi knockdown resulted in dramatic Wg retention. However, to clearly demonstrate which tissues were expressing retrograde knockdown, GFP was used to identify cells expressing *β-COP* and *Yip1A* dsRNAs.

Since we were unable to obtain antibodies specific to *Drosophila* Yip1A and β-COP, the GFP reporter was used instead to demarcate *Yip1A* and *β-COP* dsRNA expression. However, there were some issues that arose once *UAS-GFP* was placed into the background of *C96-Gal4* and *wg-Gal4*. The first was optimizing immune-fluorescent staining, as well as obtaining stable fly stocks that harbored the Gal4 driver and *UAS-GFP*. Several ER marker antibodies were used throughout the project. Inconsistencies in staining with different BiP monoclonal antibodies made comparing compartmental markers difficult. Additionally, *UAS-GFP; C96-Gal4* and *wg-Gal4/Cyo; UAS-GFP* fly stocks took several months to become stable and productive. Constant nursing and examining for *GFP* expression had to be done prior to each experimental cross. Preliminary crosses were set-up to evaluate phenotypes caused by expression *β-COP* and *Yip1A* RNAi. However, all these progeny lacked internal GFP controls. Multiple replicates were done to ensure expected numbers of animals expressed retrograde knockdown and that they showed proper segregation of balancer chromosomes. In addition, to the stocks being unstable, adding the GFP reporter to the background could have caused an additional problem.

Another problem we faced was the sufficient expression of all retrograde transport components dsRNAs and the GFP reporter. Gal4 driver, a modular protein consisting broadly of a DNA-binding domain and an activation domain, binds specifically to a UAS (upstream activation sequence) target DNA sites. In cells that express *Gal4* and have multiple *UAS* recognition sites, the pools of Gal4 proteins are divided. If the Gal4 diver did not produce sufficient quantities of Gal4, this could potentially give false negative or false positive results depending on the experiment. However, analysis of *GFP* expression in control tissues and knockdown crosses showed no decrease in GFP

expression. This suggests that both Gal4 drivers express sufficient levels of Gal4 to support both retrograde RNAi and GFP expression.

Co-expressing Wls-NHA and retrograde knockdown by C96-Gal4 driving the expression of *UAS-wls-NHA* and *UAS-Yip1A/β-COP* RNAi shows similar wing nick phenotype to retrograde knockdown alone. Furthermore, expression of *UAS-wls-NHA* with *β-COP* RNAi using *wg-Gal4* did not rescue lethality like untagged Wls. These results support the hypothesis that ER localized Wls-NHA cannot rescue the Golgi to ER retrograde knockdown. In addition, these data also demonstrates that the Gal4 drivers are sufficient to express three separate UAS controlled genes (Figure 3-9).

The expression of *Yip1A* and *β-COP* RNAi with *wg-* and *C96-Gal4* driver combinations all yielded adult phenotypes to varying degrees. *β-COP* RNAi consistently caused lethality and more severe wing nick phenotypes with *wg-Gal4* and *C96-Gal4*, respectively, than those generated by *YiP1A* RNAi. One reason for the difference in *Yip1A* and *β-COP* RNAi phenotypes could be that β-COP is more widely used for retrograde transport in Wg producing cells. Lethality in late embryonic stage by expressing *β-COP* RNAi with *wg-Gal4*, and not in *C96-Gal4*, suggests that of β-COP is required in all Wg expressing cells. This indicates that a factor needs to be recycled from the Golgi to the ER by β-COP, which is essential before Wg secretion.

4.1.3 The requirement of retrograde transport for Wg secretion can be overcome by Wls expression.

It has been established that Wg retention in retromer loss-of-function cells can be overcome by over-expression of Wls [52]. Consistent with the role of the retromer, Golgi to ER retrograde knockdown demonstrated that this process is vital for Wg secretion.

Additionally, the over-expression of Wg and Wls-NHA did not rescue Wg retention in retrograde knockdown progeny, suggesting that Wls is the limiting factor. Taken together, these results strongly suggest that Wg requires Golgi to ER retrograde transport systems in order to maintain high level of Wls in the ER to maintain for proper Wg secretion. Additionally, these data also demonstrate that Wls is recycled back from the plasma membrane to the ER and the ER is the site where Wg and Wls initially engage one another.

Previous models have suggested that due to the dogmatic function of the retromer complex and moderate colocalization of Wls with Golgi markers in Wg expressing cells, the site where Wls engages Wg is the Golgi[46]. However, our current data strongly argue a different Wls recycling mechanism. On the basis of these new findings, the following mechanism is proposed: in the ER, Wg protein is lipid modified by Porcupine. Por releases Wg after proper lipid modification to Wls. Wls then escorts Wg to the Golgi for further posttranslational processing and then onto the cell surface for Wg release. The unloaded Wls protein at the plasma membrane is subsequently internalized through dynamin-mediated endocytosis [47]. Within the endosome, Wls is trafficked to the Golgi in the presence of the retromer and in the absence of the retromer Wls is directed to the lysosome for degradation. From the Golgi, Wls is transported back to the ER via COPI dependent and independent retrograde trafficking, where it binds to newly Por modified Wg for another round of secretion.

Although our current data demonstrate that Wls recycling to the ER is important to maintain Wg secretion, it is still unknown if another mechanism controls this retrograde transport and if Wls recycling to the ER can bypass the Golgi compartment. Studies of the retromer strongly suggest that Wls has to go through the Golgi; however, it

cannot be ruled out that the recycling of Wls could bypass the Golgi membrane for direct transport from the plasma membrane to the ER. [52]. Exogenous toxin studies examining the plasma membrane to ER retrograde transport of Shiga toxin and Cholera toxin suggest mechanisms in which bypass might occur [57, 59]. Further experiments are needed to better elucidate these mechanisms.

Wingless/Wnt is a highly conserved molecule that has been shown to be vital for proper development of invertebrates and vertebrates. Proper Wnt signaling is highly controlled by Por and Wls for its palmitoylation and intracellular transport required for secretion and downstream signaling. Here we demonstrated that in order to maintain high levels of Wls for proper Wg secretion, in addition to the retromer complexes, Golgi to ER retrograde transport is required. Taken together from previous experiments done to understand the function of Por, Wls, and retromer complex, our current data reveals the complete recycling mechanism of Wls proteins within Wg producing cells. These results not only suggest that Wls and Wg initially engage in the ER, but also demonstrate that Wls requires retrograde trafficking to the ER from the plasma membrane. Although it's been known that the retrograde transport recycling mechanism is highly conserved, our current data suggest that membrane proteins can be targeted for recycling from the plasma membrane to the ER. This idea, though quite simple and logical, is unprecedented in previous work and is set to open new opportunity for future studies of Wnt ligands and other secretory proteins.

4.2 Future directions

4.2.1 Direct method to demonstrate Wls and Wg interaction in the ER

There are other methods that can be used to determine directly that Wls and Wg engagement occurs in the ER. Using indirect techniques, it was demonstrated that Wls recycles back to the ER to maintain proper Wls levels for Wg secretion. However, direct confirmation is still needed. The problem with direct confirmation is the inability to stain for endogenous Wls in *Drosophila.* The Selva laboratory has made several attempts to generate an antibody that can detect endogenous Wls but have been unsuccessful. The creation of this reagent would enable us to follow the trafficking of endogenous Wls by cellular fractionation following surface biotinylation. Other laboratories have generated a Wls antibody, but will only give out small amounts that are insufficient for these experiments. While the carboxyl-terminal HA tagged version of Wls could be used in fractionation experiments, the high-level Wls expression is likely to alter its normal trafficking. Regardless, optimization of this difficult fractionation protocol has not been completely established for optimal ER membrane isolation (Figure 3-7).

Additionally, current projects are underway to investigate the mechanism of the dynamic trafficking of Wls in Wg expressing and non-expressing cells. Wls is ER localized in non-Wg expressing cells, but cycles throughout the secretory pathway in Wg expressing cells. One proposal to explain the dynamic cycling of Wls is that Por, a resident protein, binds Wls to maintain its ER localization. Upon lipidation of Wg by Por, transfer of Wg to Wls causes a displacement of the Por-Wls interaction in favor of a Wls-Wg interaction. This initiates the release of Wls-Wg complex for anterograde trafficking

to the Golgi. Documentation of a Wg dependent Por-Wls interaction would further support the model that Wls and Wg initially engage in the ER.

In previous studies on Por and its interaction with Wg, it has been proposed that Por acts as an anchor for proper Wg modification in the ER [27, 38]. Upon completion of this modification, Por releases Wg and it is unclear whether the transfer to Wls is direct or indirect. *In vitro* expression of *por*-HA and *wls*-V5 in S2R+ cells and co-immunoprecipitation using Wg is a strategy being used to determine if Por and Wls directly interact.

4.2.2 Effects of Wls recycling on short-range Wg signaling

Wnt in vertebrates and likewise Wg in *Drosophila* is a secreted glycolipoprotein, which acts as a patterning signaling molecule in many developing organs and tissues. In *Drosophila*, this signaling is especially important during the embryonic development, and later in the imaginal discs[75, 76]. In wing imaginal discs, Wg is produced at the DV boundary and spreads symmetrically to activate downstream gene targets in the adjacent cells. Target genes within cells located closest to the Wg producing cells are activated by the high concentration of short-range Wg signaling or so called high-level target genes, such as *senseless* (*sens*)[77]. *Sens*, *Growth factor independence 1* (*Gfi1*) in the vertebrates, plays an important role in peripheral nervous system and proper development[78].

Though most of the Wg ligand is retained in Wg producing cells due to retrograde block, limited amount of Wg endocytic punctuates were detected 3-4 cell lengths away from the dorsal-ventral border (Figure 3-15-17). Consistent with this observation, *wg-Gal4* driving the expression of Y*ip1A* RNAi shows a less severe wing nick phenotype in

comparison to *C96-Gal4; UAS-Yip1A* RNAi. In the region corresponding to the posterior and anterior compartment of the adult wings (Figure 3-13), margin bristles are still present; at distal tip, dramatic wing nicks were observed. This could simply be due to a dosage dependent effect in which *C96-Gal4* expressing *Yip1A* RNAi produces higher levels of the *Yip1A* dsRNA to causes more Wg retention. However, based on the expression of *GFP* in both *wg-Gal4* and *C96-Gal4* control, the expression levels seem to be at a similar threshold, although the domain of *C96-Gal4* at the dorso-ventral boundary is much broader than *wg-Gal4*.

Another reason for this phenomenon may be that Wls recycling is more crucial for longer range Wg signaling, and that short-range signaling can still persist with limited Wls recycling. Two models consistent with this phenomenon were proposed to regulate Wg long-range and short-range signaling. Both models suggest similar pathways; they differ only in the involvement of Wls. Both propose that Wls guides Wg to the apical plasma membrane surface where it is released into the extracellular space to induce short-range target gene expression in neighboring cells. It has been proposed that Wg that encounters Reggie-1/Flotillin-2, a microdomain-associated protein, at the apical surface, which may induce Wg for endocytosis and basal surface targeting [9].

Delivery of endocytosed Wg to the basal surface established a morphogen gradient on the basal surface needed for long-range Wg signaling. In the first model, Wls releases Wg at which point it is endocytosed at the plasma membrane and is delivered to an endosomal compartment. However, the second model suggests that Wls and Wg are still associated prior to endocytosis and together they are delivered to endosomal compartments and ultimately to the basal surface. In the endosome Wg may be packaged

into lipophorin particles by means of an unknown loading mechanism. This association allows Wg to be targeted for release at the basolateral membrane [9].

Consistent with the second model, it seems that retrograde transport block decreases the Wls concentration needed for long range targeting, and shifts the mobile pool of Wg from long-range towards short-range. Examination of Wg long-range signaling targets would be required to test the molecular consequences of changes in targeting. The over-expression of Wg in the background of *Yip1A* RNAi caused Wg retention in the wing imaginal discs and did not rescue wing nicks at the margin in the adult wings (Figure 3-23 and 24). However, other regions of the wings showed Wg gain of function phenotypes, demonstrated by an abundance of wing bristles in the wing blade (Section 3-5, Figure 3-24). This suggests that short- and long-range signaling may require the retrograde transport, but autocrine Wg signaling might not. In all progeny with *C96-Gal4* driving *β-COP* and *Yip1A* RNAi knockdown and Wg over-expression, we found that most if not all adults showed similar dramatic wing nicks at the posterior and anterior margin, but not at the distal region of the wings, which shows a gain of function phenotype. We believe that within these Wg producing cells, over-expression of Wg can compensate for the lack of Yip1A or β-COP mediated retrograde transport perhaps by autocrine mechanisms.

4.2.3 Localization of Wls to the lysosome in retrograde knockdown

Wing nick phenotypes we observed in the retrograde knockdown progeny demonstrates that there is a loss of Wg signaling due to insufficient levels of Wls for proper Wg secretion. The depleted amount of Wls was due to RNAi against either Yip1A or β-COP. However, it is important to note that anterograde transport is not inhibited. As

such, newly synthesized Wls should still be present in the ER, Golgi and the plasma membrane. It would be interesting to see where the ER targeted recycling Wls is sent in the absence of retrograde transport proteins. Most logically, loss of retrograde transport would cause recycling Wls to be present in the Golgi, which would likely cause an accumulation of proteins. However, this accumulation was not observed (data not shown). The next compartment where recycled Wls would be targeted is the lysosome, similar to the loss of retromer function demonstrated by Belenkaya *et al.*, 2008. These researchers demonstrated that Wls is targeted for destruction, it may be that in the absence of retrograde transport [52], Wls is targeted for the lysosome.

4.2.4 Additional experiments

In addition of Wg retention and subsequent observed wing nicks phenotypes, the expression of *wls-NHA* resulted in high accumulation of Wls-NHA in the ER membrane causing ER stress which further suggests that the site where Wls and Wg engage have to be in the ER. The accumulation of ER proteins, BiP, has also been shown in preliminary data of *wls* homozygous mutant tissues (Figure 1-10, blue). High accumulation of chaperone proteins such as BiP could suggest ER stress. One possible reason for this stress may be because of the accumulating Wls-NHA in the ER membrane. In addition to supporting our hypothesis that Wls and Wg engagement occurs in the ER, further analyses suggested something we had not expected.

It has been known that ER stress lead by unfolded protein response (UPR) can induce capase-mediated apoptosis (Rao *et al.*, 2002). Interestingly, the accumulation of Wls-NHA within the ER causes the accumulation of chaperone protein BiP but does not seem to cause cell death, although more studies are needed to address this question.

Controlled experiments demonstrated that this effect was not due to cross-reactivity of antibodies. In addition, *wls-NHA* expression does not hinder the secretion of other secretory proteins, such as E-cadherin. Therefore, this accumulation of BiP is due to the over-expression of *wls-NHA* and its retention in the ER. The question then is how the accumulations of Wls-NHA within the ER is alleviated. In addition to the programmed cell death there are other ways to alleviate ER stress. Another way to deal with this stress is for cells to mediate ER associated protein degradation (ERAD). It would be interesting to see if the accumulation of Wls-NHA causes an increase in lysosome activities. However, due to the inconsistencies in ER protein staining in these tissues, we were not confident with our results. BiP accumulation is only an indication to ER stress. Additional experiments need to be performed to confirm *wls-NHA* expression activates UPR before a definitive conclusion can be reached.

Although it is unlikely, the accumulation of Wls-NHA in Wg producing cells at the ER may be causing other dominant negative effects. Since Wls is targeted for ER recycling by Golgi to ER retrograde transport proteins, there has to be recognition between Wls by these transport complexes. At normal levels of Wls, the regular function of retrograde transport complexes may not be hindered by Wls. However, when Wls-NHA is highly accumulating at the ER, this may be causing retrograde transport block of other proteins. However, a better understanding of retrograde transport system is needed before further hypothesis can be made.

REFERENCES

1.Nusse R, Varmus HE. Many tumors induced by the mouse mammary tumor virus contain a provirus integrated in the same region of the host genome. Cell 1982;31(1):99-109.

2.Paul P. The adenomatous polyposis coli (APC) tumor suppressor. Biochimica et Biophysica Acta (BBA) - Reviews on Cancer 1997;1332(3):F127-F147.

3.van Amerongen R, Nusse R. Towards an integrated view of Wnt signaling in development. Development 2009;136(19):3205-3214.

4.Brennan KR, Brown AMC. Wnt Proteins in Mammary Development and Cancer. Journal of Mammary Gland Biology and Neoplasia 2004;9(2):119-131.

5.Clevers H. Wnt/[beta]-Catenin Signaling in Development and Disease. Cell 2006;127(3):469-480.

6.Arias AM, Browntand AMC, Brennan K. Wnt signalling: pathway or network? Current Opinion in Genetics & Development 1999;9(4):447-454.

7.Croce JC, McClay DR. Evolution of the Wnt Pathways. In: Vincan E, editor. Wnt Signaling. Volume 469, Methods in Molecular Biology: Humana Press; 2009. p 3-18-18.

8.Hausmann G, Banziger C, Basler K. Helping Wingless take flight: how WNT proteins are secreted. Nat Rev Mol Cell Biol 2007;8(4):331-336.

9.Bartscherer K, Boutros M. Regulation of Wnt protein secretion and its role in gradient formation. EMBO Rep 2008;9(10):977-982.

10.Mayr T, Deutsch U, Kühl M, Drexler HCA, Lottspeich F, Deutzmann R, Wedlich D, Risau W. Fritz: a secreted frizzled-related protein that inhibits Wnt activity. Mechanisms of Development 1997;63(1):109-125.

11.Logan CY, Nusse R. THE WNT SIGNALING PATHWAY IN DEVELOPMENT AND DISEASE. Volume Vol. 20. Annual Review of Cell and Developmental Biology2004. p 781-810.

12.Gordon MD, Nusse R. Wnt Signaling: Multiple Pathways, Multiple Receptors, and Multiple Transcription Factors. Journal of Biological Chemistry 2006;281(32):22429-22433.

13.Umbhauer M, Djiane A, Goisset C, Penzo-Mendez A, Riou J-F, Boucaut J-C, Shi D-L. The C-terminal cytoplasmic Lys-Thr-X-X-X-Trp motif in frizzled receptors mediates Wnt/[beta]-catenin signalling. EMBO J 2000;19(18):4944-4954.

14.Arce L, Pate K, Waterman M. Groucho binds two conserved regions of LEF-1 for HDAC-dependent repression. BMC Cancer 2009;9(1):159.

15.Arce L, Yokoyama NN, Waterman ML. Diversity of LEF//TCF action in development and disease. Oncogene 0000;25(57):7492-7504.

16.Barker N, Hurlstone A, Musisi H, Miles A, Bienz M, Clevers H. The chromatin remodelling factor Brg-1 interacts with [beta]-catenin to promote target gene activation. EMBO J 2001;20(17):4935-4943.

17.Yang J, Zhang W, Evans PM, Chen X, He X, Liu C. Adenomatous polyposis coli (APC) differentially regulates beta-catenin phosphorylation and ubiquitination in colon cancer cells. The Journal of biological chemistry 2006;281(26):17751-17757.

18.Torres MA, Eldar-Finkelman H, Krebs EG, Moon RT. Regulation of Ribosomal S6 Protein Kinase-p90rsk, Glycogen Synthase Kinase 3, and beta -Catenin in Early Xenopus Development. Molecular and Cellular Biology 1999;19(2):1427-1437.

19.De Strooper B, Annaert W. Where Notch and Wnt signaling meet. The presenilin hub. J Cell Biol 2001;152(4):F17-20.

20.Li X, Yost HJ, Virshup DM, Seeling JM. Protein phosphatase 2A and its B56 regulatory subunit inhibit Wnt signaling in Xenopus. EMBO J 2001;20(15):4122-4131.

21.Yamamoto H, Kishida S, Uochi T, Ikeda S, Koyama S, Asashima M, Kikuchi A. Axil, a Member of the Axin Family, Interacts with Both Glycogen Synthase Kinase 3beta and beta -Catenin and Inhibits Axis Formation of Xenopus Embryos. Molecular and Cellular Biology 1998;18(5):2867-2875.

22.Jonkers J, Korswagen HC, Acton D, Breuer M, Berns A. Activation of a novel proto-oncogene, Frat1, contributes to progression of mouse T-cell lymphomas. EMBO J 1997;16(3):441-450.

23.Polakis P. Wnt signaling and cancer. Genes & Development 2000;14(15):1837-1851.

24.Reya T, Clevers H. Wnt signalling in stem cells and cancer. Nature 2005;434(7035):843-850.

25.Bienz M, Clevers H. Linking Colorectal Cancer to Wnt Signaling. Cell 2000;103(2):311-320.

26.Willert K, Jones KA. Wnt signaling: is the party in the nucleus? Genes & development 2006;20(11):1394-1404.

27.Kadowaki T, Wilder E, Klingensmith J, Zachary K, Perrimon N. The segment polarity gene porcupine encodes a putative multitransmembrane protein involved in Wingless processing. Genes & Development 1996;10(24):3116-3128.

28.MacDonald BT, Tamai K, He X. Wnt/[beta]-Catenin Signaling: Components, Mechanisms, and Diseases. Developmental Cell 2009;17(1):9-26.

29.Mathew D, Ataman B, Chen J, Zhang Y, Cumberledge S, Budnik V. Wingless Signaling at Synapses Is Through Cleavage and Nuclear Import of Receptor DFrizzled2. Science 2005;310(5752):1344-1347.

30.DiNardo S, Sher E, Heemskerk-Jongens J, Kassis JA, O'Farrell PH. Two-tiered regulation of spatially patterned engrailed gene expression during Drosophila embryogenesis. Nature 1988;332(6165):604-609.

31.Bartscherer K, Pelte N, Ingelfinger D, Boutros M. Secretion of Wnt Ligands Requires Evi, a Conserved Transmembrane Protein. Cell 2006;125(3):523-533.

32.Nusslein-Volhard C, Wieschaus E. Mutations affecting segment number and polarity in Drosophila. Nature 1980;287(5785):795-801.

33.Neumann CJ, Cohen SM. Long-range action of Wingless organizes the dorsal-ventral axis of the Drosophila wing. Development 1997;124(4):871-880.

34.van den Heuvel M, Harryman-Samos C, Klingensmith J, Perrimon N, Nusse R. Mutations in the segment polarity genes wingless and porcupine impair secretion of the wingless protein. Volume 12. EMBO1993. p 5293–5302.

35.Kurayoshi M, Yamamoto H, Izumi S, Kikuchi A. Post-translational palmitoylation and glycosylation of Wnt-5a are necessary for its signalling. Volume 402. Biochem J.2007. p 515-523.

36.Zhai L, Chaturvedi D, Cumberledge S. Drosophila Wnt-1 Undergoes a Hydrophobic Modification and Is Targeted to Lipid Rafts, a Process That Requires Porcupine. Journal of Biological Chemistry 2004;279(32):33220-33227.

37.Tanaka K, Kitagawa Y, Kadowaki T. Drosophila Segment Polarity Gene Product Porcupine Stimulates the Posttranslational N-Glycosylation of Wingless in the Endoplasmic Reticulum. Journal of Biological Chemistry 2002;277(15):12816-12823.

38.Takada R, Satomi Y, Kurata T, Ueno N, Norioka S, Kondoh H, Takao T, Takada S. Monounsaturated Fatty Acid Modification of Wnt Protein: Its Role in Wnt Secretion. Developmental Cell 2006;11(6):791-801.

39.Kay H. A superfamily of membrane-bound O-acyltransferases with implications for Wnt signaling. Trends in Biochemical Sciences 2000;25(3):111-112.

40.Caricasole A, Ferraro T, Rimland JM, Terstappen GC. Molecular cloning and initial characterization of the MG61/PORC gene, the human homologue of the Drosophila segment polarity gene Porcupine. Gene 2002;288(1-2):147-157.

41.Thorpe CJ, Schlesinger A, Carter JC, Bowerman B. Wnt Signaling Polarizes an Early C. elegans Blastomere to Distinguish Endoderm from Mesoderm. Cell 1997;90(4):695-705.

42.Willert K, Brown JD, Danenberg E, Duncan AW, Weissman IL, Reya T, Yates JR, Nusse R. Wnt proteins are lipid-modified and can act as stem cell growth factors. Nature 2003;423(6938):448-452.

43.Noordermeer JN, Klingensmith J, Nusse R. Differential requirements for segment polarity genes in wingless signaling. Elsevier; 1993. p 145 - 155.

44.Panakova D, Sprong H, Marois E, Thiele C, Eaton S. Lipoprotein particles are required for Hedgehog and Wingless signalling. Nature 2005;435(7038):58-65.

45.Steinhauer J, Treisman JE. Lipid-modified morphogens: functions of fats. Current Opinion in Genetics & Development 2009;19(4):308-314.

46.Bänziger C, Soldini D, Schütt C, Zipperlen P, Hausmann G, Basler K. Wntless, a Conserved Membrane Protein Dedicated to the Secretion of Wnt Proteins from Signaling Cells. Cell 2006;125(3):509-522.

47.Goodman RM, Thombre S, Firtina Z, Gray D, Betts D, Roebuck J, Spana EP, Selva EM. Sprinter: a novel transmembrane protein required for Wg secretion and signaling. Development 2006;133(24):4901-4911.

48.Giles RH, van Es JH, Clevers H. Caught up in a Wnt storm: Wnt signaling in cancer. Biochimica et Biophysica Acta (BBA) - Reviews on Cancer 2003;1653(1):1-24.

49.Dyrløv Bendtsen J, Nielsen H, von Heijne G, Brunak S. Improved Prediction of Signal Peptides: SignalP 3.0. Journal of Molecular Biology 2004;340(4):783-795.

50.Culi J, Mann RS. Boca, an Endoplasmic Reticulum Protein Required for Wingless Signaling and Trafficking of LDL Receptor Family Members in Drosophila. Cell 2003;112(3):343-354.

51.Attar N, Cullen PJ. The retromer complex. Advances in Enzyme Regulation 2010;50(1):216-236.

52.Belenkaya TY, Wu Y, Tang X, Zhou B, Cheng L, Sharma YV, Yan D, Selva EM, Lin X. The Retromer Complex Influences Wnt Secretion by Recycling Wntless from Endosomes to the Trans-Golgi Network. Developmental Cell 2008;14(1):120-131.

53.Franch-Marro X, Wendler F, Guidato S, Griffith J, Baena-Lopez A, Itasaki N, Maurice MM, Vincent J-P. Wingless secretion requires endosome-to-Golgi retrieval of Wntless/Evi/Sprinter by the retromer complex. Nat Cell Biol 2008;10(2):170-177.

54.Novick P, Field C, Schekman R. Identification of 23 complementation groups required for post-translational events in the yeast secretory pathway. Cell 1980;21(1):205-215.

55.Patil C, Walter P. Intracellular signaling from the endoplasmic reticulum to the nucleus: the unfolded protein response in yeast and mammals. Current Opinion in Cell Biology 2001;13(3):349-355.

56.Wang X-Z, Harding HP, Zhang Y, Jolicoeur EM, Kuroda M, Ron D. Cloning of mammalian Ire1 reveals diversity in the ER stress responses. EMBO J 1998;17(19):5708-5717.

57.Jackson ME, Simpson JC, Girod A, Pepperkok R, Roberts LM, Lord JM. The KDEL retrieval system is exploited by Pseudomonas exotoxin A, but not by Shiga-like toxin-1, during retrograde transport from the Golgi complex to the endoplasmic reticulum. Journal of Cell Science 1999;112(4):467-475.

58.Letourneur F, Gaynor EC, Hennecke S, Démollière C, Duden R, Emr SD, Riezman H, Cosson P. Coatomer is essential for retrieval of dilysine-tagged proteins to the endoplasmic reticulum. Cell 1994;79(7):1199-1207.

59.Majoul I, Sohn K, Wieland FT, Pepperkok R, Pizza M, Hillemann J, Söling H-D. KDEL Receptor (Erd2p)-mediated Retrograde Transport of the Cholera Toxin A Subunit from the Golgi Involves COPI, p23, and the COOH Terminus of Erd2p. The Journal of Cell Biology 1998;143(3):601-612.

60.Sandvig K, Bergan J, Dyve A-B, Skotland T, Torgersen ML. Endocytosis and retrograde transport of Shiga toxin. Toxicon 2010;56(7):1181-1185.

61.Kano F, Yamauchi S, Yoshida Y, Watanabe-Takahashi M, Nishikawa K, Nakamura N, Murata M. Yip1A regulates the COPI-independent retrograde transport from the Golgi complex to the ER. Journal of Cell Science 2009;122(13):2218-2227.

62.Bonifacino JS, Hurley JH. Retromer. Current Opinion in Cell Biology 2008;20(4):427-436.

63.Duffy JB. GAL4 system in drosophila: A fly geneticist's swiss army knife. genesis 2002;34(1-2):1-15.

64.Brand AH, Perrimon N. Targeted gene expression as a means of altering cell fates and generating dominant phenotypes. Development 1993;118(2):401-415.

65.Lavieu G, Orci L, Shi L, Geiling M, Ravazzola M, Wieland F, Cosson P, Rothman JE. Induction of cortical endoplasmic reticulum by dimerization of a coatomer-binding peptide anchored to endoplasmic reticulum membranes. Proceedings of the National Academy of Sciences 2010;107(15):6876-6881.

66.Sixma TK, Kalk KH, van Zanten BAM, Dauter Z, Kingma J, Witholt B, Hol WGJ. Refined Structure of Escherichia coli Heat-labile Enterotoxin, a Close Relative of Cholera Toxin. Journal of Molecular Biology 1993;230(3):890-918.

67.Fujinaga Y, Wolf AA, Rodighiero C, Wheeler H, Tsai B, Allen L, Jobling MG, Rapoportv T, Holmes RK, Lencer WI. Gangliosides That Associate with Lipid Rafts Mediate Transport of Cholera and Related Toxins from the Plasma Membrane to Endoplasmic Reticulm. Volume 14(12): Mol Biol Cell; 2003. p 4783–4793.

68.Moody SA. Cell Lineage and Fate Determination. Academic Press; 1999.

69.Quijano JC, Stinchfield MJ, Newfeld SJ. Wg signaling via Zw3 and Mad restricts self-renewal of sensory organ precursor cells in Drosophila. Volume 189(2): Genetics; 2011.

70.Seth S B. shaggy (zeste-white 3) and the formation of supernumerary bristle precursors in the developing wing blade of Drosophila. Developmental Biology 1992;152(2):263-278.

71.Jafar-Nejad H, Tien A-C, Acar M, Bellen HJ. Senseless and Daughterless confer neuronal identity to epithelial cells in the Drosophila wing margin. Development 2006;133(9):1683-1692.

72.Kennerdell JR, Carthew RW. Use of dsRNA-Mediated Genetic Interference to Demonstrate that frizzled and frizzled 2 Act in the Wingless Pathway. Cell 1998;95(7):1017-1026.

73.Axelrod JD, Matsuno K, Artavanis-Tsakonas S, Perrimon N. Interaction Between Wingless and Notch Signaling Pathways Mediated by Dishevelled. Science 1996;271(5257):1826-1832.

74.Kim SY, Renihan MK, Boulianne GL. Characterization of big bang, a novel gene encoding for PDZ domain-containing proteins that are dynamically expressed throughout Drosophila development. Gene Expression Patterns 2006;6(5):504-518.

75.Zecca M, Basler K, Struhl G. Direct and Long-Range Action of a Wingless Morphogen Gradient. Cell 1996;87(5):833-844.

76.Vincent JP, Briscoe J. Morphogens. Current biology : CB 2001;11(21):R851-4.

77.Piddini E, Vincent J-P. Interpretation of the Wingless Gradient Requires Signaling-Induced Self-Inhibition. Cell 2009;136(2):296-307.

78.Kazanjian A, Gross EA, Grimes HL. The growth factor independence-1 transcription factor: New functions and new insights. Critical reviews in oncology/hematology 2006;59(2):85-97.